Natural Product Reports

ROYAL SOCIETY OF CHEMISTRY

REVIEW

View Article Online
View Journal

Cite this: DOI: 10.1039/d5np00046g

Discovery, bioactivities and biosynthesis of spirooxindole alkaloids

Ruijie Chen,[ab] Lihan Zhang,[ab] Xiaoyang Zhao,[ab] Zhuangjie Fang,[a] Liping Zhang,[abc] Qingbo Zhang,[*abc] Changsheng Zhang[*abc] and Yiguang Zhu[*abc]

Covering: up to the end of August, 2025

Spirooxindole-containing natural products are widely distributed in actinomycetes, cyanobacteria, fungi, plants, and invertebrates and have attracted significant attention due to their intricate chemical skeletons and diverse biological activities. Some of these compounds have made substantial contributions to the human health, particularly in the treatment of the central nervous system disorders and cardiovascular conditions as well as in agricultural applications. Accordingly, their biosynthetic pathways have been extensively investigated. Current studies reveal that cytochrome P450 enzymes and flavin-dependent monooxygenases (FMOs) are the primary enzymes involved in triggering carbocation, radical or epoxidation reactions following semipinacol rearrangement during the formation of spirooxindole. In some cases, spontaneous intramolecular Diels–Alder cycloaddition also yields spirooxindole skeletons. This review presents a comprehensive overview of the discovery and structure of spirooxindole alkaloids (SOAs), together with their bioactivities and distinctive biosynthetic pathways.

Received 28th June 2025

DOI: 10.1039/d5np00046g

rsc.li/npr

[a]State Key Laboratory of Tropical Oceanography, Guangdong Key Laboratory of Marine Materia Medica, Laboratory of Tropical Marine Bioresources and Ecology, South China Sea Institute of Oceanology, Chinese Academy of Sciences, Guangzhou 510301, China. E-mail: zhangqingbo@scsio.ac.cn; czhang@scsio.ac.cn; ygzhu@scsio.ac.cn

[b]University of Chinese Academy of Sciences, Beijing 100049, China

[c]Sanya Institute of Ocean Eco-Environmental Engineering, Sanya 572000, China

1. Introduction

Spirooxindole alkaloids (SOAs), featuring a scaffold with an oxindole core fused with various heterocyclic motifs at the C-2 or C-3 position, have long captured attention due to their unique spatial architecture and significant biological

Ruijie Chen

Ruijie Chen obtained her BS in Biology from Shandong University in 2022 and her MS in Marine Biology from the South China Sea Institute of Oceanology, Chinese Academy of Sciences in 2025. She is currently pursuing her PhD degree in Helmholtz Institute for Pharmaceutical Research Saarland (HIPS). Her research focuses on the catalytic mechanisms of tailoring enzymes in microbial natural product biosynthesis and the mechanisms of antibiotic resistance.

Lihan Zhang

Lihan Zhang obtained her BS in Bioscience from Huazhong Agricultural University in 2024. She is currently a PhD student at the South China Sea Institute of Oceanology, Chinese Academy of Sciences. Her research interests focus on the exploration of natural products from actinomycetes and investigation of their biosynthetic pathways.

Zhuangjie Fang

Zhuangjie Fang obtained his BS in Biotechnology from Guangdong University of Petrochemical Technology in 2016 and his MS (2019) and PhD (2023) in Marine Biology from the University of Chinese Academy of Sciences. He is currently a Postdoctoral Researcher at the South China Sea Institute of Oceanology. His research focuses on the discovery and biosynthesis of bioactive compounds from marine actinomycetes.

Qingbo Zhang

Qingbo Zhang obtained his PhD in 2013 in Marine Biology from the South China Sea Institute of Oceanology, Chinese Academy of Sciences. He is currently working as a Program Professor at the same institute. His research focus on the discovery and biosynthesis of natural products from marine microorganisms.

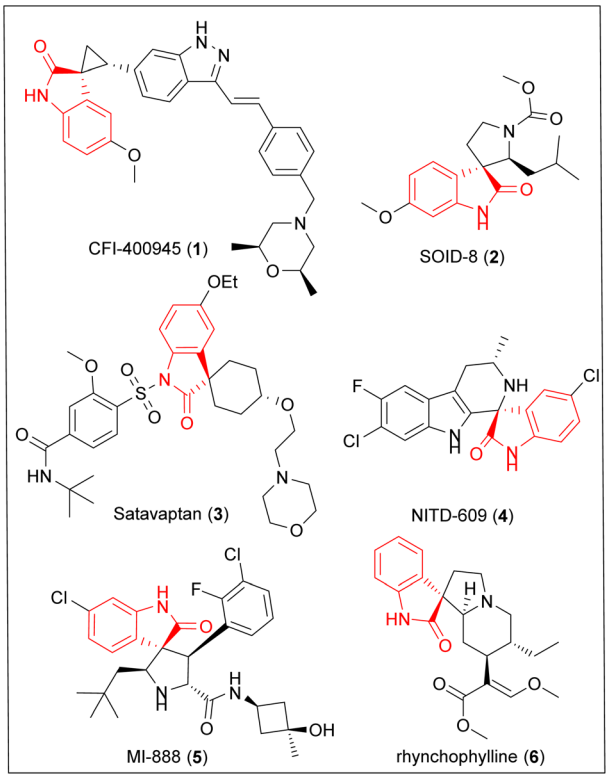

Fig. 1 Clinically and pharmaceutically active analogues of spirooxindoles.

activities, making them promising candidates for drug discovery. Several spirooxindole derivatives have already advanced to clinical trials, underscoring their therapeutic potential. For example, CFI-400945 (**1**), the first oral inhibitor of polo-like kinase, has been tested in clinical trials for patients with advanced solid tumors.[1] Other examples with demonstrated promising therapeutic efficacy include the melanoma agent SOID-8 (**2**),[2] the vasopressin receptor antagonist satavaptan (**3**) (SR121463),[3] and the antimalarial candidate NITD-609 (**4**).[4] Structural modifications of the natural spiro(oxindole-3,3′-pyrrolidine) core have led to a series of potent inhibitors of the p53-MDM2 interaction,[5] represented by MI-888 (**5**), a potent MDM2 inhibitor (Ki = 0.44 nM) with a superior pharmacokinetic profile.[6] Additionally, rhynchophylline (**6**), a plant-derived compound, is a traditional Chinese medicine used to lower blood pressure and induce sleep, and it serve as a neuroprotectant (Fig. 1).

Natural alkaloids containing a spirooxindole scaffold are widely distributed across a variety of organisms, including actinomycetes (Fig. 2), cyanobacteria (Fig. 2), fungi (Fig. 3–6), plants (Fig. 7, 8 and 10–12), and invertebrates (Fig. 13). These compounds were first chemically studied and pharmacologically evaluated in plants in the early twentieth century.[7,8] Brevianamide A, isolated in 1969, was the first reported fungus-derived spirooxindole alkaloid.[9] Later, the isolation of compounds from marine[10–14] and terrestrial[15–17] fungal species of *Aspergillus*, *Penicillium* and related genera led to the discovery of a diverse range of SOAs. SOAs from bacterial and animal origins have also garnered significant attention in structural chemistry studies. Many natural SOAs exhibit notable biological activities, including antimicrobial,[17–19] insecticidal,[20,21] anthelmintic,[22,23] anticancer,[24,25] and anti-inflammatory effects.[26,27] These remarkable activities highlight their potential for the development of new drugs and agricultural applications.

The construction of chiral spirocyclic skeletons has been challenging in organic synthesis. Methods such as the Pictet–Spengler oxidative rearrangement,[28] Mannich reaction,[29] intramolecular Heck reaction,[30] and metal-catalyzed or organo-catalyzed 1,3-dipolar cycloaddition[31,32] are commonly employed to build spirooxindole frameworks. Several books and reviews have provided insightful overviews of these methods.[33–36] However, the enzyme-mediated biosynthesis of SOAs offers a stereoselective advantage over traditional organic synthesis, and it is more efficient and environmentally friendly. In particular, the enzymatic mechanisms for spiro-formation have attracted significant interest in recent decades, which have demonstrated that cytochrome P450 enzymes and flavin-dependent monooxygenases are the primary enzymes involved in catalyzing the spiro formation. This review aims to systematically summarize the isolation, biological activities and biosynthesis of SOAs.

Changsheng Zhang

Changsheng Zhang obtained his PhD in Chemical Microbiology from the University of Wuppertal (Germany) in 2002 and completed his postdoctoral training at the University of Wisconsin Madison (USA) from 2003 to 2008. He is currently a Professor at the South China Sea Institute of Oceanology, Chinese Academy of Sciences. His research focus on the discovery, biosynthesis and drug development of natural products from marine microbes.

Yiguang Zhu

Yiguang Zhu received his PhD in Microbiology from Huazhong Agricultural University in 2011 and is currently working as a Professor at the South China Sea Institute of Oceanology, Chinese Academy of Sciences. His research focuses on the biosynthesis and enzyme biocatalysis of natural products from marine fungi and actinomycetes.

2. Structure diversity of spirooxindole alkaloids

2.1. Actinomycetes derived SOAs

2.1.1 Cyanogramide. In 2014, Zhu and co-workers isolated cyanogramide (7) from the fermentation broth of the marine-derived *Actinoalloteichus cyanogriseus* WH1-2216-6, and fully determined its structure through spectroscopic analysis and electronic circular dichroism (ECD) calculations. Compound 7 contains spirooxindole and pyrroloimidazole moieties, with the absolute configuration of the spiro carbon being *R*.[37]

2.1.2 Maremycins. Maremycins E (**8**) and F (**9**), both incorporating a sulfur atom, were discovered in the culture broth of *Streptomyces* sp. (strain GT 051237) by Tang *et al.*[38] The spirocycle is formed between the cyclopenta[f]quinoxaline moiety (C-6) and indol-2-one moiety (C-3′). Their planar structures were elucidated through detailed NMR analysis, while the absolute configurations of the spiro carbon remained uncertain. Maremycin G (**10**) is identified as a deoxy analogue of compound **9**.[39]

2.1.3 Spindomycins. In 2014, Xu *et al.* isolated spindomycins A (**11**) and B (**12**) from rhizosphere strain *Streptomyces* sp. xzqh-9, and elucidated their structures by spectroscopic analysis. ECD analysis was performed to determine the chirality of the spiro carbon C-3′, and both compounds were found to have the absolute configuration of *R*.[40]

2.2. Cyanobacteria-derived SOAs

2.2.1 Welwitindolinone A. Welwitindolinones are a unique family of indole monoterpene alkaloids that were originally isolated from the true-branching heterocystous filamentous cyanobacterium *Hapalosiphon welwitschii* by Moore and colleagues.[41] Unlike other welwitindolinones, which feature 3,4-disubstituted oxindoles with a signature bicyclo[4.3.1]decane core motif, welwitindolinone A (**13**) contains an oxindole backbone appended with a spirocyclobutane monoterpene unit. It is postulated to serve as a biosynthetic precursor to other congeners. The highly stereoselective total synthesis of welwitindolinone A isonitrile has been successfully completed.[41]

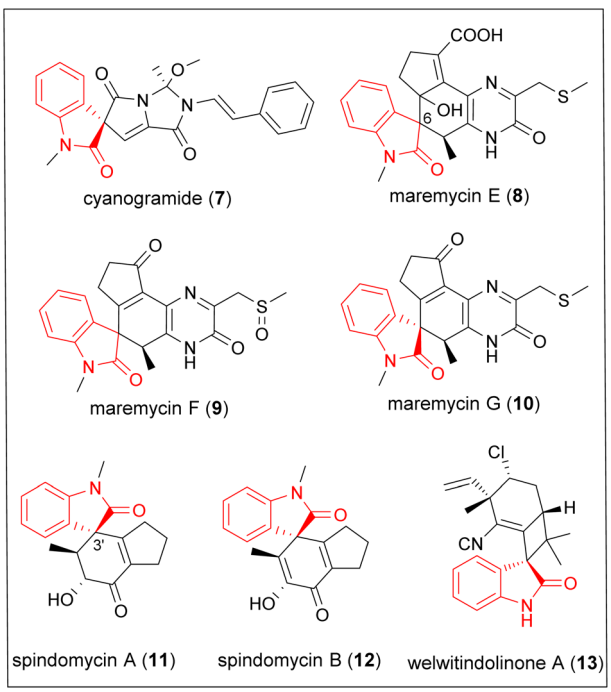

Fig. 2 SOAs from actinomycetes and cyanobacteria.

2.3. Fungal-derived SOAs

2.3.1 SOAs with bicyclo[2.2.2]diazaoctane skeleton

2.3.1.1 Brevianamides. Brevianamides are a class of isoprenylated indole alkaloids produced by filamentous fungi. In 1969, Birch and Wright reported the discovery and isolation of brevianamides A–E from *P. Brevicompactum*.[9] They elucidated the structures of brevianamides A (**14**) and B (**15**), which contain spirooxindole moieties and bicyclo[2.2.2]diazaoctane skeletons, through spectroscopic analyses in 1970 and 1972, respectively.[42,43] Brevianamide B was shown to be a stereoisomer of brevianamide A at the spiro-center through inter-conversion. They also indicated that cyclo-L-tryptophyl-L-proline is biosynthetically incorporated into brevianamide A, with the spiro ring located at C-2. Subsequently, the absolute stereochemistries of **14** and **15** were determined by Williams's group.[44] In 2017, Qi *et al.* isolated brevianamides X (**16**) and Y (**17**) from a deep-sea derived fungus. Compound **16** was inferred to be a diastereomer of (−)-depyranoversicolamide B with a relative configuration of 3*S*,11*R*,17*R*,19*R*, while **17** was confirmed to be (3*S*,11*S*,17*S*,19*R*)-brevianamide Y.[45]

2.3.1.2 Marcfortines. Marcfortines A–C (**18–20**) were isolated by Polonsky and co-workers from *P. roqueforti* in 1980.[46] Compound **18**, established by X-ray analysis, is the first fungal alkaloid with a seven-membered ring formed by the linkage of an isoprene unit to two phenolic hydroxy groups on the tryptophan unit. This spirooxindole alkaloid also features a bicyclo[2.2.2]diazaoctane system, similar to the brevianamide family. In 1981, the structure of **20** was established by X-ray diffraction analysis.[47] Chrysogenamide A (**21**), a member of the marcfortine group of alkaloids, was identified by Zhu and co-workers from *P. chrysogenum* No. 005 in 2008,[48] featuring a unique structure with methylation at C-17 and a 2-oxindole moiety possessing an isoprene unit at C-7. Penioxalamine A (**22**) was isolated by Bai *et al.* from the fungus *P. oxalicum* TW01-1 in 2014.[16] Its structure was elucidated using spectral data, single-crystal X-ray diffraction, and CD analysis, suggesting it is a prenylated spirooxindole alkaloid with a unique seven-membered nitrogen heterocycle. It possesses a rare *anti* relative configuration within the core bicyclo[2.2.2]diazaoctane ring system, and the epoxy ring at C-25 and C-26 and the acylamino group between C-11 and C-13 are β-oriented. The absolute configuration of the spiro carbon (C-3) has been determined to be *S*.[16]

2.3.1.3 Paraherquamides. Paraherquamides represent one of the largest families of prenylated indolic natural products derived from various fungal genera. Paraherquamide A (**23**) is a spirooxindole originally isolated by Yamazaki *et al.* from *P.*

paraherquei in 1981, featuring a bicyclo[2.2.2]diazaoctane moiety, one cyclopentane ring, a 1,4-dioxepine ring, and two pyrrolidine rings.[49] Similar to **18** and **19**, **23** also contains an unusual dioxygenated seven-membered ring on the tryptophan unit, as determined by X-ray diffraction analysis. Paraherquamides B-G (**24–29**) were isolated from *P. charlesii* in 1990.[50] They exhibit variations in substitution patterns, in addition to the two variants of the ring system fused to the C-6 and C-7 positions of the indole. Among them, the crystal structure of **27** was reported by Aree and co-workers in 2010.[51] Moya and co-workers isolated paraherquamides H (**30**) and I (**31**) from the culture broth of *P. cluniae* Quintanilla in 2006, which have unusual oxidative substitutions at C-16.[21] Paraherquamides J (**33**) and K (**37**) were initially named for two compounds isolated from *A. duricaulis* in 2015,[15] but were later assigned to two compounds, **34** and **38**, isolated from the marine-derived fungus *P. janthinellum* HK1-6, exhibiting different structures in 2020.[13] Along with **33** and **37**, 16-deoxo-paraherquamide B (**32**), 29-*N*-demethyl paraherquamide J (**35**), 16-deoxo-paraherquamide J (**36**), 29-*N*-demethyl-paraherquamide K (**39**), and 16-deoxo-paraherquamide K (**40**) were isolated.[15] Other members of this family, such as VM55595-VM55597 (**41–43**), contain β-methylproline similar to paraherquamides E–G.[52,53] In addition to *Penicillium* species, Everett and co-workers also isolated SB203105 (**44**), SB200437 (**45**) from *Aspergillus* species, which are members of the paraherquamide family. Comparison of their spectral data with other reported paraherquamide shows that **44** is the first paraherquamide to feature a C-4 substitution.[22,54] In 2022, a new paraherquamide, aculeaquamide A (**46**), was isolated from the marine fungus *A. aculeatinus* WHUF0198 by Wu and co-workers. This compound is similar to **27** but has a hydroxyl group replacing the aromatic proton at C-5.[55]

2.3.1.4 Notoamides. Notoamides represent another large family of prenylated indolic natural products. In 2007, Tsukamoto *et al.* reported the isolation and structural elucidation of SOAs (−)-notoamides A (**47**) and B (**49**) from the marine-derived fungus *Aspergillus* sp. isolated from the common mussel *Mytilus edulis*.[10] Williams and co-workers isolated (+)-notoamide B (**50**) from the terrestrial *A. versicolor* NRRL 35600, and subsequently reported the biomimetic total synthesis of **49**.[56,57] (+)-Notoamide A (**48**) was isolated in 2017 from *A. amoenus*.[58] Other compounds in this family containing spirooxindole moieties were gradually isolated by Tsukamoto's group from 2008 to 2010, including notoamides H (**51**), N (**52**), O (**53**).[59–61] Compound **50** is characterized as a 1-hydroxy derivative of sclerotiamide(**55**),[59] while **52** is a chlorinated derivative.[60] Compound **53** contains a hemiacetal ring connected to an indole-derived ring through a spiro hemiaminal ether carbon C-2, with the C-2 and C-10 carbon atoms in the oxidized states.[61] In 2015, (+)-isonotoamide B (**54**) was isolated from the marine-derived endophytic fungus *Paecilomyces variotii* EN-291.[62] Additionally, notoamide Y (**55**), a 19-methoxylated analogue of **55**, was isolated by Hu *et al.* from the coral-associated fungus *A. ochraceus* LZDX-32-15 in 2019.[63]

2.3.1.5 Sclerotiamides. (−)-Sclerotiamide (**56**) was first isolated by Whyte and Gloer from *A. sclerotiorum* Huber (NRRL 5167) in 1996.[64] Sclerotiamide B (**55**) was isolated from the endophytic fungus *Fusarium sambucinum* TE-6, which actually has the same structure as notoamide Y.[20] In 2013, (−)-10-*epi*-sclerotiamide (**57**) and 5-chlorosclerotiamide (**58**) were isolated from the deep-sea-derived fungus *A. westerdijkiae* DFFSCS013.[65] **57** is an isomer of **55** at C-10. In 2018, 10-*O*-ethylsclerotiamide (**59**) and 10-*O*-acetylsclerotiamide (**60**) were isolated from a co-culture of the marine-derived fungi *A. sulphureus* KMM 4640 and *Isaria felina* KMM 4639, with the presence of an ethyl ether and an acetoxy group at C-10 in **55**.[66] (−)-19-e*pi*-sclerotiamide (**61**) and (+)-19-*epi*-sclerotiamide (**62**) were isolated in 2023.[67] Sclerotiamide O (**63**) was discovered by Lin and co-workers in 2022. There was a methoxy group at C-19, and a second methoxy group located at C-8.[68]

2.3.1.6 Versicolamides. (+)-Versicolamide B (**64**) is a minor metabolite of *A. versicolor* NRRL 35600.[57] Williams and co-workers assigned the absolute configuration to this compound based on CD spectra.[57] (−)-Versicolamide B (**65**) was isolated from a marine-derived *Aspergillus* sp.[60] In 2013, (−)-versicolamide C (**66**) was isolated as the photoinduced conversion product of *N*-hydroxy-6-*epi*-stephacidin A from *A. taichungensis*.[69]

2.3.1.7 Asperversiamides. Asperversiamides B (**67**) and C (**68**) are two linearly fused prenylated indole alkaloids, featuring an unusual pyrano[3,2-f]indole unit, isolated from the marine-derived fungus *A. versicolor* in 2018.[70] Their structures and absolute configurations were confirmed by single-crystal X-ray diffraction analysis.[70]

2.3.1.8 Amoenamides. Amoenamide B (**69**) was isolated from *A. amoenus* NRRL 35600 by Tsukamoto and co-workers in 2018, which features a pyrano[2,3-*g*]indole moiety and a bicyclo[2.2.2] diazaoctane core.[71] Amoenamide C (**70**) was later isolated from the endophytic fungus *F. sambucinum* TE-6L by Xu and co-workers. Based on comprehensive spectroscopic techniques, including ECD and X-ray diffraction, it was determined to be a 10-methoxy derivative of **69**, with a different stereogenic center in the indoxyl core compared to **69**.[20] In 2022, Wang and co-workers discovered 2-*epi*-amoenamide C (**71**) from a sponge-derived fungus *A. sclerotiorum*.[72]

2.3.1.9 Mangrovamides. Mangrovamides A (**72**) and B (**73**), featuring a bicyclo [2.2.2] diazaoctane core and possess novel g-methyl proline and isoprene-derived dimethyl g-pyrone functionalities, were isolated from a *Penicillium* sp. strain derived from a mangrove soil sample in 2014.[73] Later, in 2018, mangrovamides D (**74**) and E (**75**) were isolated from *Penicillium* sp. SCSIO 041218, cultured in a 1% NaCl PDB substrate.[74]

2.3.1.10 Peniciherquamides. Peniciherquamides A (**76**) and B (**77**) were isolated from the fungal culture broth of *P. herquei* in 2016. Compound **76** is the first diazabicyclo[2.2.2]octane ring derivative to feature both β-methylproline and 2,2-dimethylchroman-4-one moieties. Compound **77** is the first diazabicyclo[2.2.2]octane ring system to be described to possesses an *O*-methyl group that forms an imidate.[75]

2.3.1.11 Asperthrin E. In 2021, asperthrins A–F were isolated from the marine-derived endophytic fungus *Aspergillus* sp. YJ191021. Asperthrin E (**78**) was identified as a spirooxindole. The planar structure of **78** was found to be identical to that of 10-*O*-acetylsclerotiamide (**60**).[76]

2.3.1.12 Taichunamide E. Taichunamides A–G were isolated by Tsukamoto and co-workers from the fungus *A. taichungensis* in 2016.[77] Among them, taichunamide E (**79**) was found to be a spirooxindole, which is the 3-epimer of **64**, corresponding to the 21-epimer of compound **48**.[77]

2.3.1.13 Spiromalbramide. Spiromalbramide (**80**) was detected by Crews and colleagues from the hyphae of the marine invertebrate-derived fungus *Malbranchea graminicola*.[78] Further NMR spectroscopy analysis revealed that **60** is a chlorinated derivative with an *S*-spiro junction at C-6a.[78]

2.3.1.14 Citrinalin C. Citrinalin C (**81**) was isolated as a minor component from *P. citrinum* F53, and unlike the minor components citrinalins A and B, it contains a bicyclo[2.2.2]diazaoctane structural moiety.[79]

2.3.1.15 Cycloexpansamine A. Cycloexpansamine A (**82**) was isolated from a marine-derived fungus *Penicillium* sp. (SF-5292) by Lee and co-workers in 2015. It is a heptacyclic spiroindolinone alkaloid consisting of a 4,5-dihydro-1*H*-pyrrolo[3,2,1-*ij*] quinoline 2,6-dione ring and an amide-bridged cyclopenta[*f*]indolizidine ring connected *via* a spiro-carbon atom. The relative configuration between the C13–C14 and C16–N24 bonds in the [2.2.2] diazaoctane core was determined as *anti*.[11]

2.3.1.16 Waikikiamide C. Waikikiamide C (**83**) was isolated from *Aspergillus* sp. FM242.[80] It features the first unique heterodimer of two notoamide analogs (notoamide B and 12,13-dihydro-13-hydroxy-12-methoxy-notoamide G) with an N–O–C bridge. Its structure was determined through X-ray crystallographic analysis.[80]

2.3.2 SOAs with cyclopentane piperidine moiety

2.3.2.1 Citrinadins. Citrinadin A (**84**) was isolated in 2004 from the marine red alga-derived fungus *P. citrinum* by Kobayashi and co-workers. It is a pentacyclic spirooxindole alkaloid with an *N*,*N*-dimethylvaline ester and an α, β-epoxy carbonyl unit. The absolute configuration at C-2′ was identified to be the L-form by chiral HPLC analysis.[81] In 2005, citrinadin B (**85**) was isolated by the same group. The absolute stereochemistries of C-21 and the pentacyclic core in both **84** and **85** were established through analysis of their ROESY spectrum and comparison of their ECD spectra.[82] Other pentacyclic SOAs, such as PF1270 A-C (**86–88**), were isolated from *P. waksmanii* in 2007 by Yaguchi and co-workers.[83] Compound **86** was confirmed by X-ray crystallographic analysis. Compound **87** is similar to **86** but lacks one methylene group in its acyl side chain, and **88** lacks two methylene groups. In 2022, citrinadin C (**89**), a *N*-demethyl derivative of citrinadin A (**84**), was isolated by Jiang and co-workers.[14] In 2025, citrinadin E (**90**) was identified from the endophytic *Penicillium* sp. NX-S-6. It closely resembles citrinadin B (**85**), but lacks a hydroxyl group at C-18.[84]

2.3.2.2 Citrinalins. Citrinalins A (**91**) and B (**92**) were identified in 2010 by Berlinck and colleagues through optimization of *P. citrinum* cultures. Similar to citrinadins, these compounds lack the bicyclo[2.2.2]diazaoctane framework but feature rare aliphatic nitro groups.[85] In 2014, Berlinck and Sarpong's groups isolated 17-hydroxycitrinalin B (**93**) and citrinalin C (**81**), and conducted a computational simulation and reanalyzed their NMR data, suggesting that citrinalins A and B involve epimerization at the C22 stereocentre.[79] It is hypothesized that **91** and **92** are the oxidative degradation products of a precursor containing a bicyclo[2.2.2]diazaoctane ring.[79]

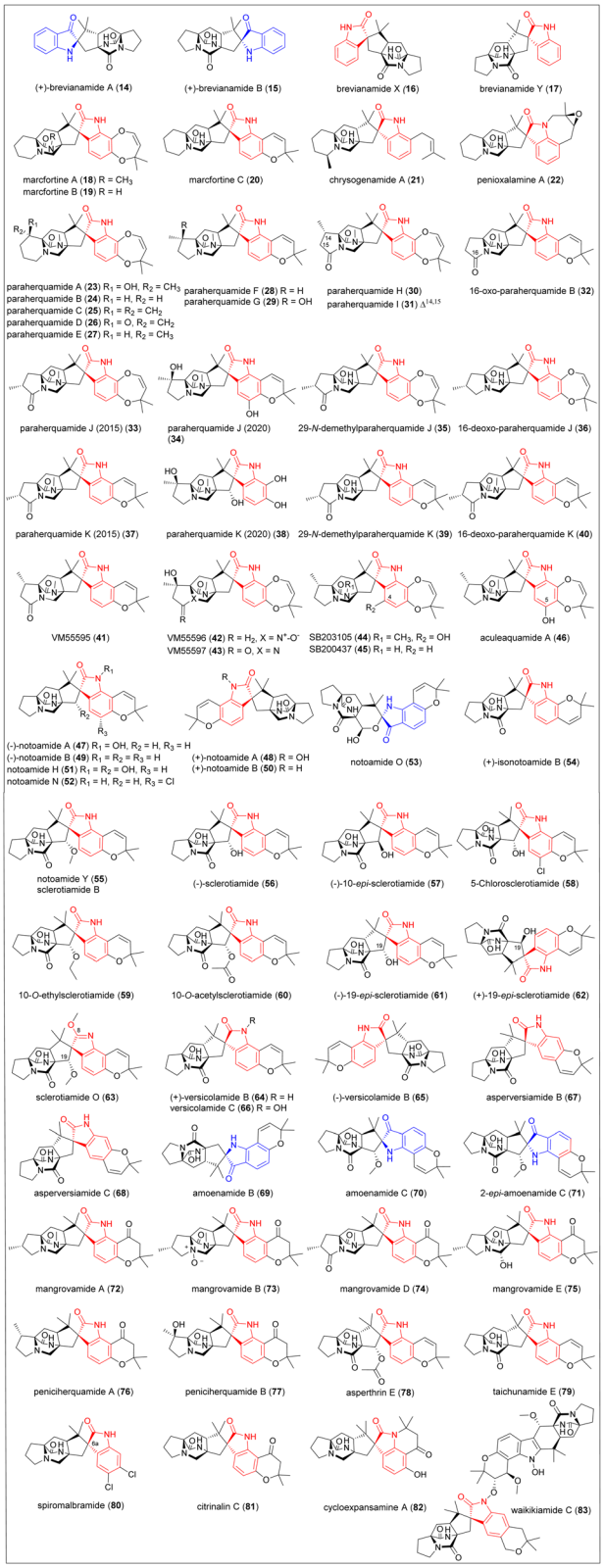

Fig. 3 Fungal-derived SOAs with a bicyclo[2.2.2]diazaoctane skeleton.

2.3.2.3 Cyclopiamines. Cyclopiamines A (**94**) and B (**95**) were discovered in 1979 in a toxinogenic strain of *P. cyclopium*.[86] 6-Hydroxycyclopiamine B (**96**) was isolated from *Aspergillus* sp. fA75 in 2012.[87] *Ent*-homocyclopiamine B (**97**) and clopiamine C (**98**) were isolated from the endophytic fungus *P. concentricum* of the liverwort *Trichocolea tomentella* (Trichocoleaceae).[88] Clopiamine C (**98**) was first isolated from *P. griseofulvum* CPCC 400528, and its relative and absolute configurations were determined by single-crystal X-ray diffraction.[89] **98** and **95** are enantiomers. Cyclopiamines C (**99**) and D (**100**) were isolated from *Penicillium* sp. CML 3020. Their NMR and MS/HRMS data suggested the presence of an epoxide unit connected to the proline-derived pyrrolidine moiety and a hydroxy group at C-5.[90]

2.3.2.4 Cycloexpansamines. Cycloexpansamine B (**101**) was isolated from a marine-derived fungus *Penicillium* sp. (SF-5292) by Lee and co-workers in 2015, along with cycloexpansamine A (**82**).[11] **101** is closely related to **99** and **100**, and is one of the few secondary metabolites possessing a 4,5-dihydro-1*H*-pyrrolo [3,2,1-*ij*]quinoline-2,6-dione ring system.[11]

2.3.2.5 Penicitrimicins. Penicitrimicins A–G (**102–108**) were discovered from the fungus *P. citrinum* YSC-1 isolated from a medicinal plant *Chloranthus japonicus*, with a rare 6/5/5/6/6

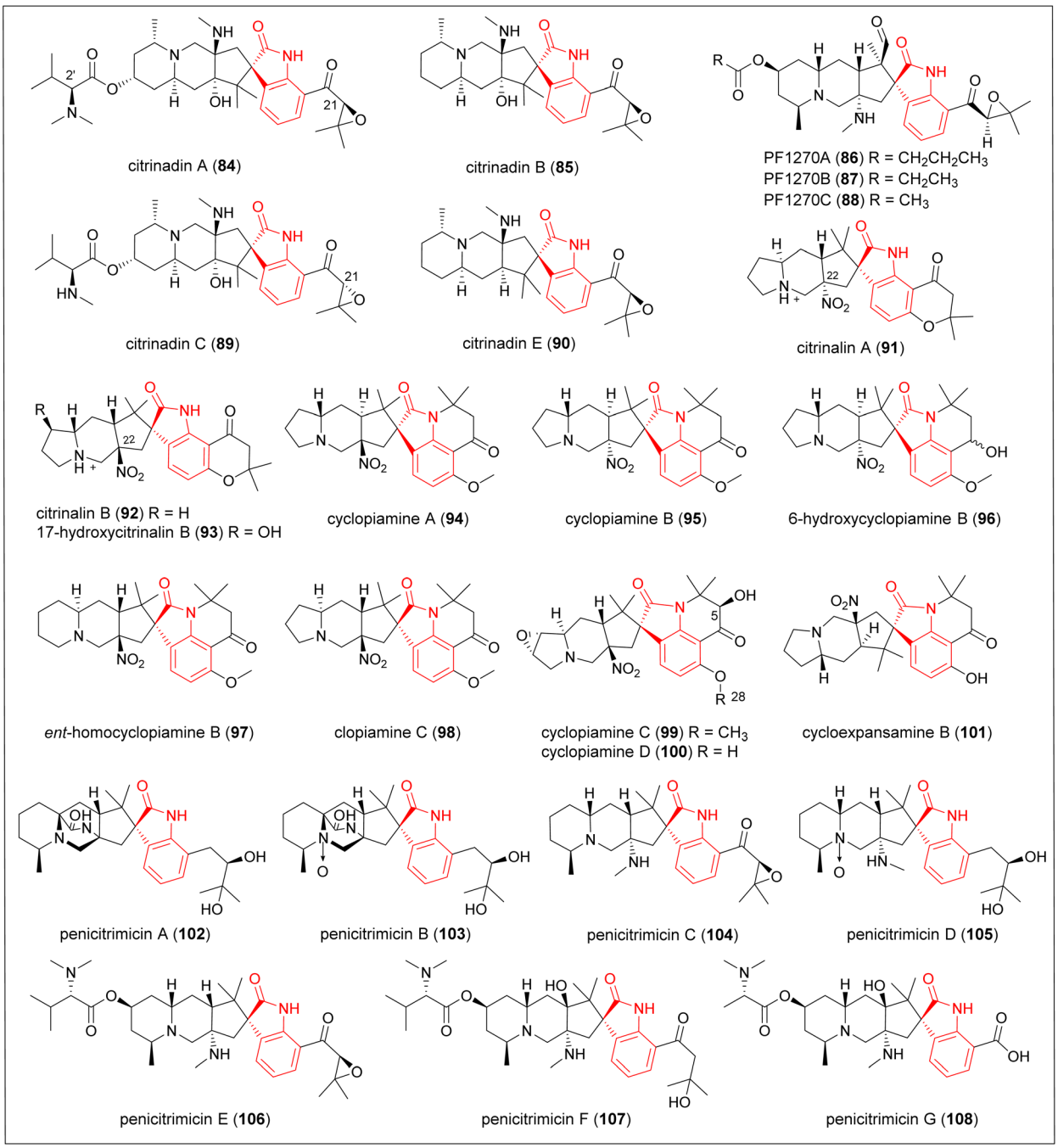

Fig. 4 Fungal-derived SOAs with a cyclopentane piperidine moiety.

polycyclic skeleton, using an OSMAC approach.[91] Instead of the isopentenyl group in chrysogenamide A (**21**), **102** has a 2,3-dihydroxy-3-methylbutyl moiety at C-7. **103** is a N-11 oxide derivative of **102**. **104** is a structural analogue of citrinadin B (**85**), with the major distinction being the presence of an extra methine and the lack of an oxygenated tertiary carbon. **106–108** have additional *N*,*N*-dimethyl-valinyl side chains at C-14.[91]

2.3.3 SOAs with diketopiperazine moiety

2.3.3.1 Spirotryprostatins. In 1996, spirotryprostatins A (**109**) and B (**110**) were isolated from *A. fumigatus* and found to contain spirooxindole and diketopiperazine moieties.[92,93] Subsequently, spirotryprostatins C–E (**111–113**) were isolated by Wang *et al.* from the holothurian-derived fungus *A. fumigatus* in 2008.[94] Compound **111** shared the same spiro-oxindole skeleton as **109** but featured two additional hydroxyl groups (8-OH and 9-OH) and an isoprenyl unit attached to the indole N-1. Compound **112** had the same skeleton as **111**, but with a 12-OH group substituted at C-1. Compound **113** featured a hydroperoxy isoprenyl group linked to N-1. In 2012, 8,9-dihydroxyspirotryprostatin A (**114**) was isolated from the endophytic fungus *A. fumigatus*.[95] Spirotryprostatin F (**115**) was discovered in 2012 from a marine fungus, *A. fumigatus*, isolated from the soft coral *Sinularia* sp.[96] In 2017, another spirooxindole, also named spirotryprostatin F (**116**), was identified from the plant endophytic *P. brefeldianum*, which was isolated from the rhizome of *Pinellia ternata*. In 2019, Zhang *et al.* isolated spirotryprostatin G (**118**) from the marine-derived fungus *P. brasilianum* HBU-136 using genomic analysis.[12] The same name spirotryprostatin G (**117**) had been used in one of the end products in the biosynthetic pathway for fumitremorgin in 2013.[97] Spirotryprostatin M (**119**) was isolated by Lin and co-workers in 2020 from an insect-derived fungus *Neosartorya fischeri*,[98] which featured an additional oxygenated isoprenyl unit attached to C-8. Most spiro centers in spirotryprostatins exhibit an *S* absolute configuration, although **111** and **118** were revised to *R* configurations based on their experimental and calculated CD spectra in 2022.[17]

2.3.3.2 Spirobrefeldins. In 2022, spirooxindole diketone piperazine alkaloids spirobrefeldins A–C (**120–122**, respectively) were isolated from the terrestrial fungus *P. brefeldianum*. The isopentenyl at C-18 in **119** was substituted by a hydroxyl group in **120**. The absolute configurations of these compounds were elucidated by computational chemistry and CD spectra, revealing that the spiro carbon at the C-2 position was *S*.[17]

2.3.3.3 Asperdiketopoids. In 2025, asperdiketopoids D–G (**123–126**, respectively) were isolated from *Aspergillus* sp. KYS-11.[99] Notably, compounds **125** and **126** feature an inverted and α-oriented isobutenyl side chain, with their C-18 position being *R*-configured.[99]

2.3.3.4 Asperfumines. In 2025, asperfumines A (**127**) and B (**128**) were isolated from *A fumigatus*.[100] **127** is similar to spirotryprostatin F (**115**), with its key difference being the absence of a hydroxyl group at C-8. Compound **128** shares similarities with **117**, expect for an additional methoxy group at C-12.[100]

2.3.3.5 Talaromycins. Talaromycins A–E (**129–133**, respectively) were isolated in 2024 from the marine-derived fungus *Talaromyces purpureogenus* SCSIO 41517.[101] These compounds contain the same A/B/C/D ring system and isoprenyl unit as spirotryprostatin A (**109**), but the proline residue in **109** was replaced by an alanine residue in the talaromycins.[101]

2.3.3.6 Austamide. Austamide (**134**) was isolated in 1971 from *A. ustus* CSIR 1128. It was assumed to be the biogenetic precursor of brevianamide A.[102] In 1973, 12,13-dihydroaustamide (**135**) was isolated.[103]

2.3.3.7 Versicoines. Versicoines N–S (**136–141**, respectively) were isolated in 2025 from the deep-sea derived fungus *A. puulaauensis* F77, collected from deep-sea sediment at a depth of −2728 m in the Pacific Ocean. These compounds represent a unique class of austamide-type alkaloids.[104] Compound **137** is a 16,17-hydrogeneated analog of **136**, while **138** is a 16,17-dihydroxylated analog of **137**. Compounds **139** and **141** are (16*S*, 17*S*)-isomers of **138** and **140**.[104]

2.3.3.8 Pseudellones. Pseudellones A (**142**) and B (**143**) were isolated from the marine-derived fungus *Pseudallescheria ellipsoidea* F42-3. They are a pair of irregularly bridged epimonothiodiketopiperazine diastereomers composed of unusual 3-indolylglycine and alanine residues.[105]

2.3.4 SOAs with a quinazoline moiety. Aspertoryadins F (**144**) and G (**145**) were isolated in 2019 from the marine-derived fungus *Aspergillus* sp. HNMF114.[106] In 2023, clavutoines J–K (**146–148**, respectively), stereoisomers isolated from the marine-derived fungus *A. clavutus* LZD32-24, were found to have planar structures similar to **144** with an oxindole unit incorporated into a quinazoline moiety. However, they differ by a hydroxy group at C-2′ replacing the acetoxy group present in **144**.[107] Trypotoquivaline T (**149**), isolated from *N. siamensis*,[108] and Scedapin E (**150**), obtained from the marine-derived fungus *Scedosporium apiospermum* F41–1,[109] both contain a pyrazinoquinazolinedione and an imidazoindolone/indolone moiety connected by a tetrahydrofuran ring. However, they exhibit distinct stereochemical configurations at C-1 and C-14. The absolute configuration of C-16 in **149** is still uncertain.

2.4. Plant-derived SOAs

Plants are the primary source of SOAs, with more than 400 distinct compounds identified to date. We have systematically categorized them based on their botanical genera, which include compounds isolated from the *Alstonia* genus (Fig. 7, **151–186**),[110–124] *Mitragyna*/*Uncaria* genus (Fig. 8 and S1, **187–258**),[7,125–139] *Gelsemium* genus (Fig. 10 and S2, **259–444**),[140–167] *Gardneria* genus (Fig. 11, **445–466**),[167–173] *Alangium*, *Mappiodoside* and *Nauclea* genera (Fig. S3, **467–478**),[174–183] *Tabernaemontana* genus (Fig. S4, **479–489**),[184–191] *Ervatamia* genus (Fig. S5, **490–497**),[192–195] *Voacanga* genus (Fig. S6, **498–507**),[18,196–199] *Catharanthus* genus (Fig. S7, **508–512**),[200,201] *Aspidosperma*, *Vinca* and *Rauvolfia* genera (Fig. S8, **513–535**),[202–206] and other genera (Fig. 12, **536–557**).[207–221]

2.4.1 SOAs from *Alstonia*. Plants of the genus *Alstonia*, which produce macroline SOAs, have been utilized in traditional medicine. In 1972, Elderfield *et al.* first isolated alstonisine (**151**) from the stem bark of *A. muelleriana*.[110] The relative configuration of **151** was determined through single-crystal X-ray analysis, which showed it was a tryptophan and an

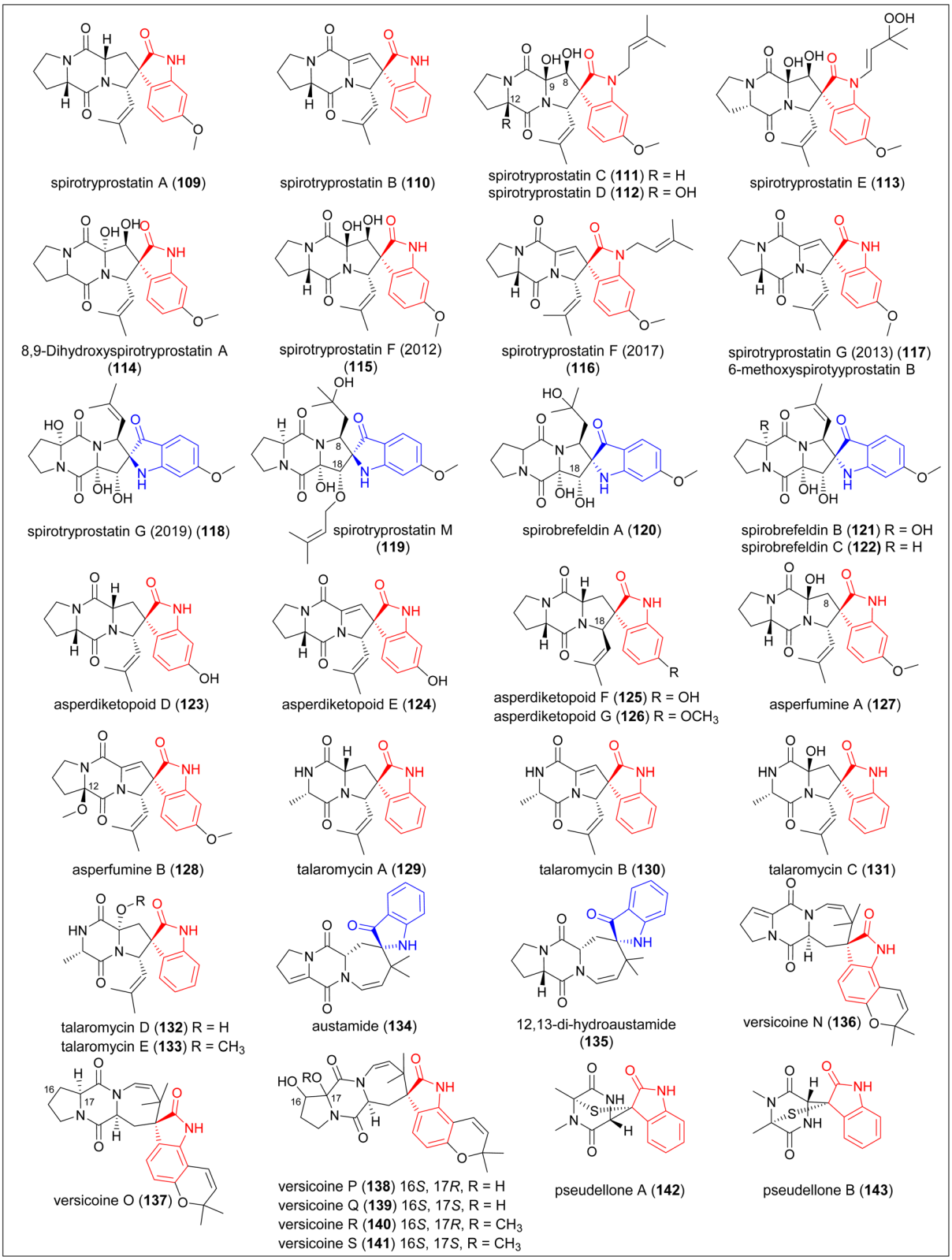

Fig. 5 Fungal-derived SOAs with a diketopiperazine moiety.

anthranilic acid-derived compound.[111] Kam and Choo later isolated its analogues isoalstonisine (**152**), N_1-demethylalsonisine (**153**) and alstofoline (**154**) from *A. macrophylla* in their study.[112] Wong *et al.* discovered alstonal (**155**) and N_b-demethylalstophyllal oxindole (**156**), which share the same core structure as **151**.[113,114] Their analogue N_b-demethylalstophylline

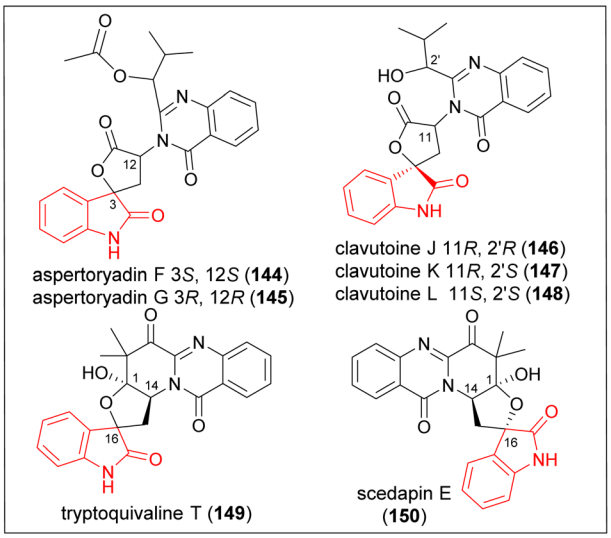

Fig. 6 Fungal-derived SOAs with a quinazoline moiety.

oxindole (**157**) was isolated in 1987.[115] Additionally, Kam and Choo isolated 16-hydroxyalstonal (**158**), N_1-demethylalstonal (**159**) and 16-hydroxy-N_4-demethylalstophyllal oxindole (**160**).[112,116] In 2018, alstonisinines A–C (**161–163**, respectively) and alstonoxine F (**164**) were isolated from *A. penangiana*.[117]

Beyond these structures, macrogentine (**165**),[112] macrogentine A (**166**) and macroxine (**167**) exhibit distinct skeletal structures.[118,119] The A, B, C, and D rings of these macroline oxindole systems are essentially intact, though cleavage and rearrangement occur within ring E. Alstonoxines A and B (**168** and **169**, respectively), isoalstonoxine B (**170**) and alstonoxine E (**171**) are ring-opened macroline SOAs.[120]

Other types of SOAs have also been found in *Alstonia* species. In 2019, alstonlarsines B–D (**172–174**, respectively), isolated from *A. scholaris,* feature a tetracyclic framework.[121] Affinisine oxindole (**175**) is an oxindole derivative of the sarpagine alkaloid affinisine.[122] Other sarpagine-type alkaloids such as alstoumerine oxindole (**176**), 7(*S*)-talpinine oxindole (**177**) and normacusine B-2(*S*)-pseudoindoxyl (**178**) were isolated from *A. angustifolia* in 2014.[118] In 2020, Yeap *et al.* isolated seven SOAs from the leaves and stem-bark extracts of *A. penangiana*, including alstopenidine B–E (**179–182**, respectively), alstomutinine C (**183**), alstomutinine D (**184**) and alstomutinine E (**185**).[123] In 2024, alstoniaine E (**186**) was isolated from the stem barks of *A. scholaris* using a silica gel-free methodology.[124]

2.4.2 SOAs from *Mitragyna*/*Uncaria*. The genera *Mitragyna* and *Uncaria* share similar nature products but differ in their content. Both belong to the subtribe *Mitragyninae Havil* of the tribe *Cinchonea*.[7] A series of investigations into alkaloids from *Mitragyna speciosa* collected across various geographic locations in Asia reported several SOAs.[125,126] In 2021, monoterpenoid SOAs (**6**, **187–239**) (Fig. S1) from the genus *Uncaria* were summarized by Yu *et al.*[127] Most SOAs in these genera are tetracyclic or pentacyclic monoterpene indole alkaloids. Notably, rhynchophylline (**6**) and its epimer (**193**) at the C-7 position of the tetracyclic oxindole alkaloid were isolated from *Uncaria* species *U. rhynchophylla* (MIQ) Jackson, and *U. sinensis* (Oliv.) Havil.[128] Mitraphyline (**201**) is an oxindole alkaloid epimer and the most ubiquitous alkaloid found in *Uncaria* species.[24] Another famous compound in this family is corynoxine (**195**), which is also a secoyohimbane-type tetracyclic oxindole.[129,130]

Following the latest review,[131] around 20 SOAs from these genera have been isolated from 2023 to 2025 (Fig. 8). In 2023, Zhang and colleagues isolated uncarialines D (**240**) and E (**241**) from the stems of *U. rhynchophylla*.[132] These compounds feature a rare rearranged scaffold originating from corynantheine-type alkaloids with C-2/C-7 oxidation.[132] Liang *et al.* isolated macrophyllines C (**242**) and D (**243**) from *U. macrophylla*.[133] These are a pair of C-20 diastereomers with an additional 2-oxopropyl group compared to isorhyncophylline (**193**) and corynoxine (**195**), respectively.[133] Ramanathan and colleagues isolated isovillocarine D (**244**) from the leaves of *U. attenuate*,[134] while Ma and co-workers extracted uncarialin J (**245**) from *U. rhynchophylla*.[135] Zhao and colleagues isolated spirophyllines A–D (**246–249**, respectively) from *U. rhynchophylla*. These compounds, featuring a spiro[pyrrolidin-3,3′-oxindole] core and a rare isoxazolidine ring, were characterized by spectroscopic analysis and confirmed by X-ray crystallography.[136] In 2024, uncarpseudoindosides A (**250**) and B (**251**), novel stereoisomers of pseudoindoxyl monoterpene alkaloids, along with compound **252**, were isolated from *U. rhynchophylla*.[137] In 2025, monoterpene indole glycoalkaloids 19-*epi*-rhynchophylloside A (**253**) and 7-*epi*-rhynchophylloside A (**254**) were isolated from the hook-bearing branches of *U. rhynchophylla*.[138] Additionally, corynanthe-type alkaloids uncamarins A–D (**255–258**, respectively) were isolated from the leaves of *U. longiflora* by Tan and co-workers.[139]

2.4.3 SOAs from *Gelsemium*. *Gelsemium* is a genus of medicinal flowering plants in the Gelsemiaceae family, renowned for producing a variety of SOAs.[140] The compounds of this genus can be divided into six distinct categories including sarpagine-, yohimbine-, koumine-, humantenine-, gelsedine-, and gelsemine-type compounds (Fig. 9).

In 2014, Jin *et al.* summarized the phytochemistry of *Gelsemium* species, including 87 SOAs (**259–345**) (Fig. S2).[141] Among them, **259–305** are gelsedine-type alkaloids, **306–319** are gelsemine-type alkaloids, and **320–345** are humantenine-type alkaloids. Compounds from this genus have continued to be discovered in significant numbers between 2014 and 2022, as exemplified by SOAs **346–400** (Fig. S2).[142–158] After the latest review in 2023,[159] approximately 40 SOAs have been isolated from 2023 to 2025. In 2023, gelselegandine F (**401**) was isolated from the aerial parts of *G. elegans,* with its structure incorporating chlorine atoms.[160] Gelsegansymines A (**402**) and B (**403**) possessed a rare cage-like gelsedine skeleton, hybridized with a bicyclic monoterpenoid. The absolute configuration of the spiro carbon remained uncertain. In 2024,[161] gelseginedine A (**404**), gelseginedine B (**405**), N_4-aldehydegelsegine (**406**), 11-methoxy-N_4-aldehydegelsegine (**407**), 11-hydroxy-N_4-aldehydegelsegine (**408**), 14-hydroxy-N_4-aldehydegelsegine (**409**), 11,14-dimethoxy-N_4-aldehydegelsegine (**410**), 14-acetoxy-N_4-aldehydegelsegine (**411**), and 11-hydroxy-14-acetoxy-N_4-

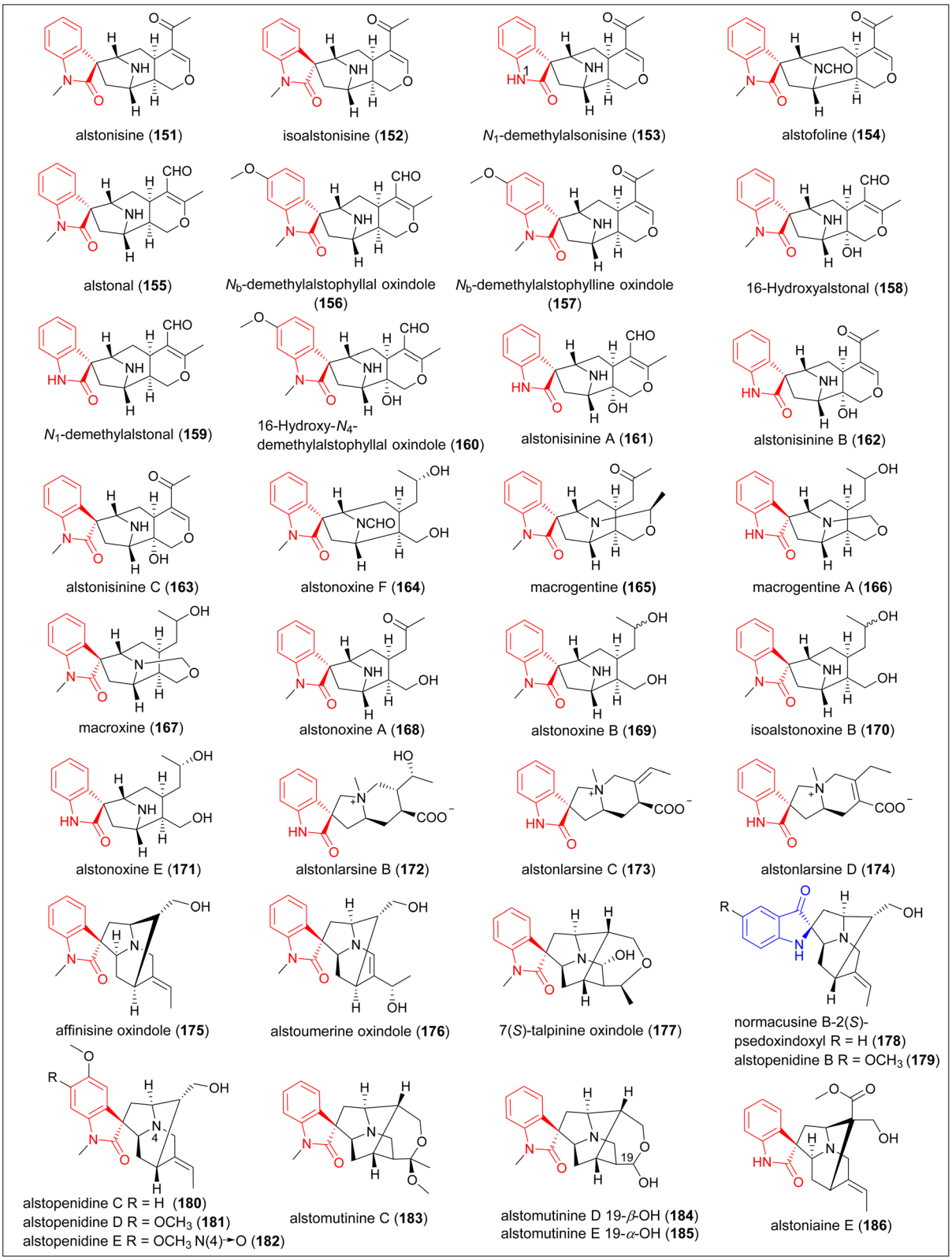

Fig. 7 SOAs from the *Alstonia* genus.

aldehydegelsegine (**412**) were isolated from *G. elegans*.[162] Notably, **404** and **405** represented the first examples of gelselegine-gelsedine type alkaloids, where two units are bridged by a double bond.[162] In 2025, gelseansdines A–H (**413**–**420**, respectively) were isolated from *G. elegans*.[163] Compound **413** was an N_4-deficient alkaloid, while gelseansdines E–H (**417**–

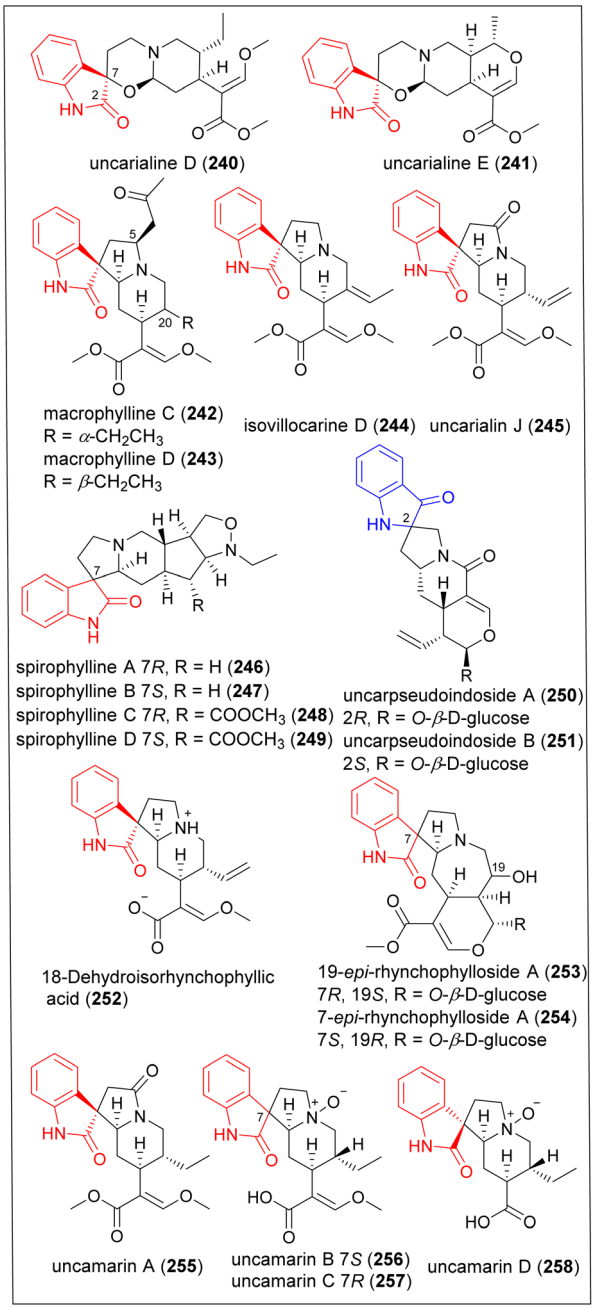

Fig. 8 SOAs from the *Mitragyna*/*Uncaria* genus (2023–2025).

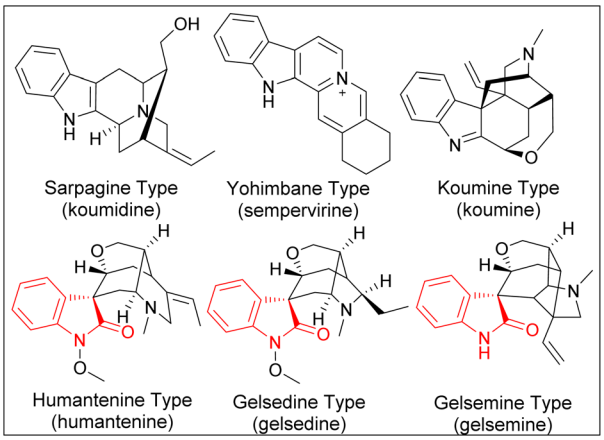

Fig. 9 Categories of compounds from *Gelsemium*.

420) represented a class of alkaloids polymerized with iridoid.[163] Li *et al.* reported 13 new toxic compounds (**421–423**, respectively) from *G. elegans*.[164] Among them, **421–427** are gelsedine-type alkaloids, **428–431** are humantenine-type alkaloids, and **432–433** are koumine-type alkaloids.[164] Eleganine A (**434**), a gelsenicine-related monoterpenoid indole alkaloid possessing an iridoid, was isolated from *G. elegans* by Wei *et al.*[165] Gelselegangmines A–D (**435–438**, respectively) are dimers connected by pyrrole rings, which were isolated by Lin *et al.*[166] Gelsepolycines A–F (**439–444**, respectively), six oligomeric monoterpenoid indole alkaloids with new skeletons, were isolated from the flowers of *G. elegans*.[167] The structure of **439** was confirm by X-ray diffraction. Compound **440** was a dimeric constructed from two gelsenicine moieties, while **441** was a dimeric gelsemium alkaloid consisting of a gelsenicine unit and a gelsemolenine B derivative. Compound **442** was formed from **441** and gelsenicine units. **443** was a similar trimeric analogue of **442**, with its difference being that its substructure was connected at a different position. Compound **444** was similar to **443** except that the α,β-unsaturated ketone moiety in **443** was replaced by a saturated ketone unit.[167]

2.4.4 SOAs from *Gardneria*. The genus *Gardneria*, belonging to the family Loganiaceae, are traditionally used as folk medicine.[168] In 1970, Sakai and co-workers reported the isolation of the dimer spirooxindole gardmultine (**445**) from *G. multiflora*, and its structure was determined in 1975 through spectroscopic analysis. Chitosenine (**446**) and voachalotine oxindole (**447**) were also isolated and proposed as the biogenetic precursors of **445**, which contain an azabicyclo[2.2.2]octane substructure and spirooxindole skeleton, in which the absolute configuration is *R* at C7.[169] In 2014, gardmutines A-F (**448–453**, respectively) and 18-hydroxy-chitosenine (**454**) were isolated from the aerial parts of *G. multiflora*,[170] and **448–453** were the first Gardneria alkaloids possessing a 7*S* configuration.[170] Gardmultimine A (**455**) was isolated from the leaves and stems of *G. multiflora* Makino by Zhang and co-workers.[171] In 2018, Zhang and co-workers isolated monoterpenoids **456–458** from the leaves and stems of *G. multiflora*.[172] In 2020, 19(*E*)-9,12-didemethoxy-11-methoxy-16-dehydroylchitosenine-17-*O*-β-D-glucopyranoside (**459**) was isolated from *G. ovata*.[168] In 2023, through MS/MS-based molecular networking-guided separation, gardistines E-G (**460–462**, respectively), gardneramine iminoether (**463**), chitosenine (**464**), 16-deoxychitosenine (**465**), and 3*H*-indole-3,1′(5′*H*)-[3,7]methanoindolizine-9′, 2″-oxirane (**466**) were discovered from the whole parts of *G. distincta*.[173]

2.4.5 SOAs from other plants. Tricyclic spirooxindole spirobrassinin (**536**) was extracted in 1987 from *Pseudomonas cichorii*-inoculated Japanese radish (*Raphanus sativus*). It contained two sulfur atoms and was the first phytoalexin identified with this ring system.[207] In 2001, Kutschy and co-workers confirmed that natural spirobrassinin has an *S* configuration

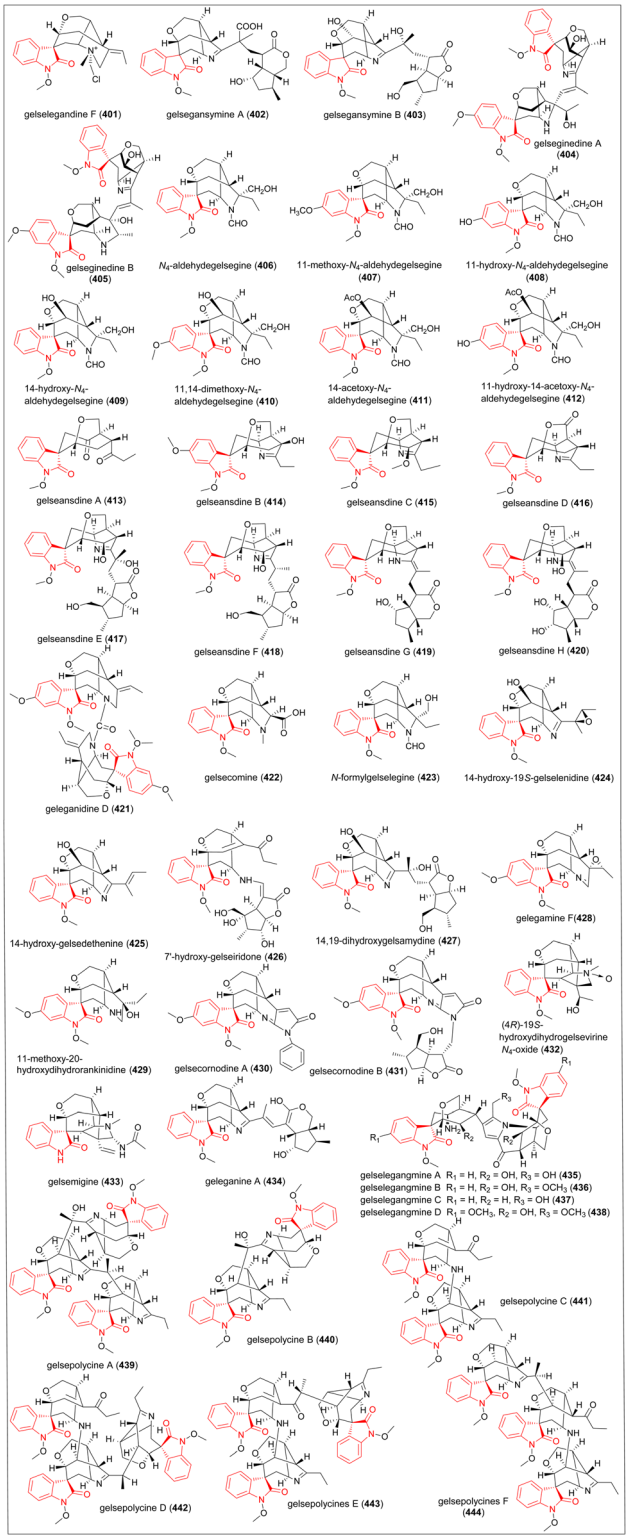

Fig. 10 SOAs from the *Gelsemium* genus (2023–2025).

based on X-ray crystallography.[208] In 1991, Jossang and co-workers extracted horsfiline (**538**) from the leaves of *Horsfieldia superba*, and determined its structure by spectral analysis.[209] Coerulescine (**539**), isolated by Colegate and co-workers in 1998, shares the same tricyclic skeleton as **538**. The stereochemistry of its spiro linkage remains undefined. It was chemically synthesized in earlier studies aimed at synthesizing horsfiline before its natural discovery.[210] Elacomine (**540**) is a hemiterpene spirooxindole alkaloid isolated from the roots of the shrub *Elaeagnus commutata* (Elaeagnaceae).[211] Moreover, tricyclic compounds including 3*S*,12*S*, (−)-perispirooxindole B (**541**) and 3*S*,12*S*, (−)-perispirooxindole B (**542**) were isolated from the extracts of the whole bodies of *Periplaneta americana*.[212] Along with **541** and **542**, tetracyclic spirooxindoles 3*S*, (−)-perispirooxindole A (**543**) and 3*S*, (−)-perispirooxindole A (**544**), which comprise pyrrole-2-carboxaldehyde derivatives, were also isolated.[212] Besides, flueindoline C (**545**) was isolated from the fruits of *Flueggea virosa* by Xie *et al.*,[213] and daturametelindole B (**546**) and C (**547**), with unconfirmed absolute configurations, were isolated from the seeds of *Datura metel* by Liu *et al.*[214] Additionally, **548** and **549** are enantiomers containing unusual dihydrothiopyran and 1,2,4-thiadiazole rings, which were isolated from the root of *Isatis indigotica* by Shi and co-workers.[215] Wincaline A (**550**) was isolated from the leaves of *Winchia calophylla*, and its structure was determined by X-ray diffraction analysis.[216]

Kopsiyunnanine B (**551**) was a pentacyclic spirooxindole isolated from the aerial part of Yunnan *Kopsia arborea*, and was a corynanthe-type oxindole alkaloid rearranged by D ring rotation.[217] Trigolutes A–D (**552–555**, respectively) were isolated from *Trigonostemon lutescens*.[218] Their structures and relative configurations were elucidated by X-ray crystallography.[218] In 2025, the total synthesis of **553** and **555** was accomplished *via* one-pot sequential allylation.[219] Palmirine (**556**) was isolated from *Hamelia Patens* Jacq, which has a similar structure to isopteropodine (**206**) but contains a –OCH_3 group at C-10.[220] The hexacyclic spirooxindole strychnofoline (**557**) was isolated in 1978 from *Strychnos usambarensis,* and its first enantioselective synthesis was conducted by Xu *et al.*[221]

2.5. Animal-derived SOAs

2.5.1 Orbicularisine. In 2017, Goudou and colleagues isolated orbicularisine (**558**, Fig. 13), a sulfur-oxidizing metabolite from the tropical bivalve *Codakia orbicularis*. It was found to feature a spiro-indolofuranone fused to a thiazine skeleton containing a single stereocenter, making this compound racemic.[222]

2.5.2 Blapspirooxindoles. In 2024, blapspirooxindoles A–C (**559–561**, respectively) were isolated from the medicinal insect *Blaps japanensis*. They contain a unique spiro[chromane-4,3′-indoline]-2,2′-dione motif and exist as racemic mixtures.[223]

3. Biological activities of SOAs

Given the diverse structures illustrated above, which encompass the arrangement of spiro rings fused with other moieties and specific substituents, it is unsurprising that SOAs exhibit a wide range of bioactivities (Table 1). Besides, the conformational constraints imposed by the spiro carbon when binding to receptors can also enhance their specificity and potency.[224]

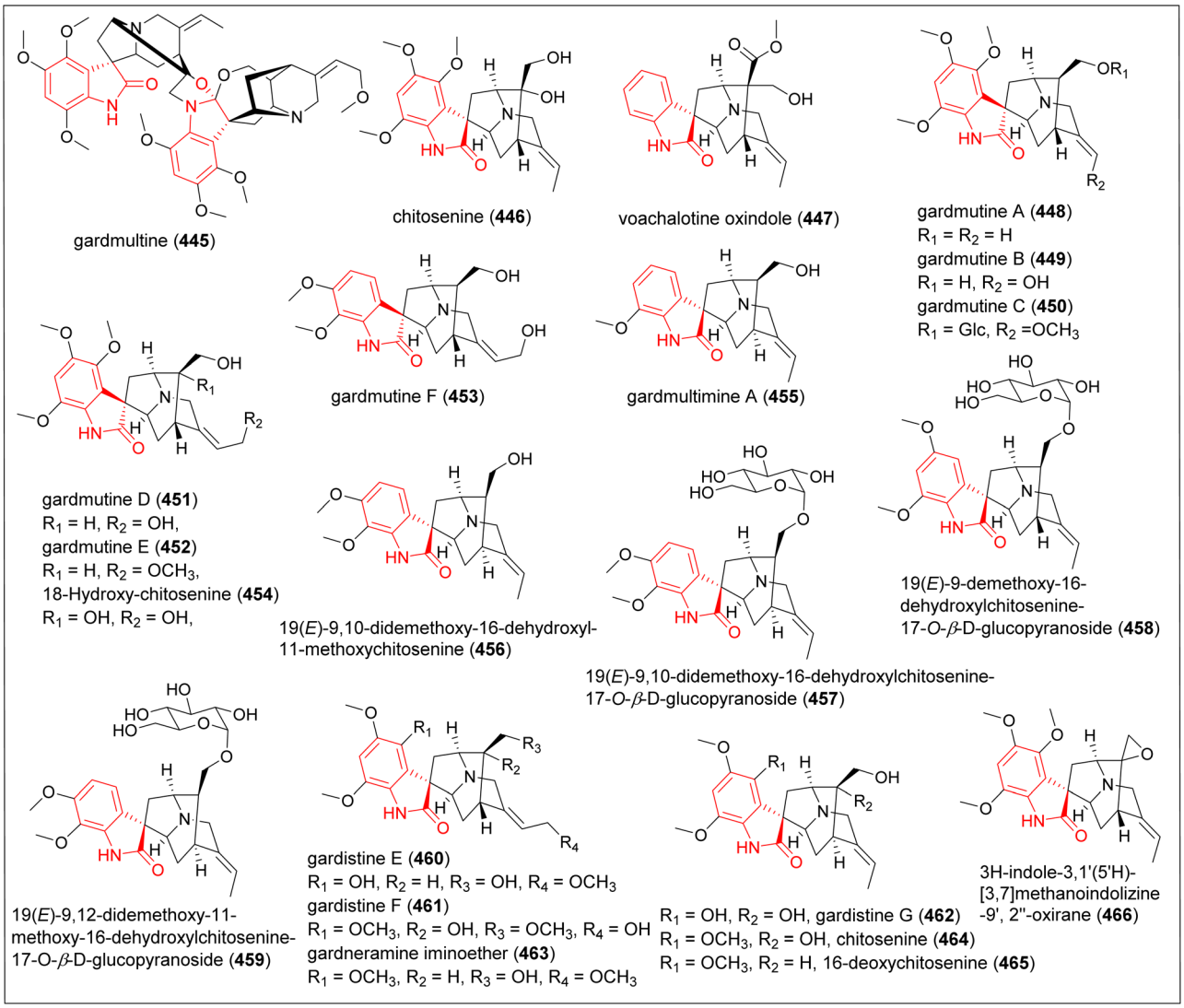

Fig. 11 SOAs from the *Gardneria* genus.

3.1. Antimicrobial activity

Amoenamide C (**70**) shows potent antibacterial activity against *P. aeruginosa* with an MIC value of 1 μg mL^{-1}, and specific activity against *F. oxysporum* and *Thielaviopsis basicola*, with an MIC value of 8 μg mL^{-1}.[20] Sclerotiamide (**55**) has been reported to display moderate antibacterial activity against *Escherichia coli*, *Micrococcus luteus*, *P. aeruginosa*, and *Ralstonia solanacearum*, with MIC values of 4, 4, 8, and 8 μg mL^{-1}, respectively.[20] It is notable for being the first non-peptide-based natural product activator of the caseinolytic protease P (ClpP), which plays an essential role in bacterial homeostasis.[225] Notoamide B (**49**), which lacks only the C-10α-oriented secondary hydroxy group, fails to activate EcClpP, indicating that the C-10α-hydroxy motif is essential. Additionally, an altered geometry also fails to activate EcClpP, highlighting the importance of the three-dimensional character imparted by the spiroindolinone moiety.[225] Voagafricines A (**500**) and G (**506**) exhibit potent antibacterial effects against ESBL-producing *E. coli* 298 and 140 by targeting biofilm formation, with an MIC value of 12.5 μg mL^{-1}.[18] Gelselegandine B (**387**) shows antibacterial activity against *S. typhi* with a minimal inhibitory concentration (MIC) value of 6.25 μg mL^{-1}.[154]

In addition to antibacterial activity, sclerotiamide (**55**) also exhibits growth-inhibitory activity toward the fungus *Alternaria alternata*.[20] Citrinadin A (**84**) and chrysogenamide A (**21**), which are derived from *P. citrinum*, also show potential as antifungal agents. Through a co-culture strategy and mass spectrometry imaging (MSi), these compounds have been found to reduce the radial growth of *P. digitatum* by 48% and 61%, respectively.[19]

SOAs are also recognized as antiviral agents.[226] Enantiomers **548** and **549** extracted from the root of *I. indigotica* by Shi and coworkers show similar antiviral activities against the herpes simplex virus 1 (HSV-1).[215] Macrophylline D (**243**), isorhynchophylline (**193**) and corynoxine (**195**) showed weak anti-HIV activities with EC_{50} values of 11.31 ± 3.29 μM, 18.77 ± 6.14 μM and 30.02 ± 3.73 μM, respectively.[133]

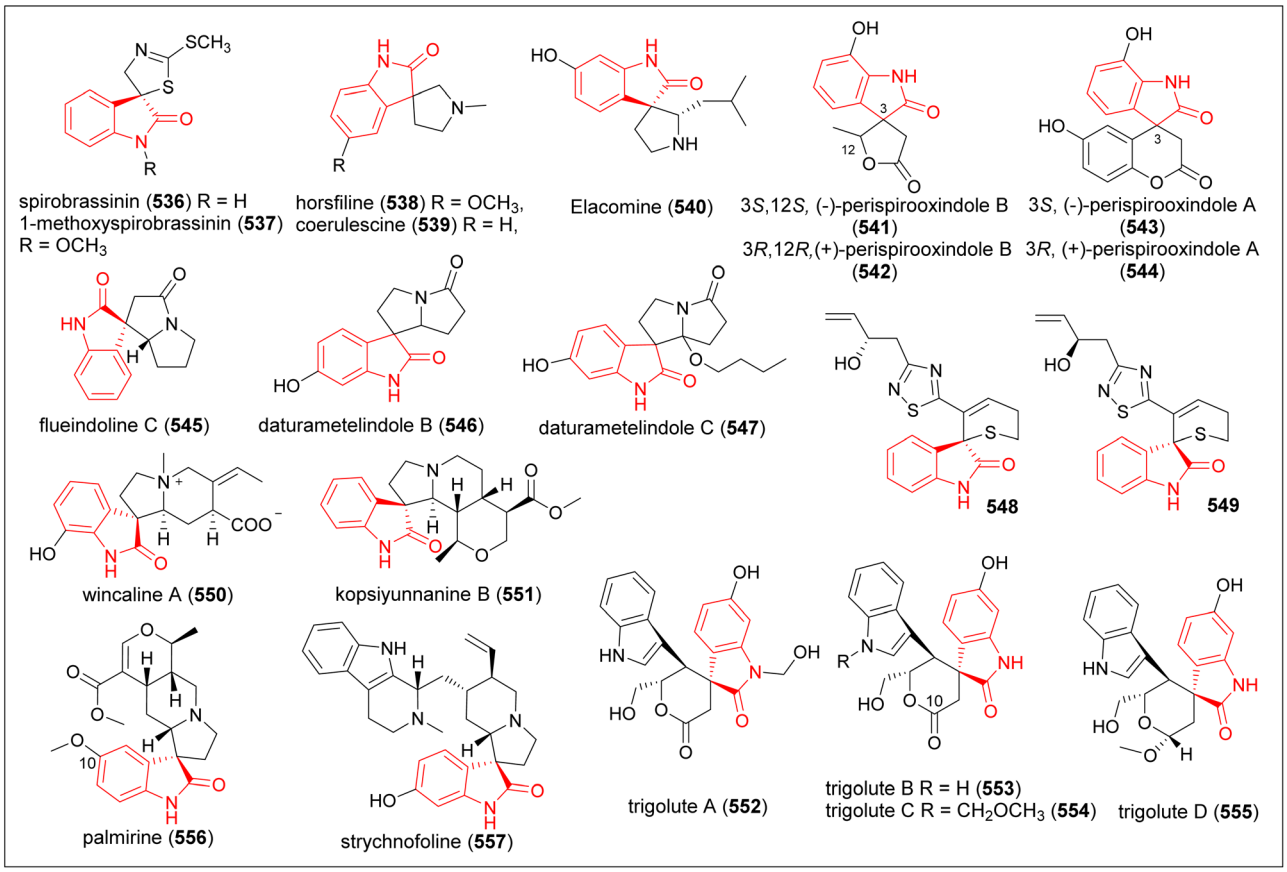

Fig. 12 Other plant-derived SOAs.

3.2. Insecticidal and anthelmintic activities

Paterson and co-workers reported that brevianamide A (**14**) exhibited effective antifeedant properties against lepidopterous larvae of *Spodoptera frugiperda* (fall armyworm) and *Heliothis virescens* (tobacco budworm).[227] Sclerotiamide (**55**) and notoamide B (**49**) exhibit remarkable insecticidal activity against first instar larvae of the cotton bollworm *Helicoverpa armigera*, with mortality rates of 83.2% and 70.5%, respectively.[20] Compound **55** can also induce significant mortality and physiological effects in the corn earworm *H. zea*.[64] Furthermore, paraherquamides show toxicity against the hemipteran *Oncopeltus fasciatus* Dallas (milkweed bug).[21] Among them, paraherquamide E (**27**) is the most active compound (LD_{50} 0.089 μg per nymph), followed by paraherquamide A (**23**) (LD_{50} 0.32 μg per nymph). Interestingly, the presence of a hydroxy group in this molecule reduces its insecticidal activity, as seen by the reduced potency of **23** compared to **27**. Conversely, paraherquamide B (**24**), which lacks a methyl group at C-14, shows the least activity (LD_{50} 16.54 μg per nymph), suggesting that the alkyl substation is crucial for insecticidal activity.[21]

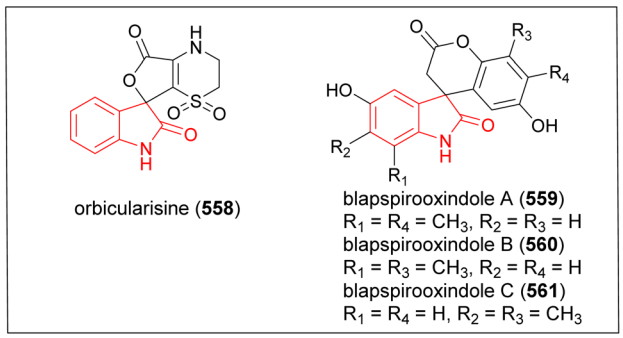

Fig. 13 Animal-derived SOAs.

Beyond agricultural pest control, SOAs also affect parasitic organisms. **23** also demonstrates significant anthelmintic activity. It has shown high efficacy in treating infections caused by the parasitic nematode *Trichostrongylus colubriformis* in gerbils,[228] as well as common gastrointestinal nematodes in sheep.[229] Especially, it shows high efficacy (>98% reduction) as a single oral treatment at dosages >0.5 mg kg^{-1} against adult *Haemonchus contortus*, *Ostertagia circumcincta*, *T. axei*, *T. colubriformis* and *Cooperia curticei*, as well as the L4 stage of *Cooperia* spp.[229] **23** has also been tested against common gastrointestinal nematodes of dogs, with good efficacy (91%) observed only against *Strongyloides stercoralis* at a high dosage level.[230] Additionally, it has demonstrated efficacy against the adult stages of nine common gastrointestinal and lung nematodes of calves, with a 0.5 mg kg^{-1} dosage being 95% or more effective against *H. placei*, *O. ostertagi*, *C. oncophora*, and *Dictyocaulus viviparus*.[231] Its mechanism of action was investigated

Table 1 Biological activities of SOAs

Reported biological activity	Congener(s)	Efficacy	Ref.
Antimicrobial activities	Amoenamide C (**70**)	Against *P. aeruginosa* with an MIC value of 1 μg mL^{-1} Against *F. oxysporum* and *T. basicola* with MIC value of 8 μg mL^{-1}	20 and 225
	Sclerotiamide (**55**)	Against *E. coli*, *M. luteus*, *P. aeruginosa* and *R. solanacearum* of MIC values of 4, 4, 8, and 8 μg mL^{-1}, respectively	
	Voagafricines A (**500**) and G (**506**)	Against ESBL producing *E. coli* 298 and 140, with an MIC value of 12.5 μg mL^{-1}	18
	Gelselegandine B (**387**)	Against *S. typhi* with a minimal inhibitory concentration (MIC) value of 6.25 μg mL^{-1}	154
	Sclerotiamide (**55**)	Exhibits growth-inhibitory activity toward the fungus *Alternaria alternata*	20
	Citrinadin A (**84**)	Reduces 48% of *P. digitatum* radial growth	19
	Chrysogenamide A (**21**)	Reduces 61% of *P. digitatum* radial growth	
	548 and **549**	Against the herpes simplex virus 1 (HSV-1) with IC_{50} values of 33.33 and 25.87 μM	215
	Macrophylline D **(242)**	Anti-HIV activities with EC_{50} values of 11.31 ± 3.29 μM	133
	Isorhynchophylline (**193**)	Anti-HIV activities with EC_{50} values of 18.77 ± 6.14 μM	
	Corynoxine (**195**)	Anti-HIV activities with EC_{50} values of 30.02 ± 3.73 μM	
Insecticidal and anthelmintic activities	Sclerotiamide B (**54**)	Against *H. armigera* with mortality rates of 70.2%	20
	Brevianamide A (**14**)	Against both *S. frugiperda* and *H. virescens*	227
	Sclerotiamide (**55**)	Against *H. armigera* with mortality rates of 83.2% Induces significant mortality and physiological effects against the corn earworm *H. zea*	64
	Notoamide B (**49**)	Against *H. armigera* with mortality rates of 70.5%	20
	Paraherquamide E (**27**)	Toxicity against *O. fasciatus* with a LD_{50} of 0.089 μg per nymph	21
	Paraherquamide A (**23**)	98–100% effective against immature *T. colubriformis* in gerbil when given as single oral doses of 1.56 mg kg^{-1} and above; highly efficacious against adult *H. contortus*, *O. circumcincta*, *T. axei*, *T. colubriformis* and *C. curticei*, and the L4 stage of *Cooperia* spp.; against the common gastrointestinal nematodes of dogs; against the adult stages of nine common gastrointestinal and lung nematodes of calves	23 and 228–231
	Caboxine A (**516**)	Antiparasitic effects at a dose of 100 μg mL^{-1}, and was more toxic against L. infantum than against *T. cruzi*	204
	Caboxine B (**517**)	Against *T. cruzi* with an ED_{50} value within the upper range of the positive control nifurtimox	10
	Cathagine B (**510**)	Moderate anti-malarial activity against *Plasmodium falciparum* 3D7	202
	Penicitrimicins A-G (**102–108**)	Antimalarial activity against *Plasmodium falciparum* Dd2 strain, with EC_{50} values spanning 0.9–2.4 μM	91
Uncarine D (**210**)	Anti-plasmodial with IC_{50} 17.03 μg mL^{-1}	126	
Cytotoxicity	Norhumantenine A (**349**)	Against HL-60, SMMC-7721, A-549 cells with IC_{50} values of 8.5 μM, 7.3 μM, and 9.3 μM, respectively	142

Table 1 (*Contd.*)

Reported biological activity	Congener(s)	Efficacy	Ref.
	Uncarine D (**210**)	High cytotoxicity, with IC_{50} values ranging from 30 to 40 μg mL^{-1} in SK-MEL, KB, BT-549, SK-OV-3 and VERO cell lines	233
	Waikikiamide C (**83**)	Against cancer cell lines HT1080 (IC_{50} 1.135 μM), PC3 (IC_{50} 1.805 μM), Jurkat (IC_{50} 1.79 μM), and A2780 (IC_{50} 1.127 μM)	80
	Spirophylline C (**248**)	Against human embryonic kidney (HEK) 293T cells with IC_{50} value 9.1 ± 0.69 μM	136
	Ervahainine A (**492**)	Growth inhibitory effects against HepG2 cells and HepG2/ADM cells with IC_{50} values of 12.47 ± 0.24 and 17.68 ± 0.31 μM, respectively	193
	Gardmutines D (**451**) and E (**452**)	Cytotoxic to HeLa (IC_{50} 4.52 ± 0.42 μM, and 2.52 ± 0.12 μM, respectively), MCF-7 breast (8.10 ± 0.36 μM, and 1.67 ± 0.21 μM, respectively), and SW-480 colon cancer cell lines (1.37 ± 0.10 μM, and 3.01 ± 0.14 μM, respectively)	170
	Spirobrassinin (**536**)	Antiproliferative effect against T-Jurkat leukemic cells	253
	Gelsemine (**306**)	IC_{50} values at 24 h were 340.3 mmoL l^{-1} in M1-treated HepG2 cells, 338.9 mmol L^{-1} in M1-treated HeLa cells, 107.1 mmol L^{-1} in M2-treated HepG2 cells, 169.8 mmol L^{-1} in M2-treated HeLa cells	25
	Penioxalamine A (**22**)	Showed moderate cytotoxicity against HL-60 cell line	16
	Spirotryprostatins A (**109**) and B (**110**)	Inhibited the cell cycle progression of tsFT210 cells at the G2/M phase with IC_{50} values of 197.5 μM and 14.0 μM, respectively	92
	Spirotryprostatins E (**113**)	Susceptivity to MOLT-4, HL-60, and A549 cells	94
	Citrinadin C (**89**)	Against human liver cancer cell line MHCC97H, with IC_{50} value of 16.7 μM	14
DNA Strand Scission	Javaniside (**467**)	Exhibited moderate DNA strand scission activity ranging from 10% conversion of supercoiled (form I) DNA to nicked, circular (form II) DNA at 10 mM in the presence of 20 mM Cu^{2+}	176
Anti-inflammatory	Rhynchophylline (**6**)	Increment of TLR2, TLR4, nuclear NF-κB and MyD88 expressions at 24 h after ischemia Upregulating miR-21–5p and miR331–5p	235 and 241
	Mitraphylline (**201**)	Inhibited around 50% of the release of interleukins 1a,1b, 17, and TNF-a Reduced almost 40% of the production of interleukin 4 (IL-4)	26
	Gelsenicine (**263**)	ED_{50} of 36–50.6 mg for inflammatory pain in human subjects weighing 60 kg	237
	Geleganimine B (**366**)	Suppresses lipopolysaccharide-induced proinflammatory factors in BV2 microglial cells with an IC_{50} value of 10.2 μM	238
	Gelsegansymines A (**402**) and B (**403**)	Exhibit the significant inhibitory effect on the osteoclast genesis induced by RANKL	161
	Gelsepolycines C (**441**) and D (**442**)	Inhibited the release of the key pro-inflammatory cytokines TNF-α and IL-6 at a concentration of 5 μM	167
	Versicoine N (**136**)	Against p65 expression and its nuclear translocation, along with the inhibition toward phosphorylation of IKK/IκB in NF-κB signaling pathway. Inhibits NLRP3 inflammasome activation and its related proteins, including caspase 1, pro-caspase1, IL-1β and pro-IL-1β	104

Table 1 (*Contd.*)

Reported biological activity	Congener(s)	Efficacy	Ref.
Novel Histamine H3 receptor ligands	PF1270A (**86**), B (**87**) and C (**88**)	Displayed high affinity for rat H3R and human H3R. Acted as potent agonists with the EC_{50} values of 0.12, 0.15 and 0.20 mM, respectively	83
Central nervous system	Chrysogenamide A (**21**)	Protective effect on neurocytes against oxidative stress-induced cell death	19
	Gelsemine (**306**)	Inhibits the CUMS-induced activation of NLRP3-inflammasome pathways and downregulated CREB and BDNF overexpression in the hypothalamus	254
	Rhynchophylline (**6**)	Attenuates migraine in trigeminal nucleus caudalis in nitroglycerin-induced rat model by suppressing MAPK/NF-kB pathway	239
	Uncamarins B (**256**) and D (**258**)	Show anti-amyloidogenic activities with uncamarins D (77.91% ± 0.22%) and B (70.40% ± 1.93%)	139
	29-*N*-Demethylparaherquamide K (**39**) and 16-deoxo-paraherquamide J (**40**)	Rescue PC12 cells by reducing the formation of Aβ aggregates and increasing Aβ monomers	15
Cardiovascular system treatment	Cycloexpansamine A (**82**)	Effectively treats type 2 diabetes mellitus and obesity, showing an IC_{50} value of 27.6 μM	11
	Isorhynchophylline (**106**)	Enhances Nrf2 and inhibits MAPK pathway in cardiac hypertrophy	250
Protective against nephrotoxicity	Gelsemine (**306**)	Against cisplatin-induced nephrotoxicity by improving redox status	252

by Zinser in 2002, who proposed that its anthelmintic activity is due to the blockade of cholinergic neuromuscular transmission.[23] According to a Ca^{2+} flux assay, 2-deoxo-paraherquamide blocked nicotinic stimulation of cells expressing a3 ganglionic (IC_{50} 9 μM) and muscle-type (IC_{50} 3 μM) nicotinic cholinergic receptors.[23] Caboxine A (**516**) had significant antiparasitic effects at a dose of 100 μg mL^{-1}, and was more toxic against *L. infantum* than against *T. cruzi*.[204] Caboxine B (**517**) was active against *T. cruzi* with an ED_{50} value within the upper range of the positive control nifurtimox.[204] Cathagine B (**510**) showed moderate anti-malarial activity against *Plasmodium falciparum* 3D7.[202] Penicitrimicins A–G (**102–108**, respectively) exhibited good biocompatibility (<5% hemolysis and >80% cell viability), while displaying obvious antimalarial activity against *P. falciparum* Dd2 strain, with EC_{50} values spanning 0.9–2.4 μM.[91]

3.3. Cytotoxicity

Cyanogramide (7) displays cytotoxic activity against human glioma U251 and U87MG cells with IC_{50} values of 2.0–7.2 μM.[232] Additionally, it efficiently reverses multidrug resistance in K562/A02, MCF-7/Adr, and KB/VCR cells at a concentration of 5 μM.[37] The fungal SOAs notoamides A (**47**) and B (**49**) show moderate cytotoxicity against HeLa and L1210 cells, with IC_{50} values of 22–52 mg mL^{-1}.[10] Aculeaquamide A (**39**) and paraherquamide E (**27**) show cytotoxicity against Bel-7402, with IC_{50} values of 3.3 and 1.9 μM, respectively.[55] Citrinadin A (**84**) exhibits cytotoxicity against murine leukemia L1210 and human epidermoid carcinoma KB cells, with IC_{50} values of 6.2 and 10 μg mL^{-1}, respectively.[81] Plant-derived SOAs, such as norhumantenine A (**349**), display cytotoxicity against HL-60, SMMC-7721, A-549 cells with IC_{50} values of 8.5 μM, 7.3 μM, and 9.3 μM, respectively.[142] Uncarine D (**210**) exhibits high cytotoxicity, with IC_{50} values ranging from 30 to 40 μg mL^{-1} in SK-MEL, KB, BT-549, SK-OV-3 and VERO cell lines.[233] Waikikiamide C (**83**) shows antiproliferative activities against the HT1080 (IC_{50} 1.135 μM), PC3 (IC_{50} 1.805 μM), Jurkat (IC_{50} 1.79 μM), and A2780 (IC_{50} 1.127 μM) cancer cell lines.[80] Spirophylline C (**248**) inhibits the currents of Kv1.5 expressed in human embryonic kidney (HEK) 293T cells in a dose-dependent manner, with an IC_{50} value of 9.1 μM and Hill coefficient of 2.39.[136] Ervahainine A (**492**) exhibited growth inhibitory effects against HepG2 cells and HepG2/ADM cells with IC_{50} values of 12.47 ± 0.24 and 17.68 ± 0.31 μM, respectively.[193] Gardmutines D (**451**) and E (**452**) were cytotoxic to HeLa (IC_{50} values of 4.52 ± 0.42 μM and 2.52 ± 0.12 μM, respectively), MCF-7 breast (IC_{50} values of 8.10 ± 0.36 μM and 1.67 ± 0.21 μM, respectively), and SW-480 colon cancer cell lines (IC_{50} values of 1.37 ± 0.10 μM and 3.01 ± 0.14 μM, respectively).[170]

The cytotoxicity of spirotryprostatins A (**109**) and B (**110**) was first studied by Cui *et al.* in 1996, which were reported to inhibit mammalian cell cycle progression at the G2/M phase in tsFT210 cells with low IC_{50} values.[92,93] In 2005, Wang and co-workers indicated that due to steric hindrance, spirotryprostatins poorly fit into the MDM2 cleft, failing to block the interaction between P53 and MDM2, which resulted in weak anti-cancer activity.[5] However, the spiro(oxindole-3,3′-pyrrolidine) core structure can mimic the p53 side chain in both hydrogen-bonding formation and hydrophobic interactions with MDM2, and further structural simplification led to the identification of

spiro-pyrrolidinyl MI-888 as a potent anticancer drug.[5] More synthetic and modified SOAs show anticancer potentials, and Yu and co-workers have reviewed SOAs as promising scaffolds for anticancer agents.[234]

3.4. Anti-inflammatory

The combination of gastrodin and rhynchophylline (**6**) alleviated the activation of inflammasomes and the down-regulation of miR-21-5p and miR-331-5p caused by middle cerebral artery occlusion.[235] Mitraphylline (**201**) regulates the release of inflammatory mediators by affecting inflammation-related signalling pathways. It inhibits the transcription of NF-kB in cell cultures and restrains the release of IL-1a, IL1b, IL-17 and TNF-α, and the production of IL-4.[26,236] Gelsenicine (**263**) is reported to attenuate inflammation at doses far below LD_{50} (95% confidence interval at 100–200 mg kg^{-1}).[237] Geleganimine B (**366**) exhibited anti-inflammatory activity indirectly by suppressing lipopolysaccharide-induced proinflammatory factors in BV2 microglial cells with an IC_{50} value of 10.2 μM.[238] Gelsegansymines A (**402**) and B (**403**) at 5 μmol L^{-1} exhibited the significant inhibitory effect on osteoclast genesis induced by RANKL.[161] Gelsepolycines C (**441**) and D (**442**) effectively inhibited the release of the key pro-inflammatory cytokines TNF-α and IL-6 at a concentration of 5 μM.[167] Versicoine N (**136**) shows significant inhibition against p65 expression and its nuclear translocation, along with the inhibition toward phosphorylation of IKK/IκB in the NF-κB signaling pathway.[104] In addition, versicoine N (**136**) also inhibited NLRP3 inflammasome activation and its related proteins, including caspase 1, pro-caspase1, IL-1β and pro-IL-1β.[104]

3.5. Central nervous system treatment

The metabolic pathways responsible for anti-inflammatory effects are closely linked to antioxidant effects and apoptosis regulation in the nervous system. SOAs have shown great importance in the treatment of nervous system conditions. Rhynchophylline (**6**) demonstrates neuroprotective properties by inhibiting MAPK/NF-kB channels, thereby reducing oxidative stress in a nitroglycerin-induced migraine rat model.[239] Additionally, **6** can alleviate early brain injury after subarachnoid hemorrhage by activating the nuclear factor E2-related factor Nrf2/ARE pathway, which resists inflammation and apoptosis in the brain.[240] In models of permanent middle cerebral artery occlusion (pMCAO), **6** not only ameliorated neurological deficits, infarct volume and brain edema, but also regulated the Akt/mTOR pathway, offering protection against ischemic damage.[241] Furthermore, **6** and its isomers are reported to alleviate ischemia-induced neuronal damage by allosterically inhibiting NMDAR binding to the NMDA recognition site to exert noncompetitive antagonism.[128] Besides brain and nerve cells protection, **6** shows an antidepressant effect by activating the BDNF-tropomyosin receptor kinase (TrkB) signaling pathway and inhibiting EphA4 signaling.[242] It has also been evaluated to be an effective therapeutic for neurodegenerative diseases, including Alzheimer's disease[243] and Parkinson's disease.[244]

Uncamarins B (**256**) and D (**258**) show anti-amyloidogenic activities, with uncamarin D showing 77.91% ± 0.22% and B 70.40% ± 1.93% inhibition. Notably, uncamarin D (**258**) also docked *in silico* to the active site of acetylcholinesterase, a key enzyme targeted in Alzheimer's disease (AD) therapy, thereby highlighting its potential for multitargeting in AD.[139]

The fungus-derived 29-*N*-demethylparaherquamide K (**39**) and 16-deoxo-paraherquamide J (**40**) show anti-Alzheimer's disease properties. These compounds do not block Aβ aggregate-induced toxicity but instead rescue PC12 cells by reducing the formation of Aβ aggregates and increasing Aβ monomers.[15]

In addition to the aforementioned antidepressant effect, gelsemicine (**262**) and gelsevirine (**307**) exhibit produce potent anxiolytic effects upon acute treatment at doses significantly lower than their LD_{50}, without significant antidepressant activity.[245]

3.6. Other bioactivities

As the primary active ingredient of *Uncaria* that has received the most research and attention, rhynchophylline (**6**) and isorhynchophylline (**193**) show great potential not only in nervous system treatment. **193** has shown protective effects against myocardial strain caused by hypertension, including lowering blood pressure, reducing heart rate, and decreasing myocardial oxygen consumption.[246–248] It also shows anti-arrhythmic effects,[249] and can be used to treat cardiac hypertrophy.[250] Interestingly, compounds from the same source show completely opposite activities. Rhynchophylline and isorhynchophylline display anticoagulant activities, while corynoxeine shows procoagulant activity.[251]

Besides the therapeutic effects of rhynchophylline (**6**) and isorhynchophylline (**193**) on cardiovascular diseases, cycloexpansamine A (**82**) is a promising therapeutic target to effectively treat type 2 diabetes mellitus and obesity by inhibiting the activity of protein tyrosine phosphatase 1B.[11] Gelsemine (**306**) is a protective agent against cisplatin-induced nephrotoxicity by improving the redox status.[252]

3.7. Biological activities of SOAs summary

Broadly speaking, SOAs offer advantages in bioactivities. According to the latest chemical investigation of *G. elegans* by Li *et al.*, toxic gelsemium alkaloids are primarily those with a spiroindole structure.[164] However, there are cases where SOAs lack the biological activity observed in their homologous counterparts.[117,173] In fact, the three-dimensional structure of spirocycles allows more pronounced and traceable interactions with the chiral binding sites of protein targets compared to their flat sp^2-hybridized analogs.[255] For instance, the spiro(-indoline-3,3′-pyrrolidine) core structure can mimic the p53 peptide by replicating key hydrogen-bonding and hydrophobic interactions with the MDM2 protein.[5] However, the relative conformational flexibility of non-SOAs enables interactions with a broader range of biological targets. The co-evolution of spiro- and non-spiro indole alkaloids likely reflects a diversified

chemical defence strategy, driven by their distinct yet complementary physiological functions.

4. Distinct biosynthetic mechanisms for spiro-formation

4.1. Cytochrome P450 monooxygenase-based

4.1.1 Cyanogramide. The biosynthetic gene cluster (BGC) of cyanogramide (**7**) was identified in *A. cyanogriseus* WH1-2216-6 and characterized to contain ten genes *cyaA-I* and *orf1* (Fig. 14A) by successful heterologous expression in *Streptomyces coelicolor* YF11. However, only eight genes are necessary and sufficient for the biosynthesis of **7**.[256] The β-carboline scaffold of **7** is constructed by three enzymes, CyaA (fatty acid CoA ligase), CyaB (Pictet-Spengler cyclase), and CyaC (glutamate decarboxylase), following the biosynthetic strategy of marinacarbolines *via* a Pictet–Spengler cyclization pathway to form marinacarboline C (**562**) (Fig. 14B).[257–259] After that, the functions of five tailoring enzymes were characterized by *in vivo* gene inactivation and feeding experiments to enable the proposal of a concise biosynthetic pathway for **7** (Fig. 14B). Briefly, marinacarboline C (**562**) was *N*-methylated by CyaF to yield marinacarboline E (**563**),[260] which was converted to cyanogramide B (**564**) by the cytochrome P450 monooxygenase CyaI to form the unusual imidazolidin-4-one group. After CyaE-catalyzed *O*-methylation of **562**, the product cyanogramide C (**565**) was oxidized by CyaG to generate a double bond (E $\Delta^{1',2'}$) in cyanogramide D (**566**). Additionally, the CyaI-catalyzed conversion of **563** to **564** was proposed to involve both enzymatic and nonenzymatic steps, leading to the formation of enantiomeric mixtures of cyanogramides, including **564–566** and **7**.

Notably, the cytochrome P450 enzyme CyaH was biochemically characterized to catalyze the formation of the unique spirooxindole skeleton in **7** from **566**, which can accept both enantiomers but displayed a clear preference for **566** (12*S*). Two potential reaction routes were proposed for spirooxindole formation mediated by CyaH, *i.e.*, a carbocation route and an epoxidation route. Due to the lack of an intrinsic driving force to open an epoxy intermediate, spirooxindole formation is suggested to be more favorable *via* the carbocationic route. In the carbocationic route, electrophilic attack of compound I (Fe^{IV}=O) to C9 of substrate **566** is proposed to form a free radical at the C-1 position. Subsequently, one electron is rapidly transferred from the C-1 to Fe^{IV} ion to form a carbocation at C-1, driving a semipinacol-type rearrangement by the migration of C-10 to C-1 to yield the spirooxindole in **7**, accompanied by the release of Fe^{III} (Fig. 14C).[256] According to the DFT calculations carried out by Wang and co-workers in 2021, the epoxide route cannot compete with the carbocationic route due to its significantly higher barrier of 5 kcal mol^{-1}. In addition, the delocalized charge-shift bond facilitates the formation of the spirooxindole mainly through elongation of the C1–C9 bond to eliminate the

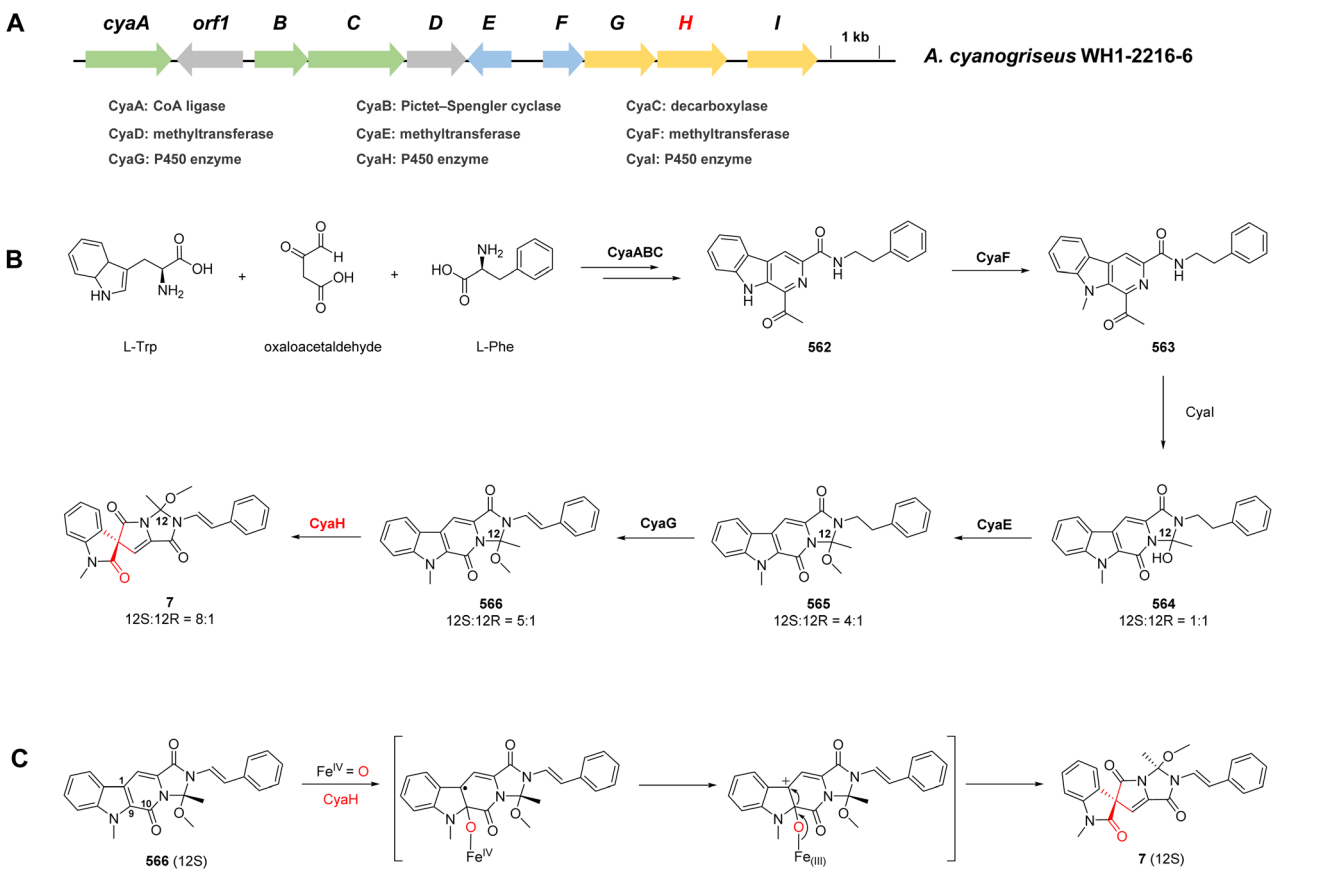

Fig. 14 Biosynthesis of cyanogramides. (A) BGC of cyanogramides in *A. cyanogriseus* WH1-2216-6. (B) Proposed biosynthetic pathway of cyanogramides. (C) Putative mechanism for spirooxindole formation catalyzed by CyaH.

aromatization of the tricyclic beta-carboline and partial cleavage of the C9–C10 bond by strong electrostatic interaction in the carbocationic route.[261]

4.1.2 Spirotryprostatins B and G. The BGCs of spirotryprostatins and fumitremorgins were first identified from *A. fumigatus* AF293, and later from *A. fumigatus* A1163, *A. fumigatus* BM939 and *N. fischeri* NRRL181,[262] all of which contained conserved 9 genes (Fig. 15A). Several enzymes in the biosynthetic pathway were analyzed, including a nonribosomal peptide synthetase (NRPS) FtmA responsible for the formation of brevianamide F (**567**) from L-tryptophan and L-proline,[263] a prenyltransferase FtmB catalyzing prenylation to yield tryprostatin B (**568**),[264] a cytochrome P450 FtmC catalyzing subsequent aromatic hydroxylation to yield desmethyltryprostatin A (**570**),[265] and methylation of the hydroxyl group by a methyltransferase FtmD to form tryprostatin A (**571**).[266] Another cytochrome, P450 FtmE, catalyzed the fusion of the indole ring to the diketopiperazine core to form a pentacyclic fumitremorgin C (**572**) (Fig. 15B).[265] However, no enzymes responsible for spirocarbon formation in the biosynthesis of spirotryprostatins had been identified during earlier studies.

In 2013, Watanabe and co-workers utilized *S. cerevisiae* BY4705 and *A. niger* A1179 as heterologous hosts to efficiently express the entire biosynthetic pathways of spirotryprostatin. They identified two distinct mechanisms for spiro-carbon formation, *i.e.*, a radical route catalyzed by the cytochrome P450 enzyme FtmG for spirotryprostatins B (**110**) and G (**117**), and an epoxide route catalyzed by the flavin-dependent monooxygenase (FMO) FqzB (see 4.2.4) for spirotryprostatin A (**109**).[97] Both bioconversion and *in vitro* experiments indicate that the FtmG-catalyzed pathway seemed to proceed through radical-mediated two-step hydroxylation, followed by dehydration and semipinacol rearrangement (Fig. 15C). Interestingly, FtmG could process both substrates **569** and **572** to produce **110** and **117**, respectively.[267]

4.1.3 Spirobrassinin. Tryptophan-derived brassinin (**575**) is produced through the indole glucosinolate pathway, and isotope feeding studies have suggested that **575** acts as

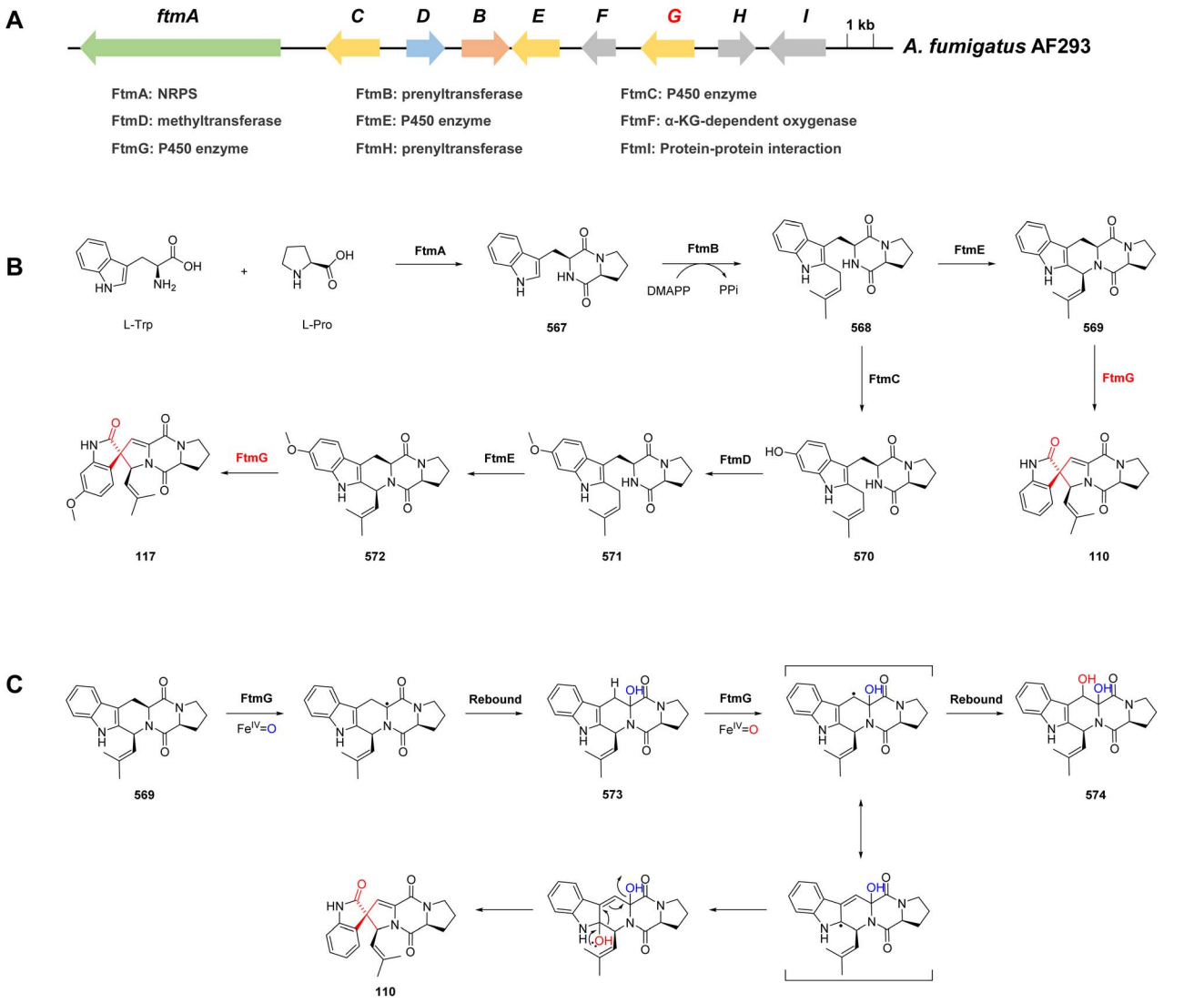

Fig. 15 Biosynthesis of spirotryprostatin B and G. (A) BGC of spirotryprostatins in *A. fumigatus* AF293. (B) Proposed biosynthetic pathway of spirotryprostatins B and G. (C) Putative mechanism for spirooxindole formation catalyzed by FtmG.

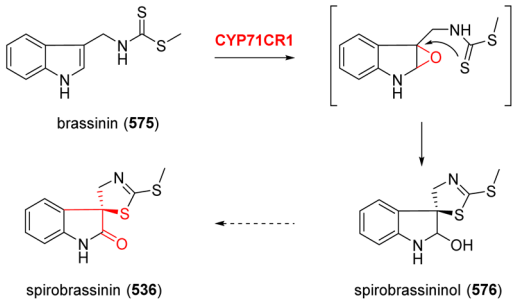

Fig. 16 Biosynthesis of spirobrassinin.

a precursor to spirobrassinin (**536**).[268] Following RNA sequencing and bioinformatic analysis, five candidate cytochrome P450 genes were individually cloned and expressed in *Saccharomyces cerevisiae* strain WAT11, along with the cytochrome P450 reductase ATR1. *In vitro* biochemical analysis revealed that the incubation of **575** with the cytochrome P450 Bra005870 (CYP71CR1) resulted in an NADPH-dependent conversion of **575** to spirobrassininol (**576**), a biosynthetic precursor for **536** (Fig. 16).[268]

The CYP71CR1-catalyzed mechanism is proposed to most likely proceed through an initial epoxidation intermediate at the C2 and C3 positions, followed by *S*-heterocyclization at the C3 position, leading to the formation of spirobrassinol (**576**) (Fig. 16).[268]

4.1.4 Corynoxeines. In 2023, Dang and co-workers characterized a cytochrome P450 enzyme from *Mitragyna speciosa* (kratom).[129] The enzyme, designated 3eCIS (MsCYP72056), belongs to the CYP71 family and was confirmed to be responsible for the formation of the tetracyclic SOAs isocorynoxeine (3*S*, 7*S*) (**194**) and 3-*epi*-corynoxeine (3*R*, 7*R*) (**578**) from 3*R*-hirsuteine (**577**) *via* both *in vivo* and *in vitro* assays. The formation of carbocation at C-7 is proposed to occur *via* an epoxide ring-opening mechanism (Fig. 17). Subsequently, through a semi-pinacol mechanism, the alkyl chain at C-3 could undergo rearrangement on both sides of the indole ring, partially influenced by pH, resulting in the production of the 3*R* and 3*S* spirooxindoles.[129]

4.1.5 Uncarines. Based on the finding that the cytochrome P450 enzyme MsCYP72056 catalyzes the formation of tetracyclic SOAs, Jiang and co-workers attempted to extend its catalytic activity toward pentacyclic SOAs and evaluate the potential of

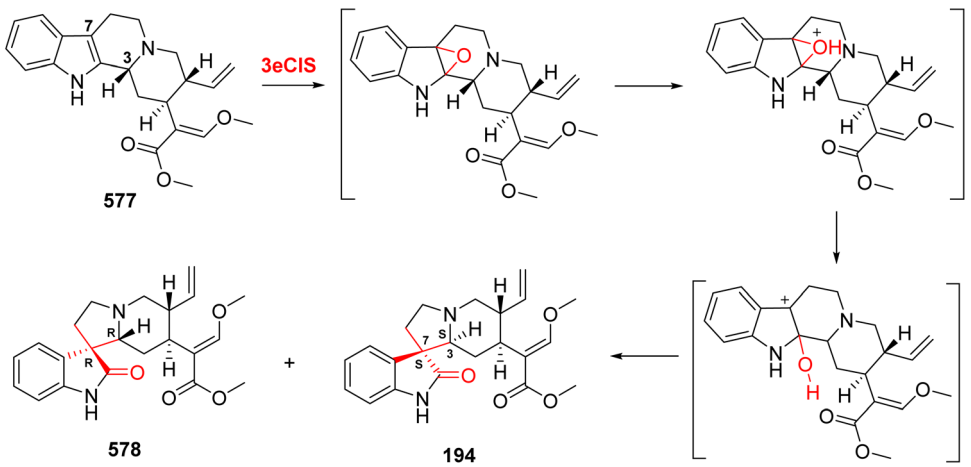

Fig. 17 Biosynthesis of corynoxeines.

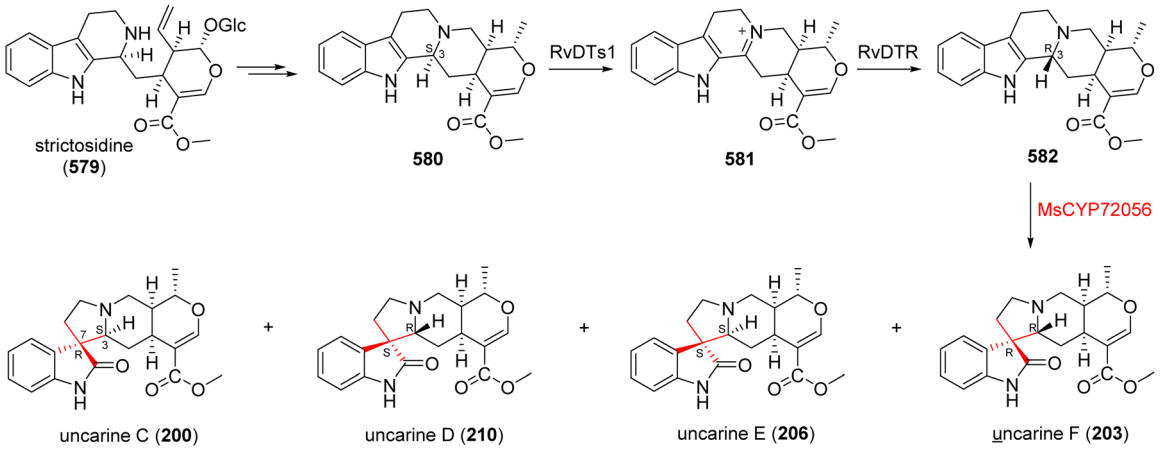

Fig. 18 Biosynthesis of uncarines.

this enzyme for collective biosynthesis. When various pentacyclic alkaloids were treated with MsCYP72056, only those with a 3*R* configuration were converted into the corresponding pentacyclic SOAs. For instance, 3*R*-akuammigine (**582**) was transformed into SOA isomers including uncarines C (**200**), D (**210**), E (**206**), F (**203**) (Fig. 18).[269] The cooccurrence of both 3*S*-tetrahydroalstomine (**580**) and (**582**) in the same plants suggested that 3*R*-configured alkaloid might be derived from its 3*S* counterparts *via* epimerization. Through transcriptome mining and bioinformation analysis, two enzymes, a flavin-dependent enzyme RvDTS1 and a medium-chain dehydrogenase RvDTR, were identified and functionally confirmed to catalyze the sequential reaction in the stereospecific epimerization of **580** to **582** through an iminium intermediate (**581**).[269]

4.2. Flavin-dependent monooxygenase-based

4.2.1 Paraherquamides. The BGC of paraherquamides from *P. fellutanum* ATCC 20841 was characterized (Fig. 19A).[270] The initial step in the biosynthesis of paraherquamides was catalyzed by an NRPS PhqB, which incorporates L-tryptophan and L-*β*-methylproline into the production of the monoketopiperazine precursor **583**.[270–272] The product **583** underwent spontaneous oxidation to generate zwitterion **584**. The reverse prenyltransferase PhqI catalyzed prenylation at the indole C2 position to produce **586**,[54,273] which was then reduced and cyclized by a bifunctional reductase and intramolecular [4 + 2] Diels-Alderase PhqE to generate preparaherquamide (**587**) and furnish the bicyclo[2.2.2]diazaoctane scaffold.[274]

Two compounds, paraherquamides K (**588**) and L (**589**), with oxidation and prenylation modifications were isolated from the

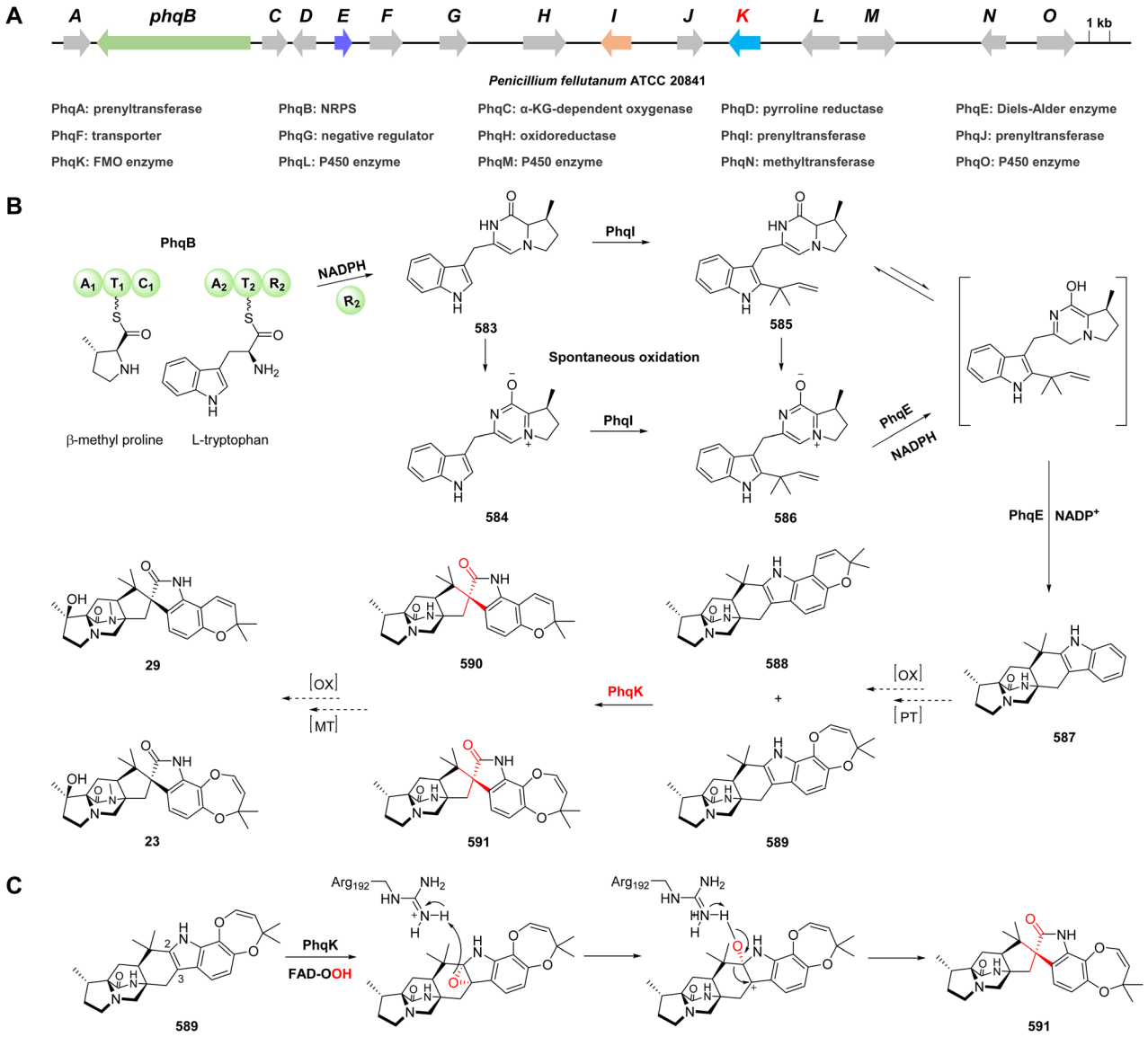

Fig. 19 Biosynthesis of paraherquamides. (A) BGC of paraherquamides in *P. fellutanum* ATCC 20841. (B) Proposed biosynthetic pathway of paraherquamides. (C) Putative mechanism for spirooxindole formation catalyzed by PhqK.

phqK mutant, suggesting that the pyran and dioxepin rings are both formed prior to spirocyclization, and the FMO PhqK is responsible for spirooxindole formation in paraherquamide M (**590**) and paraherquamide N (**591**) (Fig. 19B). The reaction kinetics indicated that dioxepin-containing **589** is the favoured substrate for PhqK.[275] The crystal structures of PhqK in the complex with the substrates and computational studies revealed that the precise substrate orientation promotes α-epoxidation at the indole C2=C3 position, followed by collapse of the epoxide at C3 to generate a C2 hydroxyl carbocation through general acid catalysis *via* Arg192. Finally, the migration of the reverse prenyl group from C2 to C3 generated the spirooxindole product *via* semipinacol rearrangement (Fig. 19C).[275] This study provided the first insights into the catalytic mechanism of selective spirocyclization.

4.2.2 Citrinadins. The BGCs of citrinadins were initially characterized from *P. citrinum* DSM 1997 (*cnd*),[276] and subsequently reidentified and functionally characterized from *P. citrinum* ATCC 9849 (*ctd*) (Fig. 20A).[277–279] The NRPS CtdQ was proposed to incorporate L-tryptophan and 6-methyl-L-pipecolate to produce the monoketopiperazine precursor **592.** The reverse prenyltransferase CtdH and the α-*anti*-selective NmrA-like Diels–Alder enzyme catalyzed the production of 2,5-diazabicyclo[2.2.2]octane-containing intermediate **594.**[278] Following *C*-prenylation catalyzed by another prenyl-transferase CtdU, the product **595** was oxidized by the flavoprotein monooxygenase CtdE to generate a 3*S*-spirooxindole moiety in **596** *via*

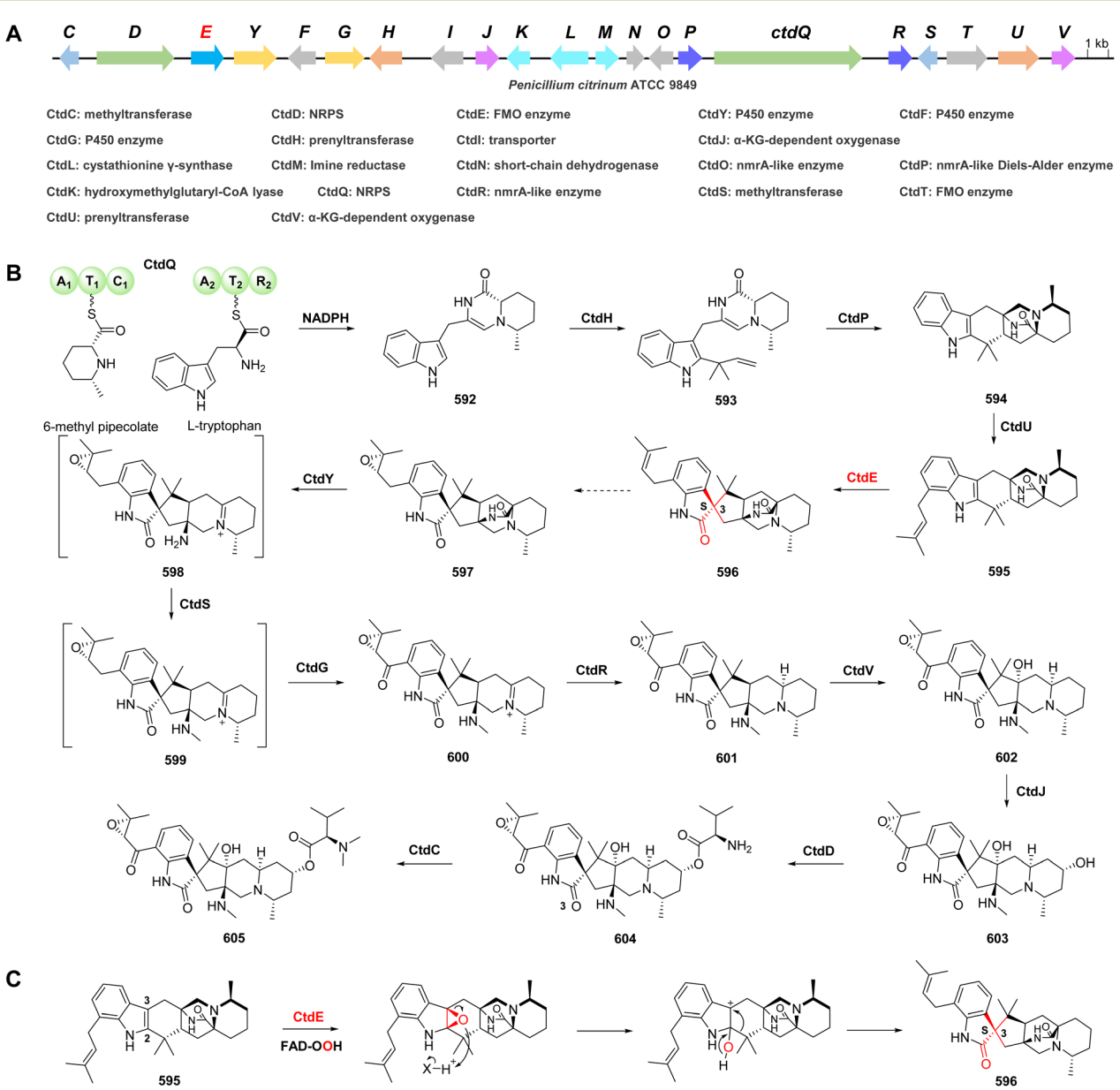

Fig. 20 Biosynthesis of citrinadins. (A) BGC of citrinadins in *P. citrinum* ATCC 9849. (B) Proposed biosynthetic pathway of citrinadins. (C) Putative mechanisms for spirooxindole formation catalyzed by CtdE.

semipinacol rearrangement.[277] Subsequently, the cytochrome P450 enzyme CtdY catalyzed the unique amide cleavage and decarboxylation to form a 6/5/5/6/6 pentacyclic scaffold in **598**.[279] In addition, seven other proteins contributed to the biosynthesis, including a cytochrome P450 enzyme (CtdG), NmrA-like enzyme (CtdR) and two α-ketoglutarate (KG)-dependent oxygenases (CtdV and CtdJ) catalyzed multistep regio- and stereo-selective redox reactions, two methyltransferases (CtdS and CtdC) mediated *N*-methylation and the NRPS enzyme CtdD assembled L-valine onto the core structure, completing the synthesis of 21*R*-citrinadin A (**605**) (Fig. 20B).[279] In contrast to the 3*R* spiro ring presented in paraherquamides and notoamides, citrinadins has a 3*S* spiro ring system.

To elucidate the formation mechanism, the high-resolution X-ray crystal structure of the CtdE-FAD-substrate complex, together with site-directed mutagenesis and computational study was used to characterized the function of CtdE.[277] The cofactor FAD undergoes a significant conformational change in the presence or absence of the substrate. The C4a atom of the flavin in the "in" position is close to the C2 and C3 of **595**, with distances of 5.6 and 5.5 Å, respectively, which are suitable for the proposed $C_{(4a)}$-hydroperoxide flavin (Fl_{OOH}) to perform epoxidation on the C2═C3 bond in substrate **595**. Importantly, the structures of the enzyme–substrate complex reveal that FAD is positioned on the β-face of substrate **595**, indicating CtdE could catalyze β-face epoxidation of the substrate (Fig. 20C). Combined with a site-specific mutation experiment, residue R122 was suggested to play multiple roles in the catalytic reaction of CtdE, including orienting and stabilizing the "in" FAD conformation and participating in directing the regio-selective collapse of the epoxide intermediate, which is similar to the function of R192 in PhqK.[275,277] Although the planar structures of CtdE substrate **595** and PhqK substrate paraherquamide L (**589**) are similar, their entire molecules exhibit a significant three-dimensional structure difference due to their different configurations, and the binding posture of the two enzymes is nearly a 180° reversal. The theoretical calculations also support that the β-face of the substrate is more stable in CtdE and shows a preference for forming a C_2-hydroxyl carbocation intermediate and subsequent C2 to C3 migration to yield 3*S* spirooxindole. CtdE is the first reported biocatalyst responsible for the formation of the 3*S* spirooxindole framework by 2,3-β-face epoxidation triggering semipinacol rearrangement (Fig. 20C), representing an evolutionary branch in specific 3*S* spirocyclization.[277]

4.2.3 Notoamides

4.2.3.1 Not/not′. The BGCs of notoamides were characterized from marine-derived *A. protuberus* (*not*) and the terrestrial-derived *A. amoenus* (*not′*), where both displayed identical genetic organization and high sequence identity (70.8%) (Fig. 21A).[280] Brevianamide F (**606**) is synthesized from L-Trp and L-Pro by the NRPS NotE/NotE′, and then reverse-prenylated by prenyltransferase NotF/NotF′ to yield deoxybrevianamide E (**607**), respectively.[281] The cytochrome P450 monooxygenases NotG/NotG′ likely catalyze the hydroxylation of the indole ring. Following this, other prenyltransferases, NotC/NotC′, catalyze normal prenylation to form the intermediate notoamide S (**609**).[281] Oxidoreductases NotD/NotD′ are proposed to mediate oxidative ring closure to construct the pyran moiety, generating notoamide E (**610**), which is further oxidized by FMO NotB to yield notoamide C (**611**) and notoamide D (**612**), respectively.[282] The conversion of notoamide S (**609**) to stephacidin A is likely catalyzed by P450 NotH/NotH′ and oxidoreductase NotD/NotD′, producing (+)-stephacidin A (**615**) and (−)-stephacidin A (**616**). However, the actual substrate for Diels–Alder reaction remains uncertain. The FMOs NotI/NotI′ were proven to be responsible for generating the spirooxindole moiety in the biosynthesis of notoamides, employing a catalytic mechanism similar to that of Phq.[275] *In vitro* biochemical assays of NotI/NotI′ demonstrated the conversion of (+)-stephacidin A (**615**) and (−)-stephacidin A (**616**) into (−)-notoamide B (**49**) and (+)-notoamide B (**50**), with a clear preference for the substrate (−)-stephacidin A (**616**) (Fig. 21B), respectively.[283] Despite the elucidated function of NotI/NotI′, the identity of the enzyme responsible for the alternative stereoisomeric outcome of (+)– and (−)-notoamides A and B in A. *amoenus* and *A. protuberus* remains unresolved, respectively. In addition, both NotI/NotI′ can also catalyze the conversion of (+)-6-*epi*-stephacidin A (**617**) to (+)-versicolamide B (**64**), but no reaction with (−)-6-*epi*-stephacidin A (**618**) is detected (Fig. 21B).[283]

4.2.3.2 Spe. The *spe* gene cluster, identified in *A. Ochraceus* CGMCC 3.4414, is also responsible for the biosynthesis of notoamides (Fig. 22A).[284] Interestingly, this BGC lacks the key homologous gene of notI, which has been previously shown to play a critical role in generating the spirooxindole moiety in notoamide biosynthesis.[283] Through systematic pathway reconstitution, substrate feeding, *in vitro* biochemical assays and computation studies, the *spe* BGC-mediated biosynthesis pathway of (+)-notoamide B (**50**) and (+)-versicolamide B (**64**) was established. The NRPS SpeA initially forms a diketopiperazine skeleton by incorporating L-tryptophan and L-proline. Following two-step prenylation, hydroxylation and cyclization reactions generate the key intermediate notoamide E (**610**). Subsequently, FMO SpeF, a homologue of NotB, catalyzes the 2,3-epoxidation of the indole moiety with stereoselectivity control. This is followed by coupling oxidation of its diketopiperazine unit at C-17 by SpeG. Finally, (+)-notoamide B (**50**) and (+)-versicolamide B (**64**) are produced through tandem isomerization, a nonenzymatic inverse electron-demand Diels–Alder (IEDDA) reaction and semipinacol rearrangement (Fig. 22B). To prevent the formation of shunt products, including notoamides C (**611**), D (**612**), M (**619**) and speramide B (**620**), it was shown through fluorescence co-localization and yeast two-hybrid assays that SpeF and SpeG form a fungal metabolon.[284] These findings exemplify the diverse biosynthetic pathways leading to notoamides in different microbial species.

It is intriguing that different fungal species employ distinct biosynthetic pathways to produce notoamides. These differences primarily arise from two factors, as follows: (1) functional divergence of key enzymes: the FMO NotB(B′) and NotI(I′), as well as SpeF exhibit functional differences despite catalyzing similar reactions. Notably, they differ in substrate specificities, where NotB acts on notoamide E (**610**), NotI/NotI′ on stephacidin A, while SpeF accepts notoamide E (**610**) as the substrate. (2)

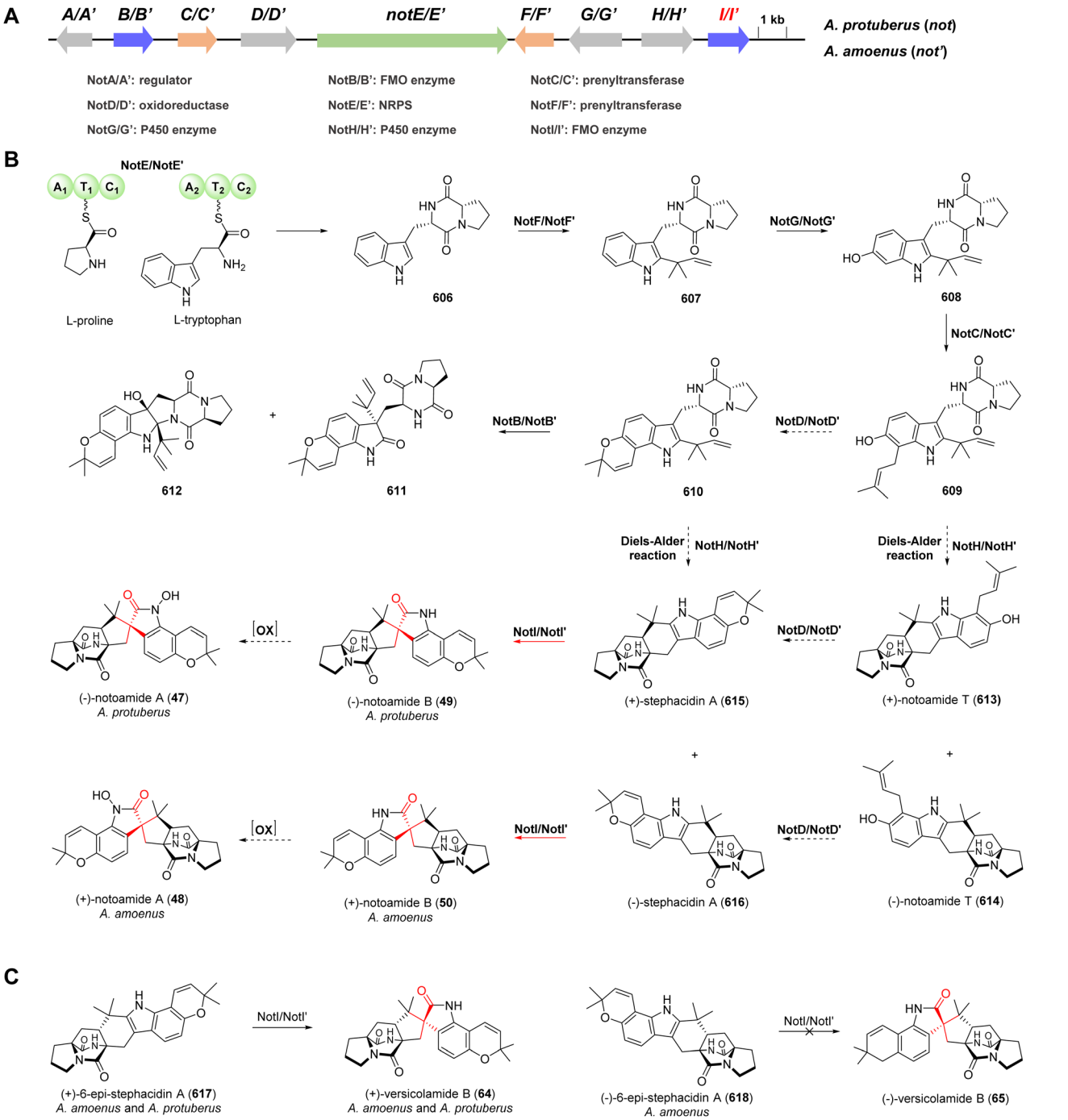

Fig. 21 Biosynthesis of notoamides (*not*/*not'*). (A) BGC of notoamides in *A. protuberus* (*not*) and *A. amoenus* (*not'*). (B) Proposed biosynthetic pathway of (+)- and (−)- notoamide B. (C) Substrate specificity analysis of NotI/NotI.

Variations in research methodologies: functional analysis of NotB and NotI/NotI′ was carried out through individual enzyme assays.[282,283] In contrast, studies on SpeF employed heterologous expression in strains transformed with either the full gene cluster (*spe*ABCDEFG) or with partially constituent genes, which provided relatively clear results. The studies also suggested that FMO SpeF and P450 SpeG may closely interact with each other. The spatial organization of the reactants in enzyme cascades is essential for orchestrating sequential reactions, guiding intermediate flow, and enhancing selectivity in the biosynthesis of natural products.[284] Therefore, systematic studies on the Not/Not′ gene cluster could help explain previously unresolved aspects of the pathway and lead to a more detailed understanding of the reaction mechanisms.

4.2.4 Spirotryprostatin A. In the spirotryprostatin biosynthetic pathway, the cytochrome P450 monooxygenase FtmG was found to be incapable of converting fumitremorgin C (**572**) into spirotryprostatin A (**109**).[97] However, a FMO, FqzB, originating from an unrelated biosynthetic pathway for the formation of fumiquinazolines, was found to be responsible for the oxidation

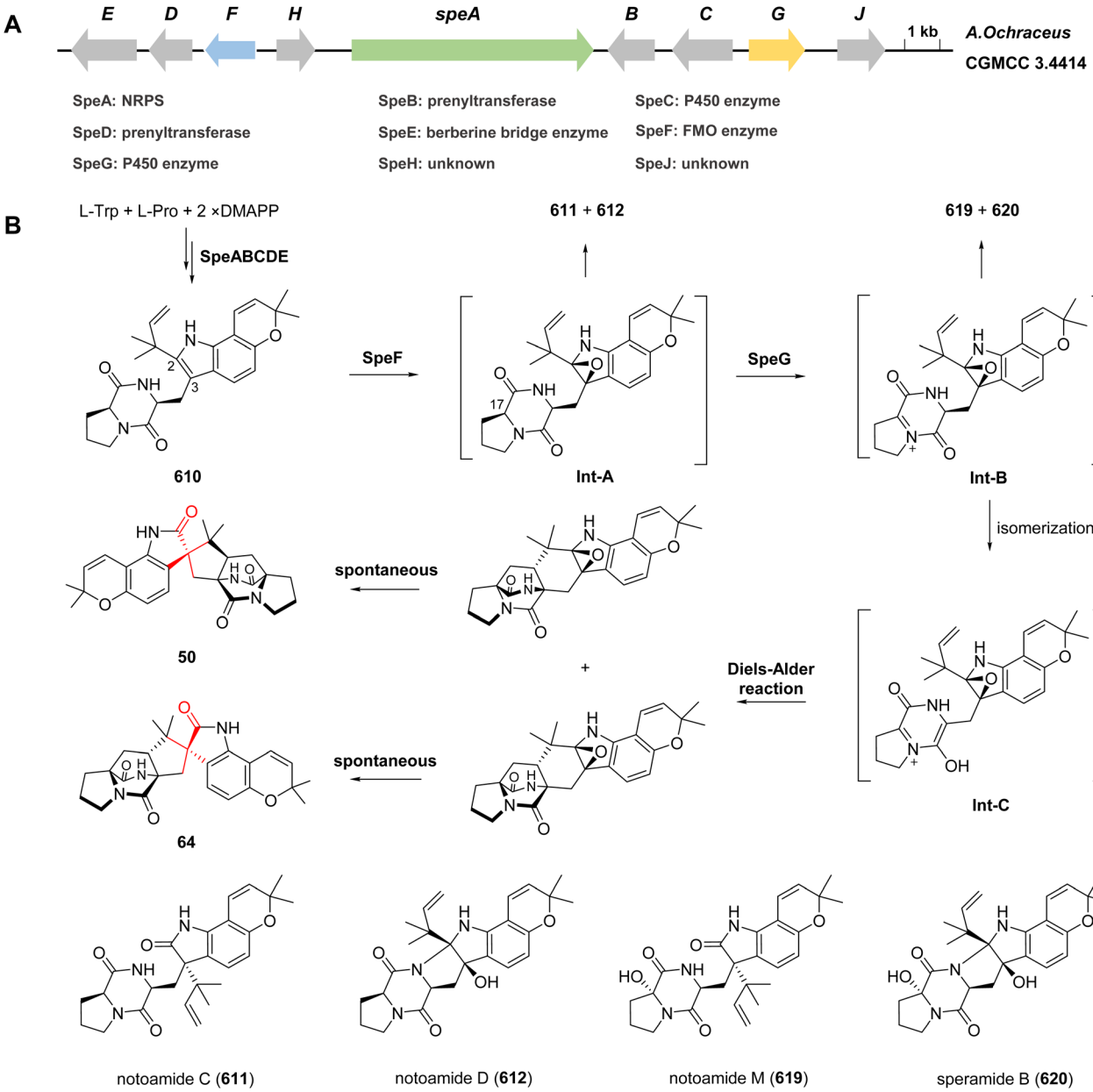

Fig. 22 Biosynthesis of notoamides (*spe*). (A) BGC of notoamides in *A. Ochraceus* CGMCC 3.4414 (*spe*). (B) Proposed biosynthetic pathway of (+)-notoamide B and (+)-versicolamide B.

steps necessary to convert tetrahydro-β-carboline fumitremorgin C (**572**) into spirotryprostatin A (**109**) *via* an epoxidation route. The proposed mechanism involves epoxide ring opening initiated by the donation of the methoxy oxygen lone pair, followed by semipinacol rearrangement (Fig. 23).[267,285] Subsequently, structural analysis, kinetic analysis and computational docking studies indicated that the flexible active site pocket of FqzB was the key reason for it to accept different substrates *via* nonspecific hydrophobic interactions. The Asp56, Arg115, Arg194 and His171 residues, which were found to have close interactions with the bound FAD and NADPH, were shown to be responsible for the catalytic function of FqzB. However, the exact mechanism of substrate recognition and catalysis by

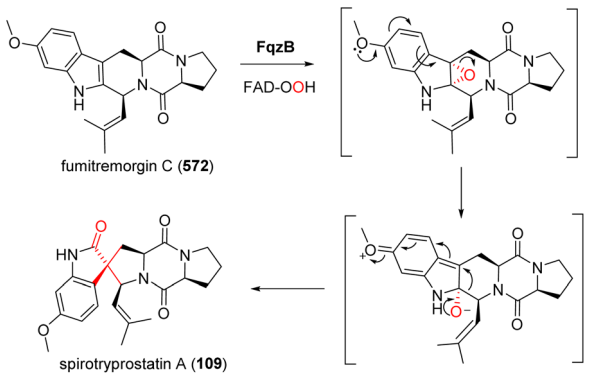

Fig. 23 Biosynthesis of spirotryprostatin A.

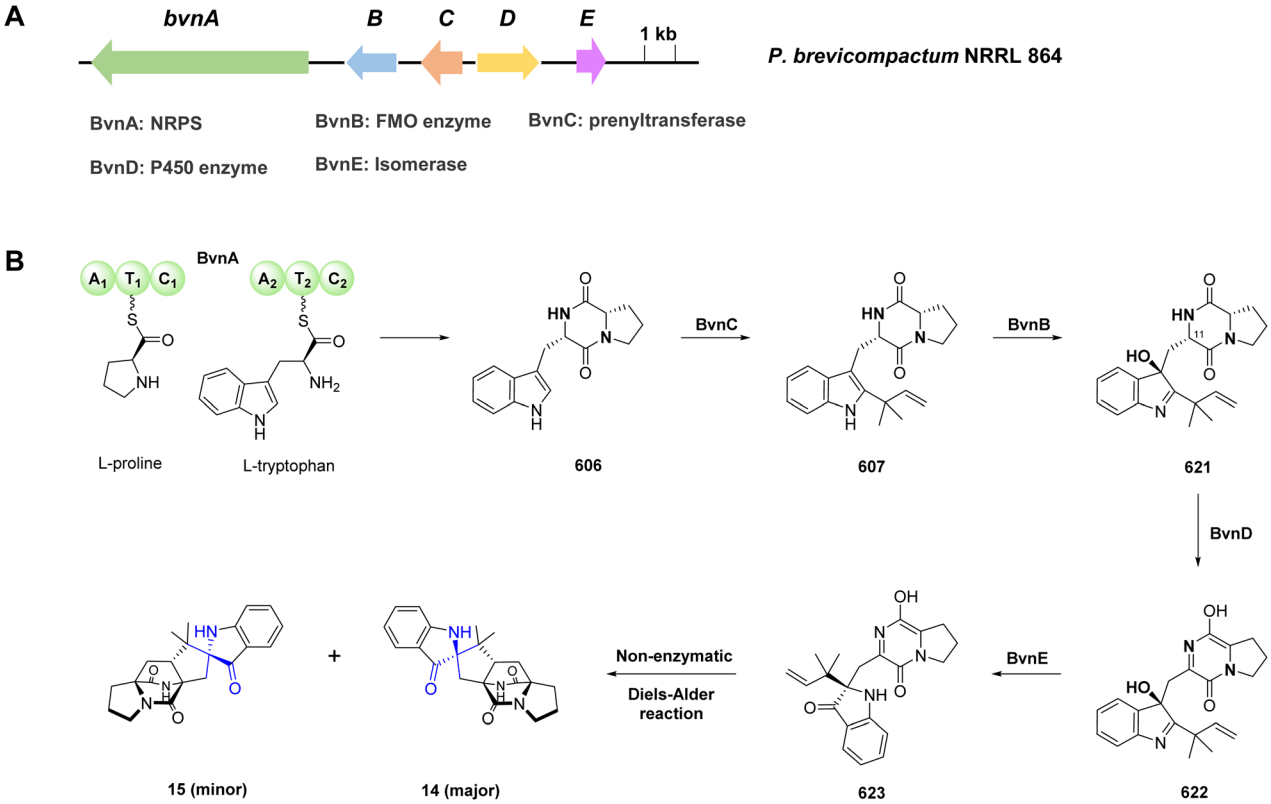

Fig. 24 Biosynthesis of brevianamides. (A) BGC of brevianamides in *P. brevicompactum* NRRL 864. (B) Proposed biosynthetic pathway of brevianamides.

FqzB is still uncertain due to the lack of the co-crystallization of the enzyme with different substrates.[285]

4.3. Other mechanisms

4.3.1 Brevianamides. The BGC of brevianamides was characterized from *P. brevicompactum* NRRL 864, which contains five genes designated as bvnA–E (Fig. 24A).[286] The NRPS BvnA was confirmed to catalyze the formation of brevianamide F (**606**) by incorporating L-tryptophan and L-proline. The production was suggested to involve "reverse" prenylation by BvnC to yield deoxybrevianamide E (**607**), which was then converted to **621** by the FMO BvnB *via* β-face epoxidation, followed by ring-opening. Interestingly, the cytochrome P450 enzyme BvnD was proposed to catalyse the C11 hydroxylation of **621**, followed by spontaneous dehydration/tautomerization to generate a diene moiety in **622**. Subsequently, the isomerase BvnE was found to catalyze stereospecific semipinacol rearrangement to produce **623** from **622**, which then undergoes a spontaneous intramolecular Diels–Alder cycloaddition to form the spirooxindole skeleton present in brevianamide A (**14**) and brevianamide B (**15**) (Fig. 24B).[286]

5. Conclusions and perspectives

SOAs, known for their remarkable structural diversity, are widely distributed across various organisms. Over 560 natural SOAs have been isolated to date and reported to exhibit a broad range of bioactivities. Among them, plant-derived SOAs are the largest proportion and primarily isolated from *Alstonia*, *Mitragyna*, *Gelsemium*, *Gardneria* and *Voacanga* genera, with a total number of 407 SOAs. Fungi-derived SOAs have also been extensively studied. In addition to the SOA moiety, compounds from fungi are found to contain diverse moieties such as bicyclo [2.2.2]diazaoctane skeleton, cyclopentane piperidine moiety, and diketopiperazine unit. However, challenges remain in the research on fungal SOAs, such as issues with duplicated name for the same structure, redundancy, and vague categorization. To date, only six SOAs have been reported from actinomycetes, and four from animals. The complexity of these structures, coupled with their potential activities, underscores the significance of continued research in this field. Recent advances in promoter engineering,[287] CRISPR editing tools,[288] and genome mining-based heterologous expression[289] are paving the way for the discovery of a wealth of SOAs with diverse structures. The antimicrobial, insecticidal, anthelmintic, anti-cancer, and anti-inflammatory properties of these compounds suggest significant potential in future drug development and agricultural applications. For instance, rhynchophylline, a representative SOA, is already utilized in the treatment of central nervous system disorders.[290]

In the biosynthesis studies of spirooxindoles, cytochrome P450 enzymes and flavin-dependent monooxygenases have been shown to play crucial roles in catalyzing spiro formation. These enzymes trigger semipinacol rearrangement, following carbocation, radical, or epoxidation, which leads to the

formation of spirooxindoles. Spirooxindole alkaloids featuring a bicyclo[2.2.2]diazaoctane ring system constitute a significant class of fungal spirooxindole alkaloids and are currently the most extensively studied in terms of their biosynthetic mechanisms. The biosynthesis generally involves three key steps including intramolecular Diels–Alder cycloaddition, formation of an epoxide intermediate, and semipinacol rearrangement. Based on the sequence of these reactions and whether they are enzyme-catalyzed, the biosynthetic pathways can be categorized into three pathways, as follows: (a) enzyme-catalyzed Diels–Alder reaction and epoxidation yield an intermediate, which subsequently undergoes semipinacol rearrangement to form the spirooxindole scaffold, as exemplified in the biosynthesis of paraherquamides[275] and citrinadins.[277] (b) Enzyme-catalyzed epoxidation and semipinacol rearrangement generate an intermediate, followed by a spontaneous Diels–Alder reaction to afford the spirooxindole framework, as observed in the biosynthesis of brevianamides.[286] (c) Enzyme-catalyzed epoxidation and desaturation produce an intermediate, which then undergoes spontaneous Diels–Alder cyclization and semipinacol rearrangement to from the spirooxindole, as demonstrated in the biosynthesis of notoamides (*spe*).[284] It has been proposed that the *not*/*not*′ BGC may biosynthesize notoamides *via* pathway a, although, pathway b also remains a plausible route.[283] Further systematic investigation of *not*/*not*′ BGC will help elucidate the detailed reaction mechanisms.

Despite the large number of known gelsemium alkaloid congeners, elucidating the biosynthetic pathways responsible for the formation of their spirooxindole scaffolds has long remained a formidable challenge. Based on the evidence from organic synthetic chemistry, it has been hypothesized that the yohimbane-type skeleton serves as a precursor to monoterpenoid indole alkaloids such as the sarpagine-type, which subsequently give rise to SOA groups including humantenine-type, gelsemine-type, and gelsedine-type groups.[291] Recent studies have revealed the role of the cytochrome P450 enzyme 3eCIS (MsCYP72056) in catalyzing the conversion of tetracyclic hirsutine and pentacyclic akuammigine into their respective spirooxindole products.[129,269] These findings imply that plants employ a collective biosynthetic strategy to assemble the spirooxindole framework, thereby motivating further research into the mechanism of oxindole spirocycle formation in plants. Furthermore, the intricate enzymatic mechanism governing spiro formation in the biosynthesis of maremycin, cyanogramides and spirotryprostatins can be further explored. The comprehensive characterization of these complex SOA biosynthetic pathways, and their combination with a better understanding of functions of biosynthetic enzymes, hold promise to facilitate the more efficient biomimetic synthesis of SOAs.

In summary, this review provides a comprehensive overview of the current understanding of the isolation, bioactivity, and biosynthesis of SOAs.

6. Author contributions

Writing – review & editing: R. C., L-H. Z., Z. F., Q. Z., C. Z. and Y. Z.; writing – original draft: R. C., L-H. Z., Q. Z. and Y. Z.; visualization: X. Z. and L-P. Z.; conceptualization: R. C., C. Z. and Y. Z.; funding acquisition: C. Z. and Y. Z.

7. Conflicts of interest

There are no conflicts to declare.

8. Data availability

No primary research results, software or code have been included, and no new data were generated or analysed as part of this review.

Supplementary information (SI): SOAs isolated from *Mitragyna*/*Uncaria* genus (before 2023), *Gelsemium* genus (before 2023), *Alangium*, *Mappiodoside* and *Nauclea* genera, *Tabernaemontana* genus, *Ervatamia* genus, *Voacanga* genus, *Catharanthus* genus, *Aspidosperma*, *Vinca* and *Rauvolfia* genera. See DOI: https://doi.org/10.1039/d5np00046g.

9. Acknowledgments

This work was supported by the National Key Research and Development Program of China (2024YFC2816000); the National Natural Science Foundation of China (22177119, 22193072); Key Science and Technology Plan Projects in Nansha District (2023ZD010); Hainan Provincial Natural Science Foundation of China (823CXTD393) and Guangdong Basic and Applied Basic Research Foundation (2024A1515011277, 2022B1515120075).

10. References

1 Z. W. Veitch, D. W. Cescon, T. Denny, L. M. Yonemoto, G. Fletcher, R. Brokx, P. Sampson, S. W. Li, T. J. Pugh, J. Bruce, M. R. Bray, D. J. Slamon, T. W. Mak, Z. A. Wainberg and P. L. Bedard, *Br. J. Cancer*, 2019, **121**, 318–324.
2 Y. Tian, S. Nam, L. Liu, F. Yakushijin, K. Yakushijin, R. Buettner, W. Liang, F. Yang, Y. Ma, D. Horne and R. Jove, *PLoS One*, 2012, **7**, e49306.
3 M. Ranieri, A. D. Mise, G. Tamma and G. Valenti, *Compr. Pharmacol.*, 2022, **4**, 656–669.
4 H. Turner, *Future Med. Chem.*, 2016, **8**, 227–238.
5 K. Ding, Y. Lu, Z. N. Coleska, S. Qiu, Y. Ding, W. Gao, J. Stuckey, K. Krajewski, P. P. Roller, Y. Tomita, D. A. Parrish, J. R. Deschamps and S. Wang, *J. Am. Chem. Soc.*, 2005, **127**, 10130–10131.
6 Y. Zhao, S. Yu, W. Sun, L. Liu, J. Lu, D. McEachern, S. Shargary, D. Bernard, X. Li, T. Zhao, P. Zou, D. Sun and S. Wang, *J. Med. Chem.*, 2013, **56**, 5553–5561.
7 C. E. Ridsdale, *Blumea*, 1987, **24**, 43–100.
8 L. Z. Lin and G. A. Cordell, *J. Nat. Prod.*, 1989, **52**, 588–594.
9 A. J. Birch and J. J. Wright, *J. Chem. Soc. D*, 1969, 644b–645.
10 H. Kato, T. Yoshida, T. Tokue, Y. Nojiri, H. Hirota, T. Ohta, R. M. Williams and S. Tsukamoto, *Angew. Chem., Int. Ed.*, 2007, **46**, 2254–2256.

11 C. Lee, J. H. Sohn, J. H. Jang, J. S. Ahn, H. Oh, J. Baltrusaitis, I. H. Hwang and J. B. Gloer, *J. Antibiot.*, 2015, **68**, 715–718.
12 Y. H. Zhang, C. Geng, X. W. Zhang, H. J. Zhu, C. L. Shao, F. Cao and C. Y. Wang, *Mar. Drugs*, 2019, **17**, 514.
13 Y. Y. Zheng, N. X. Shen, Z. Y. Liang, L. Shen, M. Chen and C. Y. Wang, *Nat. Prod. Res.*, 2020, **34**, 378–384.
14 J. Jiang, H. Jiang, D. Shen, Y. Chen, H. Shi and F. He, *J. Antibiot.*, 2022, **75**, 301–303.
15 J. Kwon, Y. H. Seo, J. E. Lee, E. K. Seo, S. Li, Y. Guo, S. B. Hong, S. Y. Park and D. Lee, *J. Nat. Prod.*, 2015, **78**, 2572.
16 X.-L. Hu, X.-Q. Bian, X. Wu, J.-Y. Li, H.-M. Hua, Y.-H. Pei, A.-H. Han and J. Bai, *Tetrahedron Lett.*, 2014, **55**, 3864–3867.
17 H. Shi, J. Jiang, H. Zhang, H. Jiang, Z. Su, D. Liu, L. Jie and F. He, *Front. Microbiol.*, 2022, **13**, 1046099.
18 M. Qin, Y. Li, W. Xu, W. Gao, S. Yin, X. Hu, R. Zhang and C. Ding, *Bioorg. Chem.*, 2023, **140**, 106780.
19 J. H. Costa, C. I. Wassano, C. F. F. Angolini, K. Scherlach, C. Hertweck and T. Pacheco Fill, *Sci. Rep.*, 2019, **9**, 18647.
20 P. Zhang, X. L. Yuan, Y. M. Du, H. B. Zhang, G. M. Shen, Z. F. Zhang, Y. J. Liang, D. L. Zhao and K. Xu, *J. Agric. Food Chem.*, 2019, **67**, 11994–12001.
21 M. P. Lopez-GresaI, M. C. Gonzalez, L. Ciavatta, I. Ayala, P. Moya and J. Primo, *J. Agric. Food Chem.*, 2006, **54**, 2921–2925.
22 R. M. Banks, S. E. Blanchflower, J. R. Everett, B. R. Manger and C. Reading, *J. Antibiot.*, 1997, **50**, 840–846.
23 E. W. Zinser, M. L. Wolfe, S. J. Alexander-Bowman, E. M. Thomas, J. P. Davis, V. E. Groppi, B. H. Lee, D. P. Thompson, T. G. Geary and J. Vet, *Pharmacol. Ther.*, 2002, **25**, 241–250.
24 S. Montserrat-de la Paz, A. Fernandez-Arche, R. de la Puerta, A. M. Quilez, F. J. Muriana, M. D. Garcia-Gimenez and B. Bermudez, *Phytomedicine*, 2016, **23**, 141–148.
25 Q.-C. Zhao, W. Hua, L. Zhang, T. Guo, M.-H. Zhao, M. Yan, G.-B. Shi and L.-J. Wu, *J. Asian. Nat. Prod. Res.*, 2010, **12**, 731–739.
26 R. Rojas-Duran, G. González-Aspajo, C. Ruiz-Martel, G. Bourdy, V. H. Doroteo-Ortega, J. Alban-Castillo, G. Robert, P. Auberger and E. Deharo, *J. Ethnopharmacol.*, 2012, **143**, 801–804.
27 B. C. Azevedo, E. J. Crevelin, B. W. Bertoni, M. Roxo, M. C. Borges, H. Peixoto, S. H. T. Contini, A. A. Lopes, S. C. França, A. M. S. Pereira and M. Wink, *Molecules*, 2019, **24**, 3299.
28 S.-I. Bascop, J. Sapi, J.-Y. Laronze and J. Levy, *Heterocycles*, 1994, **38**, 725–732.
29 F. v. Nussbaum and S. J. Danishefsky, *Angew. Chem., Int. Ed.*, 2000, **39**, 2175–2178.
30 L. E. Overman and M. D. Rosen, *Angew. Chem., Int. Ed.*, 2000, **39**, 4596–4599.
31 T. L. Liu, Z. Y. Xue, H. Y. Tao and C. J. Wang, *Org. Biomol. Chem.*, 2011, **9**, 1980–1986.
32 X.-H. Chen, Q. Wei, S.-W. Luo, H. Xiao and L.-Z. Gong, *J. Am. Chem. Soc.*, 2009, **131**, 13819–13825.
33 M. Uroos, A. Hameed, S. Naz and M. R. Shah, *Indole Alkaloids: Spirooxindole*, Elsevier, 2022.
34 G. Patel, V. R. Shah, T. A. Nguyen and K. Deshmukh, *Spirooxindole*, Elsevier, 2024.
35 A. R. Liandi, A. H. Cahyana, D. N. Alfariza, R. Nuraini, R. W. Sari and T. P. Wendari, *Green. Synth. Catal.*, 2024, **5**, 1–13.
36 H. Jeon, J. H. Kim and S. Kim, *Nat. Prod. Rep.*, 2024, **41**, 228–250.
37 P. Fu, F. Kong, X. Li, Y. Wang and W. Zhu, *Org. Lett.*, 2014, **16**, 3708–3711.
38 Y. Q. Tang, I. Sattler, R. Thiericke, S. Grabley and X. Z. Feng, *Eur. J. Org Chem.*, 2001, **2001**, 261–267.
39 Y. Lan, Y. Zou, T. Huang, X. Wang, N. L. Brock, Z. Deng and S. Lin, *Sci. China. Chem.*, 2016, **59**, 1224–1228.
40 K. Guo, T. Fang, J. Wang, A. A. Wu, Y. Wang, J. Jiang, X. Wu, S. Song, W. Su, Q. Xu and X. Deng, *Bioorg. Med. Chem. Lett.*, 2014, **24**, 4995–4998.
41 K. Stratmann, R. E. Moore, R. Bonjouklian, J. B. Deeter, G. M. L. Patterson, S. Shaffer, C. D. Smith and T. A. Smitka, *J. Am. Chem. Soc.*, 1994, **116**, 9935–9942.
42 A. J. Birch and J. J. Wright, *Tetrahedron*, 1970, **26**, 2329–2344.
43 A. J. Birch and R. A. Russell, *Tetrahedron*, 1972, **28**, 2999–3008.
44 J. F. Sanz-Cervera, T. Glinka and R. M. Williams, *J. Am. Chem. Soc.*, 1993, **115**, 347–348.
45 X. Xu, X. Zhang, X. Nong, J. Wang and S. Qi, *Mar. Drugs*, 2017, **15**, 43.
46 J. Polonsky, M.-A. Merrien, T. Prange and C. Pasca, *J. Chem. Soc., Chem. Commun.*, 1980, 601–602.
47 T. Prangé, M.-A. Billion, M. Vuilhorgne, C. Pascard, J. Polonsky and S. Moreau, *Tetrahedron Lett.*, 1981, **22**, 1977–1980.
48 Z. Lin, J. Wen, T. Zhu, Y. Fang, Q. Gu and W. Zhu, *J. Antibiot.*, 2008, **61**(2), 81–85.
49 M. Yamazaki, E. Emi Okuyama, M. Kobayashi and H. Inoue, *Tetrahedron Lett.*, 1981, **22**, 135–136.
50 J. M. Liesch and C. F. Wichmann, *J. Antibiot.*, 1990, **43**, 1380–1386.
51 T. Aree, B. S. Antia, O. D. Ekpa and P. Kittakoop, *Acta. Crystallogr. E*, 2010, **E66**, o2227.
52 S. E. Blanchflower, R. M. Banks and J. R. Everett, *J. Antibiot.*, 1993, **46**, 1355–1363.
53 E. M. Stocking, J. F. Sanz-Cervera and R. M. Williams, *J. Am. Chem. Soc.*, 1996, **118**, 7008–7009.
54 E. M. Stocking, J. F. Sanz-Cervera and R. M. Williams, *Angew. Chem., Int. Ed.*, 2001, **40**, 1296–1298.
55 J. Wu, F. Wang, L. M. He, S. Y. Zhou, S. B. Wang, J. Jia, K. Hong and Y. S. Cai, *Nat. Prod. Res.*, 2022, **36**, 4388–4393.
56 T. J. Greshock, A. W. Grubbs, S. Tsukamoto and R. M. Williams, *Angew. Chem., Int. Ed.*, 2007, **46**, 2262–2265.
57 T. J. Greshock, A. W. Grubbs, P. Jiao, D. T. Wicklow, J. B. Gloer and R. M. Williams, *Angew. Chem., Int. Ed.*, 2008, **47**, 3573–3577.
58 K. Sugimoto, Y. Sadahiro, I. Kagiyama, H. Kato, D. H. Sherman, R. M. Williams and S. Tsukamoto, *Tetrahedron Lett.*, 2017, **58**, 2797–2800.

59 S. Tsukamoto, H. Kato, M. Samizo, Y. Nojiri, H. Onuki, H. Hirota and T. Ohta, *J. Nat. Prod.*, 2008, **71**, 2064–2067.
60 S. Tsukamoto, T. Kawabata, H. Kato, T. J. Greshock, H. Hirota, T. Ohta and R. M. Williams, *Org. Lett.*, 2009, **11**, 1297–1300.
61 S. Tsukamoto, H. Umaoka, K. Yoshikawa, T. Ikeda and H. Hirota, *J. Nat. Prod.*, 2010, **73**, 1438–1440.
62 P. Zhang, X.-M. Li, J.-N. Wang, X. Li and B.-G. Wang, *Chin. Chem. Lett.*, 2015, **26**, 313–316.
63 L. Hu, T. Zhang, D. Liu, G. Guan, J. Huang, P. Proksch, X. Chen and W. Lin, *RSC Adv.*, 2019, **9**, 19855–19868.
64 A. C. Whyte and J. B. Gloer, *J. Nat. Prod.*, 1996, **59**, 1093–1095.
65 J. Peng, X.-Y. Zhang, Z.-C. Tu, X.-Y. Xu and S.-H. Qi, *J. Nat. Prod.*, 2013, **76**, 983–987.
66 S. S. Afiyatullov, O. I. Zhuravleva, A. S. Antonov, D. V. Berdyshev, M. V. Pivkin, V. A. Denisenko, R. S. Popov, A. V. Gerasimenko, G. von Amsberg, S. A. Dyshlovoy, E. V. Leshchenko and A. N. Yurchenko, *J. Antibiot.*, 2018, **71**, 846–853.
67 J. S. Hu, Y. P. He, F. G. Zhou, P. P. Wu, L. Y. Chen, C. Ni, Z. K. Zhang, X. J. Xiao, L. K. An, X. X. He and C. X. Zhang, *Chem. Biodivers.*, 2023, **20**, e202300301.
68 Q. Meng, X. Guo, J. Wu, D. Liu, Y. Gu, J. Huang, A. Fan and W. Lin, *Phytochemistry*, 2022, **203**, 113424.
69 S. Cai, Y. Luan, X. Kong, T. Zhu, Q. Gu and D. Li, *Org. Lett.*, 2013, **15**, 2168–2171.
70 H. Li, W. Sun, M. Deng, Q. Zhou, J. Wang, J. Liu, C. Chen, C. Qi, Z. Luo, Y. Xue, H. Zhu and Y. Zhang, *J. Org. Chem.*, 2018, **83**, 8483–8492.
71 A. Kai, H. Kato, D. H. Sherman, R. M. Williams and S. Tsukamoto, *Tetrahedron Lett.*, 2018, **50**, 4236–4240.
72 C. Y. Wang, X. H. Liu, Y. Y. Zheng, X. Y. Ning, Y. H. Zhang, X. M. Fu, X. Li, C. L. Shao and C. Y. Wang, *Front. Microbiol.*, 2022, **13**, 808532.
73 B. Yang, J. Dong, X. Lin, X. Zhou, Y. Zhang and Y. Liu, *Tetrahedron*, 2014, **70**, 3859–3863.
74 B. Yang, H. Tao, X. Lin, J. Wang, S. Liao, J. Dong, X. Zhou and Y. Liu, *Tetrahedron*, 2018, **74**, 77–82.
75 S. Nishikori, K. Takemoto, S. Kamisuki, S. Nakajima, K. Kuramochi, S. Tsukuda, M. Iwamoto, Y. Katayama, T. Suzuki, S. Kobayashi, K. Watashi and F. Sugawara, *J. Nat. Prod.*, 2016, **79**, 442–446.
76 J. Yang, L. Gong, M. Guo, Y. Jiang, Y. Ding, Z. Wang, X. Xin and F. An, *Mar. Drugs*, 2021, **19**, 157.
77 I. Kagiyama, H. Kato, T. Nehira, J. C. Frisvad, D. H. Sherman, R. M. Williams and S. Tsukamoto, *Angew. Chem., Int. Ed.*, 2016, **55**, 1128–1132.
78 K. R. Watts, S. T. Loveridge, K. Tenney, J. Media, F. A. Valeriote and P. Crews, *J. Org. Chem.*, 2011, **76**, 6201–6208.
79 E. V. Mercado-Marin, P. Garcia-Reynaga, S. Romminger, E. F. Pimenta, D. K. Romney, M. W. Lodewyk, D. E. Williams, R. J. Andersen, S. J. Miller, D. J. Tantillo, R. G. S. Berlinck and R. Sarpong, *Nature*, 2014, **509**, 318–324.
80 F. Wang, A. M. Sarotti, G. Jiang, J. C. Huguet-Tapia, S.-L. Zheng, X. Wu, C. Li, Y. Ding and S. Cao, *Org. Lett.*, 2020, **22**, 4408–4412.
81 M. Tsuda, Y. Kasai, K. Komatsu, T. Sone, M. Tanaka, Y. Mikami and J. i. Kobayashi, *Org. Lett.*, 2004, **6**, 3087–3089.
82 T. Mugishima, M. Tsuda, Y. Kasai, H. Ishiyama, E. Fukushi, J. Kawabata, M. Watanabe, K. Akao and J. i. Kobayashi, *J. Org. Chem.*, 2005, **70**, 9430–9435.
83 N. Kushida, N. Watanabe, T. Okuda, F. Yokoyama, Y. Gyobu and T. Yaguchi, *J. Antibiot.*, 2007, **60**, 667–673.
84 H. Peng, J. Sun, R. Zhang, Y. Qiu, Y. Hong, F. Zhou, C. Wang, Y. Hu and X. Wang, *Mar. Drugs*, 2025, **23**, 280.
85 E. F. Pimenta, A. M. Vita-Marques, A. Tininis, M. H. R. Seleghim, L. D. Sette, K. Veloso, A. G. Ferreira, D. E. Williams, B. O. Patrick, D. S. Dalisay, R. J. Andersen and R. G. S. Berlinck, *J. Nat. Prod.*, 2010, **73**, 1821–1832.
86 R. F. Bond, J. C. A. Boeyens, C. W. Holzapfel and P. S. Steyn, *J. Chem. Soc., Perkin Trans. 1*, 1979, 1751–1761.
87 T. Kawahara, A. Nagai, M. Takagi and K. Shin-ya, *J. Antibiot.*, 2012, **65**, 535–538.
88 T. Ali, T. M. Pham, K. S. Ju and H. L. Rakotondraibe, *Molecules*, 2019, **24**, 218.
89 D. Zhang, L. Zhao, L. Wang, X. Fang, J. Zhao, X. Wang, L. Li, H. Liu, Y. Wei, X. You, S. Cen and L. Yu, *J. Nat. Prod.*, 2017, **80**, 371–376.
90 S. Kildgaard, L. S. de Medeiros, E. Phillips, C. H. Gotfredsen, J. C. Frisvad, K. F. Nielsen, L. M. Abreu and T. O. Larsen, *J. Nat. Prod.*, 2018, **81**, 785–790.
91 P. Q. Wu, J. S. Zhou, L. S. Do Amaral, M. B. Cassera, J. M. Yue and B. Zhou, *Bioorg. Chem.*, 2025, **164**, 108825.
92 C.-B. Cui, H. Kakeya and H. Osada, *Tetrahedron*, 1996, **52**, 12651–12666.
93 C. B. Cui, *J. Antibiot.*, 1996, **49**, 832–835.
94 F. Wang, Y. Fang, T. Zhu, M. Zhang, A. Lin, Q. Gu and W. Zhu, *Tetrahedron*, 2008, **64**, 7986–7991.
95 Y. X. Liu, S. G. Ma, X. J. Wang, N. Zhao, J. Qu, S. S. Yu, J. G. Dai, Y. H. Wang and Y. K. Si, *Helv. Chim. Acta*, 2012, **95**, 1401–1408.
96 S. S. Afiyatullov, O. I. Zhuravleva, E. L. Chaikina and M. M. Anisimov, *Chem. Nat. Compd.*, 2012, **48**, 95–98.
97 Y. Tsunematsu, N. Ishikawa, D. Wakana, Y. Goda, H. Noguchi, H. Moriya, K. Hotta and K. Watanabe, *Nat. Chem. Biol.*, 2013, **9**, 818–825.
98 S. Lin, Y. He, F. Li, B. Yang, M. Liu, S. Zhang, J. Liu, H. Li, C. Qi, J. Wang, Z. Hu and Y. Zhang, *Phytochemistry*, 2020, **175**, 112374.
99 J. Liu, W.-J. Gao, C.-H. Fang, Y. Li, X.-Y. Liu, M.-J. Lv, J.-M. Yue and J.-H. Yu, *Fitoterapia*, 2025, **185**, 106697.
100 J. Yang, D. Lin, L. Yang, F. Li, Y. Yang, X. Cui, R. Zhang and X. Yang, *Fitoterapia*, 2025, **185**, 106708.
101 X. Liang, Z.-H. Huang, W.-B. Shen, X.-H. Lu, X.-X. Zhang, X. Ma and S.-H. Qi, *Phytochemistry*, 2024, **223**, 114119.
102 P. S. Steyn, *Tetrahedron Lett.*, 1971, **36**, 3331–3334.
103 P. S. Steyn, *Tetrahedron*, 1973, **29**, 107–120.
104 J. Wu, Y. Kang, Q. Meng, H. Jia, D. Liu, J. Huang, A. Fan and W. Lin, *Bioorg. Chem.*, 2025, **154**, 108099.

105 W. Liu, H.-J. Li, M.-Y. Xu, Y.-C. Ju, L.-Y. Wang, J. Xu, D.-P. Yang and W.-J. Lan, *Org. Lett.*, 2015, **17**, 5156–5159.
106 F.-D. Kong, S.-L. Zhang, S.-Q. Zhou, Q.-Y. Ma, Q.-Y. Xie, J.-P. Chen, J.-H. Li, L.-M. Zhou, J.-Z. Yuan, Z. Hu, H.-F. Dai, X.-L. Huang and Y.-X. Zhao, *J. Nat. Prod.*, 2019, **82**, 3456–3463.
107 X. Guo, A. Fan, X. Qi, D. Liu, J. Huang and W. Lin, *Bioorg. Chem.*, 2023, **141**, 106873.
108 B. Wu, G. Chen, Z. G. Liu and Y. H. Pei, *Rec. Nat. Prod.*, 2015, **9**, 271–275.
109 L.-H. Huang, M.-Y. Xu, H.-J. Li, J.-Q. Li, Y.-X. Chen, W.-Z. Ma, Y.-P. Li, J. Xu, D.-P. Yang and W.-J. Lan, *Org. Lett.*, 2017, **19**, 4888–4891.
110 R. C. Elderfield and R. E. Gilman, *Phytochemistry*, 1972, **11**, 339–343.
111 R. L. Garnick and P. W. L. Quesne, *J. Am. Chem. Soc.*, 1977, 4213–4219.
112 T.-S. Kam and Y.-M. Choo, *Tetrahedron*, 2000, **56**, 6143–6150.
113 W. H. Wong, P. B. Lim and C. H. Chuah, *Phytochemistry*, 1996, **41**, 313–315.
114 T.-S. Kam, I.-H. Iek and Y.-M. Choo, *Phytochemistry*, 1999, **51**, 839–844.
115 W.-H. Wong, P.-B. Lim and C.-H. Chuah, *Phytochemistry*, 1987, **26**, 865–868.
116 T.-S. Kam and Y.-M. Choo, *J. Nat. Prod.*, 2004, **67**, 547–552.
117 J. S. Yeap, S. Navanesan, K. S. Sim, K. T. Yong, S. Gurusamy, S. H. Lim, Y. Y. Low and T. S. Kam, *J. Nat. Prod.*, 2018, **81**, 1266–1277.
118 S. J. Tan, J. L. Lim, Y. Y. Low, K. S. Sim, S. H. Lim and T. S. Kam, *J. Nat. Prod.*, 2014, **77**, 2068–2080.
119 R. Atta ur, F. Nighat, A. Nelofer, K. Zaman, M. I. Choudhary and K. T. D. DeSilva, *Tetrahedron*, 1991, **47**, 3129–3136.
120 T.-S. Kam and Y.-M. Choo, *Tetrahedron*, 2000, **56**, 6143–6150.
121 X.-X. Zhu, Y.-Y. Fan, L. Xu, Q.-F. Liu, J.-P. Wu, J.-Y. Li, J. Li, K. Gao and J.-M. Yue, *Org. Lett.*, 2019, **21**, 1471–1474.
122 T. S. Kam and Y. M. Choo, *Phytochemistry*, 2004, **65**, 603–608.
123 J. S.-Y. Yeap, C.-H. Tan, K.-T. Yong, K.-H. Lim, S.-H. Lim, Y.-Y. Low and T.-S. Kam, *Phytochemistry*, 2020, **176**, 112391.
124 P. Q. Wu, Z. D. Liu, Y. H. Ren, J. S. Zhou, Q. F. Liu, Y. Wu, J. L. Zhang, B. Zhou and J. M. Yue, *Phytochemistry*, 2024, **220**, 113993.
125 A. A. Leslie Gunatilaka, in *The Alkaloids*, 1999, vol. 52, pp. 1–101.
126 M. E. Heitzman, C. C. Neto, E. Winiarz, A. J. Vaisberg and G. B. Hammond, *Phytochemistry*, 2005, **66**, 5–29.
127 L. Z. X. Yu, J. Liu, Y. Hua, S. Guo, M. Zhou, Y. Jiang and B. liu, *Zhong Cao Yao*, 2021, **52**, 6052–6065.
128 T.-H. Kanga, Y. Murakamia, K. Matsumotoa, H. Takayamab, M. Kitajimab, N. Aimib and H. Watanabea, *Eur. J. Pharmacol.*, 2002, **455**, 27–34.
129 T.-A. M. Nguyen, D. Grzech, K. Chung, Z. Xia, T.-D. Nguyen and T.-T. T. Dang, *Front. Plant Sci.*, 2023, **14**, 1125158.
130 A. S. Ravipati, N. Reddy and S. R. Koyyalamudi, *Stud. Nat. Prod. Chem.*, 2014, **43**, 381–408.
131 Z. L. Zhang, Y. Z. Li, G. Q. Wu, Y. M. Li, D. D. Zhang and R. Wang, *Arab. J. Chem.*, 2023, **16**, 104638.
132 K. P. Huang, L. L. Xu, S. Li, Y. L. Wei, L. Yang, X. J. Hao, H. P. He and Y. Zhang, *Nat. Prod. Bioprospect.*, 2023, **13**, 13.
133 X. X. Liang, J. X. Yang, J. M. Li, J. B. Huang, L. M. Yang, T. T. Sun, R. H. Luo, W. L. Xiao, Y. T. Zheng and X. L. Li, *Nat. Prod. Res.*, 2023, **37**, 1258–1264.
134 N. J. Chear, T. A. F. Ching-Ga, K. Y. Khaw, F. Leon, W. N. Tan, S. R. Yusof, C. R. McCurdy, V. Murugaiyah and S. Ramanathan, *Metabolites*, 2023, **13**, 390.
135 Z.-L. Yu, R. Bai, J.-J. Zhou, H.-L. Huang, W.-Y. Zhao, X.-K. Huo, Y.-H. Yang, Z.-L. Luan, B.-J. Zhang, C.-P. Sun and X.-C. Ma, *Chinese. J. Chem.*, 2021, **39**, 1331–1343.
136 H.-F. Zhou, W.-Y. Li, Q. Wu, J. Ren, L.-Y. Peng, X.-N. Li and Q.-S. Zhao, *Org. Lett.*, 2023, **25**, 4434–4438.
137 Q. Zhang, X. Q. Lei, F. T. Wei, J. Q. Ren, J. G. Shi and Q. L. Guo, *J. Asian. Nat. Prod. Res.*, 2024, **26**, 4–17.
138 L. Rao, F. Chen, M. H. Gao, J. J. Tan, S. J. Qu and C. H. Tan, *J. Asian. Nat. Prod. Res.*, 2025, **27**, 31–37.
139 S. G. Castro, E. Hosoya, M. Kitajima, H. Nakamura, J. A. H. Manzano, G. J. D. Alejandro, M. A. Tan and H. Ishikawa, *Phytochemistry*, 2025, **238**, 114585.
140 Z. J. Liu and R. R. Lu, *The Alkaloids*, Brossi, A., Academic Press, San Diego, 1988, vol. 33, pp. 83–140.
141 G.-L. Jin, Y.-P. Su, M. Liu, Y. Xu, J. Yang, K.-J. Liao and C.-X. Yu, *J. Ethnopharmacol.*, 2014, **152**, 33–52.
142 Y. K. Xu, L. Yang, S. G. Liao, P. Cao, B. Wu, H. B. Hu, J. Guo and P. Zhang, *J. Nat. Prod.*, 2015, **78**, 1511–1517.
143 M.-X. Sun, H.-H. Gao, J. Zhao, L. Zhang and K. Xiao, *Tetrahedron Lett.*, 2015, **56**, 6194–6197.
144 H. T. Wang, Y. C. Yang, X. Mao, Y. Wang and R. Huang, *J. Asian. Nat. Prod. Res.*, 2018, **20**, 321–327.
145 Q. Xue, J. Hu, X. C. Liu and J. Gu, *J. Asian. Nat. Prod. Res.*, 2020, **22**, 1138–1144.
146 L. Wang, J. F. Wang, X. Mao, L. Jiao and X. J. Wang, *Fitoterapia*, 2017, **120**, 131–135.
147 P. Jin, G. Zhan, G. Zheng, J. Liu, X. Peng, L. Huang, B. Gao, X. Yuan and G. Yao, *J. Nat. Prod.*, 2021, **84**, 1326–1334.
148 X. Wei, X. T. Huang, L. Y. Zhang, X. Y. Hu, W. Zhang, Y. Q. Zhou, H. F. Yu, C. F. Ding, L. C. Zhang, X. Liu and Y. Zhou, *Nat. Prod. Res.*, 2022, **36**, 2630–2636.
149 Y. K. Xu, L. Yang, S. G. Liao, P. Cao, B. Wu, H. B. Hu, J. Guo and P. Zhang, *J. Nat. Prod.*, 2015, **78**, 1511–1517.
150 M. X. Sun, Y. Cui, Y. Li, W. Q. Meng, Q. Q. Xu, J. Zhao, J. C. Lu and K. Xiao, *Phytochemistry*, 2019, **162**, 232–240.
151 W. Zhang, X. J. Huang, S. Y. Zhang, D. M. Zhang, R. W. Jiang, J. Y. Hu, X. Q. Zhang, L. Wang and W. C. Ye, *J. Nat. Prod.*, 2015, **78**, 2036–2044.
152 N. P. Li, M. Liu, X. J. Huang, X. Y. Gong, W. Zhang, M. J. Cheng, W. C. Ye and L. Wang, *J. Org. Chem.*, 2018, **83**, 5707–5714.
153 W. Zhang, W. Xu, G. Y. Wang, X. Y. Gong, N. P. Li, L. Wang and W. C. Ye, *Org. Lett.*, 2017, **19**, 5194–5197.
154 X. Wei, J. Yang, H. X. Ma, C. F. Ding, H. F. Yu, Y. L. Zhao, Y. P. Liu, A. Khan, Y. F. Wang, Z. F. Yang, W. Y. Huang, X. H. Wang and X. D. Luo, *Tetrahedron Lett.*, 2018, **59**, 2066–2070.

155 X. Wei, R. Guo, X. Wang, J. J. Liang, H. F. Yu, C. F. Ding, T. T. Feng, L. Y. Zhang, X. Liu, X. Y. Hu and Y. Zhou, *Molecules*, 2021, **26**, 7457.
156 M. X. Sun, H. H. Gao, J. Zhao, L. Zhang and K. Xiao, *Tetrahedron Lett.*, 2015, **56**, 6194–6197.
157 J. H. Gu, W. Zhang, W. Y. Cai, X. X. Fu, H. L. Zhou, N. P. Li, H. Y. Tian, J. S. Liu, W. C. Ye and L. Wang, *Org. Chem. Front.*, 2021, **8**, 1918–1925.
158 A. Saito, C. Fujita, N. Kogure, N. T. Vung, L. A. Hao, H. Takayama and M. Kitajima, *Tetrahedron*, 2022, **104**, 132572.
159 L. Wang, S. Chen, X. Gao, X. Liang, W. Lv, D. Zhang and X. Jin, *J. Enzyme Inhib. Med. Chem.*, 2023, **38**, 2155639.
160 D. Song, J. J. Liang, S. B. Pu, P. P. Zhang, Y. L. Peng, X. Liu, T. T. Feng, X. Pu, Y. Zhou, X. W. Liu and X. Wei, *Molecules*, 2023, **28**, 2531.
161 P. P. Zhang, J. J. Liang, Q. Y. Lu, X. Yin, Y. Q. Zhou, T. T. Feng, Y. Zhou, D. Chang and X. Wei, *Chem. Biodivers*, 2023, **20**, e202301665.
162 J. Lin, J. Wu, M. F. Bao, S. Kongkiatpaiboon and X. H. Cai, *Phytochemistry*, 2024, **222**, 114077.
163 L. L. Ye, M. Y. Yang and X. H. Cai, *Fitoterapia*, 2025, **184**, 106644.
164 N. Li, Y. Yang, S. Zhang, B. Jiang, W. Zhang, H. Wang, L. Chen, L. Wang, Y. Li, L. Shi, W. Ye and L. Wang, *Acta Pharm. Sin. B*, 2025, **15**, 4872–4885.
165 Q. H. Wei, J. P. Zhang, Z. Y. Lu, X. H. Jia, X. D. Zhao, Z. W. Wang and X. J. Wang, *Nat. Prod. Res.*, 2025, **39**, 233–240.
166 J. Lin, H. Q. Dong, M. F. Bao, J. X. Liu and X. H. Cai, *Org. Lett.*, 2025, **27**, 3019–3023.
167 J. H. Gu, N. P. Li, H. T. Lin, L. N. Dai, M. J. Cheng, J. Hong, Y. Y. Li, J. S. Liu, W. C. Ye and L. Wang, *Org. Chem. Front.*, 2025, **12**, 5387–5394.
168 M. J. Ren, Y. D. Wang, Y. P. Liu, Q. M. Cui, J. X. Cao, G. G. Cheng, W. B. Zhou and T. R. Zhao, *Biochem. Syst. Ecol.*, 2020, **90**, 104032.
169 S. Sakai, N. Aimi, K. Yamaguchi, E. Yamanaka and J. Haginiwa, *Tetrahedron Lett.*, 1975, **10**, 719–722.
170 X. H. Zhong, L. Xiao, Q. Wang, B. J. Zhang, M. F. Bao, X. H. Cai and L. Peng, *Phytochem. Lett.*, 2014, **10**, 55–59.
171 P. Chen, H. Yang, H. Zhang, W. Chen, Z. Zhang, J. Zhang, H. Li, X. Wang, X. Xie and X. She, *Org. Lett.*, 2020, **22**, 2022–2025.
172 W. X. Yang, Y. F. Chen, J. Yang, T. Huang, L. L. Wu, N. Xiao, X. J. Hao and Y. H. Zhang, *Fitoterapia*, 2018, **124**, 8–11.
173 S. F. Teng, J. J. He, X. Q. Wang, Y. Q. Li, A. Khan, T. R. Zhao, Y. D. Wang, G. G. Cheng and Y. P. Liu, *Phytochemistry*, 2023, **209**, 113639.
174 X.-Y. Hu, X. Wei, Y.-Q. Zhou, X.-W. Liu, J.-X. Li, W. Zhang, C.-B. Wang, L.-Y. Zhang and Y. Zhou, *Fitoterapia*, 2020, **147**, 104773.
175 H. J. Cong, Q. Zhao, S. W. Zhang, J. J. Wei, W. Q. Wang and L. J. Xuan, *Phytochemistry*, 2014, **100**, 76–85.
176 J. Ma and S. M. Hecht, *Chem. Commun.*, 2004, 1190–1191.
177 V. C. Pham, J. Ma, S. J. Thomas, Z. Xu and S. M. Hecht, *J. Nat. Prod.*, 2005, **68**, 1147–1152.
178 L. Fan, X. J. Huang, C. L. Fan, G. Q. Li, Z. L. Wu, S. G. Li, Z. D. He, Y. Wang and W. C. Ye, *Nat. Prod. Commun.*, 2015, **10**, 2087–2090.
179 X. X. Pi, G. Z. Tu, T. Z. Cai, R. Yang, Q. Wu and H. Z. Fu, *J. Chin. Pharm. Sci.*, 2014, **23**, 306–310.
180 L. Fan, C. H. Liao, Q. R. Kang, K. Zheng, Y. C. Jiang and Z. D. He, *Molecules*, 2016, **21**, 968.
181 G. Wang, L. Hou, Y. Wang, H. Liu, J. Yuan, H. Hua and L. Sun, *Fitoterapia*, 2022, **160**, 105228.
182 G. Wang, H. Wang, Z. Lin, L. Hou, J. Y. Wang and L. Sun, *J. Ethnopharmacol.*, 2022, **282**, 114560.
183 Y. L. Li, T. Wang, H. Wang, Q. Wang, C. H. Cai, G. P. Zhu, W. L. Mei, F. Q. Xu, H. F. Dai and S. Z. Huang, *J. Ethnopharmacol.*, 2025, **344**, 119533.
184 A. ATHIPORNCHAI, *Asian J. Pharm. Clin. Res.*, 2018, **11**, 45–53.
185 K. H. Lim, K. M. Sim, G. H. Tan and T. S. Kam, *Phytochemistry*, 2009, **70**, 1182–1186.
186 K. H. Lim, N. F. Thomas, Z. Abdullah and T. S. Kam, *Phytochemistry*, 2009, **70**, 424–429.
187 D. S. Sim, K. W. Chong, C. E. Nge, Y. Y. Low, K. S. Sim and T. S. Kam, *J. Nat. Prod.*, 2014, **77**, 2504–2512.
188 K. H. Lim, V. J. Raja, T. D. Bradshaw, S. H. Lim, Y. Y. Low and T. S. Kam, *J. Nat. Prod.*, 2015, **78**, 1129–1138.
189 A. E. Nugroho, M. Moue, T. Sasaki, O. Shirota, A. H. A. Hadi and H. Morita, *Nat. Prod. Commun.*, 2018, **13**, 347–350.
190 Y. Yu, M.-F. Bao, J. Wu, J. Chen, Y.-R. Yang, J. Schinnerl and X.-H. Cai, *Org. Lett.*, 2019, **21**, 5938–5942.
191 F. Traxler, H. Zhang, W. Mahavorasirikul, K. Krivanek, X. H. Cai, W. Aiyakool, M. Pfeiffer, L. Brecker and J. Schinnerl, *Molecules*, 2023, **28**, 6664.
192 Y. Yu, J. M. Gao and J. K. Liu, *Chinese. Chem. Lett.*, 1999, **10**, 575–578.
193 Z. W. Liu, T. T. Yang, W. J. Wang, G. Q. Li, B. Q. Tang, Q. W. Zhang, C. L. Fan, D. M. Zhang, X. Q. Zhang and W. C. Ye, *Tetrahedron Lett.*, 2013, **54**, 6498–6500.
194 D. B. Zhang, D. G. Yu, M. Sun, X. X. Zhu, X. J. Yao, S. Y. Zhou, J. J. Chen and K. Gao, *J. Nat. Prod.*, 2015, **78**, 1253–1261.
195 P. Clivio, B. Richard, J.-R. Deverre, T. Sevenet, M. Zeches and L. Le Men-Oliver, *Phytochemistry*, 1991, **30**, 3785–3792.
196 M. P. Cava, Y. Watanabe and K. Bessho, *J. Org. Chem.*, 1968, **33**, 3350–3352.
197 M. Qin, W. Gao, H. Wang, S. Yin, J. Hu, W. Gao and C. Ding, *Biochem. Syst. Ecol.*, 2024, **116**, 104863.
198 J.-C. Braekman, M. Tirions-Lampe and J. Pecher, *Bull. SOC. Chim. Belges*, 1969, **78**, 523–538.
199 C.-F. Ding, M.-L. Qin, K.-Y. Zhao, W. Gao, S.-Z. Yin, X.-G. Hu, G.-G. Cheng, R.-P. Zhang and W.-Y. Hu, *Phytochemistry*, 2025, **231**, 114361.
200 Z. T. Deng, W. Y. Li, L. Wang, Z. P. Zhou, X. D. Wu, Z. T. Ding and Q. S. Zhao, *Molecules*, 2021, **26**, 6516.
201 Y. Hirasawa, C. Kasagi, E. Koyama, H. Myojin, T. Tougan, T. Horii, N. Uchiyama, T. Kaneda and H. Morita, *J. Nat. Med.*, 2024, **79**, 134–142.

202 B. Gilbert, J. A. Brissolese, N. Finch, W. I. Taylor, H. Budzikiewicz, J. M. Wilson and C. Djerassi, *J.Am.Chem.Soc*, 1963, **85**, 1523–1528.
203 G. M. T. Robert, A. Ahond, C. Poupat, P. Potier, H. Jacquemin and S. K. Kan, *J. Nat. Prod.*, 1983, **46**, 708–722.
204 M. Reina, W. Ruiz-Mesia, L. Ruiz-Mesia, R. Martinez-Diaz and A. Gonzalez-Coloma, *Z. Naturforsch. C. J. Biosci.*, 2011, **66**, 225–234.
205 R. Vrabec, P. Drasar, L. Opletal, S. Kosturko, G. Blunden and L. Cahliková, *Phytochem. Rev.*, 2025, **24**, 3665–3735.
206 S. Kumar, D. Kumari and B. Singh, *J. Ethnopharmacol.*, 2022, **295**, 115327.
207 M. Takasugi, K. Monde, N. Katsui and A. Shirata, *Chem. Lett.*, 1987, **16**, 1631–1632.
208 M. r. Suchy, P. Kutschy, K. Monde, H. Goto, N. Harada, M. Takasugi, M. Dzurilla and E. Balentova, *J. Org. Chem.*, 2001, **66**, 3940–3947.
209 A. Jossang, P. Jossang, H. A. Hadi, T. Sévenet and B. Bodo, *J. Org. Chem.*, 1991, **56**, 6527–6530.
210 N. Anderton, P. A. Cockrum, S. M. Colegate, J. A. Edgar, K. Flower, I. Vit and R. I. Willing, *Phytochemistry*, 1998, **48**, 437–439.
211 C. Pellegrini, M. Weber and H. J. Borschberg, *Helv. Chim. Acta*, 1996, **79**, 151–168.
212 H.-F. Bai, S.-Y. Zhang, Y.-M. Yan and Y.-X. Cheng, *Phytochemistry*, 2024, **218**, 113936.
213 Q. J. Xie, W. Y. Zhang, Z. L. Wu, M. T. Xu, Q. F. He, X. J. Huang, C. T. Che, Y. Wang and W. C. Ye, *Chin. J. Nat. Med.*, 2020, **18**, 385–392.
214 Y. Liu, H. B. Jiang, Y. Liu, A. M. Algradi, A. Naseem, Y. Y. Zhou, X. She, L. Li, B. Y. Yang and H. X. Kuang, *Fitoterapia*, 2020, **146**, 104726.
215 M. Chen, S. Lin, L. Li, C. Zhu, X. Wang, Y. Wang, B. Jiang, S. Wang, Y. Li, J. Jiang and J. Shi, *Org. Lett.*, 2012, **14**, 5668–5671.
216 J. Zhao, F.-R. Pang, R. Luo, F. Li and D.-B. Zhang, *Fitoterapia*, 2022, **163**, 105317.
217 Y. Q. Wu, M. Kitajima, N. Kogure, R. P. Zhang and H. Takayama, *Tetrahedron Lett.*, 2008, **49**, 5935–5938.
218 S.-S. Ma, W.-L. Mei, Z.-K. Guo, S.-B. Liu, Y.-X. Zhao, D.-L. Yang, Y.-B. Zeng, B. Jiang and H.-F. Dai, *Org. Lett.*, 2013, **15**, 1492–1495.
219 B. Qing, Z. Yang, Z. Wu, Z. Zhang, Y. Zhou, X. Yan, Y. Liu and X. Feng, *J. Am. Chem. Soc.*, 2025, **147**, 7729–7740.
220 J. Borges, M. T. Manresa, J. L. M. Ramon and C. Pascual, *Tetrahedron Lett.*, 1979, **20**, 3197–3200.
221 Q. Yu, P. Guo, J. Jian, Y. Chen and J. Xu, *Chem. Comm.*, 2018, **54**, 1125–1128.
222 F. Goudou, P. Petit, C. Moriou, O. Gros and A. Al-Mourabit, *J. Nat. Prod.*, 2017, **80**, 1693–1696.
223 Y.-M. Yan, Q. Luo, J.-J. Li, Z.-C. Tu and Y.-X. Cheng, *Bioorg. Chem.*, 2023, **141**, 106845.
224 D. F. Veber, S. R. Johnson, H. Y. Cheng, B. R. Smith, K. W. Ward and K. D. Kopple, *J. Med. Chem.*, 2002, **45**, 2615–2623.
225 N. P. Lavey, J. A. Coker, E. A. Ruben and A. S. Duerfeldt, *J. Nat. Prod.*, 2016, **79**, 1193–1197.
226 N. Ye, H. Chen, E. A. Wold, P. Y. Shi and J. Zhou, *ACS Infect. Dis.*, 2016, **2**, 382–392.
227 R. R. M. Paterson, M. J. S. Simmonds, C. Kemmelmeier and W. M. Blaney, *Mycol. Res.*, 1990, **94**, 538–542.
228 D. A. Ostlind, W. G. Mickle, D. V. Ewanciw, F. J. Andriuli, W. C. Campbell, S. Hernandez, S. Mochales and E. Munguira, *Res. Vet. Sci.*, 1990, **48**, 260–261.
229 W. L. Shoop, J. R. Egerton, C. H. Eary and D. Suhayda, *J. Parasitol.*, 1990, **76**, 349–351.
230 W. L. Shoop, C. H. Eary, B. F. Michael, H. W. Haines and R. L. Seward, *Vet. Parasitol.*, 1991, **40**, 339–341.
231 W. L. Shoop, B. F. Michael, H. W. Haines and C. H. Eary, *Vet. Parasitol.*, 1992, **43**, 259–263.
232 L. Qin, W. Yi, X. Y. Lian and Z. Zhang, *J. Nat. Prod.*, 2020, **83**, 2686–2695.
233 I. Muhammad, D. C. Dunbar, R. A. Khan, M. Ganzera and I. A. Khan, *Phytochemistry*, 2001, **57**, 781–785.
234 B. Yu, D. Q. Yu and H. M. Liu, *Eur. J. Med. Chem.*, 2015, **97**, 673–698.
235 H. S. Zhang, M. F. Liu, X. Y. Ji, C. R. Jiang, Z. L. Li and B. OuYang, *Life Sci.*, 2019, **239**, 116935.
236 B. C. Azevedo, L. J. F. Morel, F. Carmona, T. M. Cunha, S. H. T. Contini, P. G. Delprete, F. S. Ramalho, E. Crevelin, B. W. Bertoni, S. C. Franca, M. C. Borges and A. M. S. Pereira, *J. Ethnopharmacol.*, 2018, **218**, 76–89.
237 M. Liu, J. Shen, H. Liu, Y. Xu, Y. P. Su, J. Yang and C. X. Yu, *Biol. Pharm. Bull.*, 2011, **34**, 1877–1880.
238 J. Qu, L. Fang, X. D. Ren, Y. Liu, S. S. Yu, L. Li, X. Q. Bao, D. Zhang, Y. Li and S. G. Ma, *J. Nat. Prod.*, 2013, **76**, 2203–2209.
239 T. Lai, L. Chen, X. Chen, J. He, P. Lv and H. Ge, *Mol. Cell. Biochem.*, 2019, **461**, 205–212.
240 Y. Zhang, J. Sun, S. Zhu, T. Xu, J. Lu, H. Han, C. Zhou and J. Yan, *Brain Res.*, 2016, **1631**, 92–100.
241 H. Huang, R. Zhong, Z. Xia, J. Song and L. Feng, *Molecules*, 2014, **19**, 11196–11210.
242 J. C. Zhang, W. Yao, Y. Qu, M. Nakamura, C. Dong, C. Yang, Q. Ren, M. Ma, M. Han, Y. Shirayama, A. Hayashi-Takagi and K. Hashimoto, *Sci. Rep.*, 2017, **7**, 7133.
243 H.-Q. Lia, S.-P. Ip, Q.-J. Yuan, G.-Q. Zheng, K. K. W. Tsim, T. T. X. Dong, G. Lin, Y. Han, Y. Liu, Y.-F. Xian and Z.-X. Lin, *Brain. Behav. Immun.*, 2019, **82**, 264–278.
244 Y. L. Lan, J. J. Zhou, J. Liu, X. K. Huo, Y. L. Wang, J. H. Liang, J. C. Zhao, C. P. Sun, Z. L. Yu, L. L. Fang, X. G. Tian, L. Feng, J. Ning, B. J. Zhang, C. Wang, X. Y. Zhao and X. C. Ma, *Cell. Physiol. Biochem.*, 2018, **47**, 1453–1464.
245 M. Liu, H. H. Huang, J. Yang, Y. P. Su, H. W. Lin, L. Q. Lin, W. J. Liao and C. X. Yu, *Psychopharmacology*, 2013, **225**, 839–851.
246 W. B. Zhang, C. X. Chen, S. M. Sim and C. Y. Kwan, *Naunyn Schmiedebergs Arch. Pharmacol.*, 2004, **369**, 232–238.
247 C. Li, F. Jiang, Y. L. Li, Y. H. Jiang, W. Q. Yang, J. Sheng, W. J. Xu and Q. J. Zhu, *Acta Pharmacol. Sin.*, 2018, **39**, 345–356.
248 L. Lin, L. Zhang, X. T. Li, J. K. Ji, X. Q. Chen, Y. L. Li and C. Li, *Front. Pharmacol.*, 2019, **10**, 1617.

249 R. Gan, G. Dong, J. Yu, X. Wang, S. Fu and S. Yang, *Planta Med.*, 2011, **77**, 1477–1481.
250 Y. Zhang, Y. Cui, S. Dai, W. Deng, H. Wang, W. Qin, H. Yang, H. Liu, J. Yue, D. Wu, J. Wang and H. Guo, *Naunyn Schmiedebergs Arch. Pharmacol.*, 2020, **393**, 203–212.
251 L. Zou, F. Lu, B. Lin, Y. Zhou, T. Liu and Y. Sun, *J. Anal. Methods. Chem.*, 2019, **2019**, 7895152.
252 L. Lin, J. Zheng, W. Zhu and N. Jia, *Cell Biochem. Biophys.*, 2015, **71**, 535–541.
253 M. Pilatova, M. Sarissky, P. Kutschy, A. Mirossay, R. Mezencev, Z. Curillova, M. Suchy, K. Monde, L. Mirossay and J. Mojzis, *Leuk. Res.*, 2005, **29**, 415–421.
254 H. Yu, M. H. Tang, Z. Y. Zeng, S. J. Huang, X. F. Zheng and Z. Y. Liu, *Brain. Sci.*, 2022, **12**, 191.
255 M. Ganesh and S. Suraj, *Org. Biomol. Chem.*, 2022, **20**, 5651–5693.
256 Y. Zhu, Q. Zhang, C. Fang, Y. Zhang, L. Ma, Z. Liu, S. Zhai, J. Peng, L. Zhang, W. Zhu and C. Zhang, *Angew. Chem., Int. Ed.*, 2020, **59**, 14065–14069.
257 Q. Chen, C. Ji, Y. Song, H. Huang, J. Ma, X. Tian and J. Ju, *Angew. Chem., Int. Ed.*, 2013, **52**, 9980–9984.
258 T. Mori, S. Hoshino, S. Sahashi, T. Wakimoto, T. Matsui, H. Morita and I. Abe, *Chem. Biol.*, 2015, **22**, 898–906.
259 M. Petchey, A. Cuetos, B. Rowlinson, S. Dannevald, A. Frese, P. W. Sutton, S. Lovelock, R. C. Lloyd, I. J. S. Fairlamb and G. Grogan, *Angew. Chem., Int. Ed.*, 2018, **57**, 11584–11588.
260 R. Chen, Q. Zhang, L. Zhang, C. Fang, H. Zhu, W. Zhu, C. Zhang and Y. Zhu, *J. Nat. Prod.*, 2025, **88**, 715–722.
261 H. Chen, A. Zhou, D. Sun, Y. Zhao and Y. Wang, *J. Phys. Chem. B*, 2021, **125**, 8419–8430.
262 S. M. Li, *J. Antibiot.*, 2011, **64**, 45–49.
263 S. Maiya, A. Grundmann, S. M. Li and G. Turner, *Chembiochem*, 2006, **7**, 1062–1069.
264 A. Grundmann and S. M. Li, *Microbiology*, 2005, **151**, 2199–2207.
265 N. Kato, H. Suzuki, H. Takagi, Y. Asami, H. Kakeya, M. Uramoto, T. Usui, S. Takahashi, Y. Sugimoto and H. Osada, *Chembiochem*, 2009, **10**, 920–928.
266 N. Kato, H. Suzuki, H. Okumura, S. Takahashi and H. Osada, *Biosci. Biotechnol. Biochem.*, 2013, **77**, 1061–1067.
267 Y. Tsunematsu, *J. Nat. Med.*, 2021, **75**, 261–274.
268 A. P. Klein and E. S. Sattely, *Nat. Chem. Biol.*, 2015, **11**, 837–839.
269 D. Chu, H. Wang, Z. Nie, K.-L. Li, J. Cao, M. Yang, Q. Yin, Y. Gu and Y. Jiang, *J. Am. Chem. Soc.*, 2025, **147**, 21600–21609.
270 S. Li, K. Anand, H. Tran, F. Yu, J. M. Finefield, J. D. Sunderhaus, T. J. McAfoos, S. Tsukamoto, R. M. Williams and D. H. Sherman, *Med. Chem. Comm*, 2012, **3**, 987–996.
271 E. M. Stocking, R. A. Martinez, L. A. Silks, J. F. Sanz-Cervera and R. M. Williams, *J. Am. Chem. Soc.*, 2001, **123**, 3391.
272 E. M. Stocking, J. F. Sanz-Cervera, C. J. Unkefer and R. M. Williams, *Tetrahedron*, 2001, **57**, 5303–5320.
273 E. M. Stocking, R. M. Williams and J. F. Sanz-Cervera, *J. Am. Chem. Soc.*, 2000, **122**, 9089–9098.
274 Q. Dan, S. A. Newmister, K. R. Klas, A. E. Fraley, T. J. McAfoos, A. D. Somoza, J. D. Sunderhaus, Y. Ye, V. V. Shende, F. Yu, J. N. Sanders, W. C. Brown, L. Zhao, R. S. Paton, K. N. Houk, J. L. Smith, D. H. Sherman and R. M. Williams, *Nat. Chem.*, 2019, **11**, 972–980.
275 A. E. Fraley, K. Caddell Haatveit, Y. Ye, S. P. Kelly, S. A. Newmister, F. Yu, R. M. Williams, J. L. Smith, K. N. Houk and D. H. Sherman, *J. Am. Chem. Soc.*, 2020, **142**, 2244–2252.
276 M. Chen, C. T. Liu and Y. Tang, *J. Am. Chem. Soc.*, 2020, **142**, 10506–10515.
277 Z. Liu, F. Zhao, B. Zhao, J. Yang, J. Ferrara, B. Sankaran, B. V. Venkataram Prasad, B. B. Kundu, G. N. Phillips Jr, Y. Gao, L. Hu, T. Zhu and X. Gao, *Nat. Commun.*, 2021, **12**, 4158.
278 Z. Liu, S. Rivera, S. A. Newmister, J. N. Sanders, Q. Nie, S. Liu, F. Zhao, J. D. Ferrara, H. W. Shih, S. Patil, W. Xu, M. D. Miller, G. N. Phillips, K. N. Houk, D. H. Sherman and X. Gao, *Nat. Chem.*, 2023, **15**, 526–534.
279 S. Liu, Q. Nie, Z. Liu, S. Patil and X. Gao, *J. Am. Chem. Soc.*, 2023, **145**, 14251–14259.
280 K. R. Klas, H. Kato, J. C. Frisvad, F. Yu, S. A. Newmister, A. E. Fraley, D. H. Sherman, S. Tsukamoto and R. M. Williams, *Nat. Prod. Rep.*, 2018, **35**, 532–558.
281 Y. Ding, J. R. d. Wet, J. Cavalcoli, S. Li, T. J. Greshock, K. A. Miller, J. M. Finefield, J. D. Sunderhaus, T. J. McAfoos, S. Tsukamoto, R. M. Williams and D. H. Sherman, *J. Am. Chem. Soc.*, 2010, **132**, 12733–12740.
282 S. Li, J. M. Finefield, J. D. Sunderhaus, T. J. McAfoos, R. M. Williams and D. H. Sherman, *J. Am. Chem. Soc.*, 2012, **134**, 788–791.
283 A. E. Fraley, H. T. Tran, S. P. Kelly, S. A. Newmister, A. Tripathi, H. Kato, S. Tsukamoto, L. Du, S. Li, R. M. Williams and D. H. Sherman, *Chembiochem*, 2020, **21**, 2449–2454.
284 S. Liu, W.-Q. Xu, Y.-T. Di, M.-C. Tang, D.-K. Chen, M.-M. Cao, Y.-W. Chang, H.-Y. Tang, C.-M. Yuan, J.-B. Yang, Z.-L. Zuo, H. Guo, Z.-F. Xu, Y. Zeng, Y.-D. Wu and X.-J. Hao, *Sci. China. Chem.*, 2025, **68**, 288–296.
285 T. Matsushita, S. Kishimoto, K. Hara, H. Hashimoto and K. Watanabe, *Biochemistry*, 2020, **59**, 4787–4792.
286 Y. Ye, L. Du, X. Zhang, S. A. Newmister, M. McCauley, J. V. Alegre-Requena, W. Zhang, S. Mu, A. Minami, A. E. Fraley, M. L. Adrover-Castellano, N. A. Carney, V. V. Shende, F. Qi, H. Oikawa, H. Kato, S. Tsukamoto, R. S. Paton, R. M. Williams, D. H. Sherman and S. Li, *Nat. Catal.*, 2020, **3**, 497–506.
287 C.-H. Ji, H.-W. Je, H. Kim and H.-S. Kang, *Nat. Prod. Rep.*, 2024, **41**, 672–699.
288 C. Woodcraft, Y.-H. Chooi and I. Roux, *Nat. Prod. Rep.*, 2023, **40**, 158–173.
289 C.-Y. Chiang, M. Ohashi and Y. Tang, *Nat. Prod. Rep.*, 2023, **40**, 89–127.
290 W. Yang, S.-P. Ip, L. Liu, Y.-F. Xian and Z.-X. Lin, *Curr. Vasc. Pharmacol.*, 2020, **18**, 346–357.
291 G.-Z. Chen and R. Hong, *Cell. Rep. Phys Sci.*, 2022, **3**, 101097.